Eur. Phys. J. C (2022) 82:234
https://doi.org/10.1140/epjc/s10052-022-10174-7

THE EUROPEAN PHYSICAL JOURNAL C

Regular Article - Theoretical Physics

Next-to SV resummed Drell–Yan cross section beyond leading-logarithm

A. H. Ajjath[a], **Pooja Mukherjee**[b], **V. Ravindran**[c], **Aparna Sankar**[d], **Surabhi Tiwari**[e]

The Institute of Mathematical Sciences, HBNI, IV Cross Road, Taramani, Chennai 600113, India

Received: 29 October 2021 / Accepted: 26 February 2022 / Published online: 18 March 2022

Abstract We present the resummed predictions for inclusive cross section for Drell–Yan (DY) production up to next-to-next-to leading logarithmic ($\overline{\text{NNLL}}$) accuracy taking into account both soft virtual (SV) and next-to SV (NSV) threshold logarithms. We restrict ourselves to resummed contributions only from quark anti-quark ($q\bar{q}$) initiated channels. The resummation is performed in Mellin-N-space. We derive the N-dependent coefficients and the N-independent constants to desired accuracy for our study. The resummed results are matched through the minimal prescription procedure with the fixed-order results. We find that the resummation, taking into account the NSV terms, appreciably increases the cross section while decreasing the sensitivity to renormalisation scale. We observe that, at 13 TeV LHC energies, the SV + NSV resummation at $\overline{\text{NLL}}$($\overline{\text{NNLL}}$) gives about 8% (2%) corrections respectively to the NLO (NNLO) results for the considered Q range: 150–3500 GeV. In addition, the absence of quark gluon initiated contributions to NSV part in the resummed terms leaves large factorisation scale dependence indicating their importance at NSV level. We also study the numerical impact of N-independent constants and explore the ambiguity involved in exponentiating them. Finally we present our predictions for the neutral Drell–Yan process at various center of mass of energies.

1 Introduction

Standard Model (SM) has been extremely successful in describing the physics of elementary particles. Thanks to precise predictions of various observables from SM and their measurements at the collider experiments with unprecedented accuracy, we could validate the SM and at the same time set stringent constraints on the parameters present in various beyond SM (BSM) scenarios. While there have been strenuous efforts in search of new physics signatures at the large hadron collider (LHC), it is important to improve the level of precision in SM and BSM predictions to arrive at sensible conclusions. Precise predictions of observables require the use of complex mathematical techniques and a deeper understanding of the underlying theory. The spin-offs include new developments in various branches of mathematics and other fields, and in addition, the perturbative predictions dealing with Feynman loop and phase space integrals demonstrate rich mathematical structure in gauge theories. In particular, these results have shed light on the underlying structure of the ultraviolet (UV) and infrared (IR) sectors of the SM.

Among innumerous final states produced in hadron collisions, leptons are relatively easy to observe due to the clean environment and the corresponding measurements are less plagued by experimental uncertainties. The production of a pair of leptons, called Drell–Yan (DY) production is customarily used for luminosity monitoring at the hadron colliders. Theoretically, for very long, the observables in DY production belong to the category of "well studied" quantities in the SM and as well as in various BSMs. Note that the next-to-next-to leading order (NNLO) quantum chromodynamics (QCD) correction [1–3] to this process was computed more than three decades ago, see also [1–17]. Similar results are also available in certain BSMs, see [18–20]. More recently, a series of results on inclusive cross sections for the production of a pair of leptons, single Z/$W^{\pm}$ at N^{3}LO in perturbative QCD has become available [17]. These corrections [17] are already found to be tiny, and at the invariant mass $Q = 150$ GeV of a pair of leptons, they reduce the cross section by 1%. The renormalisation and factorisation scale

[a] e-mail: ajjathah@imsc.res.in
[b] e-mail: poojamukherjee@imsc.res.in
[c] e-mail: ravindra@imsc.res.in
[d] e-mail: aparnas@imsc.res.in (corresponding author)
[e] e-mail: surabhit@imsc.res.in

uncertainties as well as the uncertainties from the choice of PDFs give about 2.5%.

Dedicated efforts like in [17] to obtain perturbative QCD results provide a theoretical laboratory to understand the structure of the perturbation series. Due to the complexity involved in performing many body phase space integrals in higher order computations, one resorts to the method of threshold expansion. For example, at every perturbative order in the strong coupling constant, the Feynman diagrams are computed as a series expansion around the threshold region denoted by $Q^2 \approx \hat{s}$, where Q is the invariant mass of the pair of leptons produced in the partonic reaction whose center of mass energy is $\sqrt{\hat{s}}$. Such an expansion not only provides reliable estimates of the higher order effects but also shed light on the logarithmic structure in higher order perturbative results. The leading terms in the threshold region contain contributions from virtual subprocesses as well as from soft gluons from real emissions. These are often called soft plus virtual contributions (SV). The SV terms at third order were known for some time, see [10–13,15,21–24]. In addition, using the resummation framework developed in [25,26] for threshold logarithms in SV contributions, several numerical studies were carried out to NNLL accuracy to improve the predictions, see [15,27–29]. In [30], we reported the numerical impact of threshold corrections within the resummation framework. We found that the inclusion of large threshold logarithms to $\mathrm{N^3LL}$ accuracy further reduces theoretical uncertainties.

The subleading terms in the threshold expansion contain logarithms of the form $\ln^j(1-z)$, $j \geq 0$ and numerically they are found to be as important as leading SV terms in the expansion, see [31–34] in the context of Higgs production. These are called next-to-soft virtual (NSV) logarithms. There have been several dedicated studies to understand the structure of these logarithms in inclusive reactions at higher orders and efforts to resum them like one does for SV terms, see [33,35–46]. Using the resummation framework of NSV terms at LL proposed in [35], their numerical impact was studied in [47] taking into account SV terms at $\mathrm{N^3LL}$ for DY and Higgs boson productions. Similar studies were done for the scalar and pseudo scalar Higgs boson productions in [32,48]. All these studies were at LL level as far as NSV logarithms are concerned and also restricting to diagonal partonic channels, namely quark anti-quark for Drell–Yan, gluon fusion or bottom quark annihilation for Higgs boson productions.

Recently, in [49], we set up a formalism for the first time to study all order structure of these NSV logarithms in order to go beyond LL approximation. While NSV logarithms show up both in diagonal and off-diagonal partonic channels, we have restricted to only to the former. We found that unlike SV logarithms, the NSV ones were controlled in addition to the process independent anomalous dimensions, the functions that depend on the process under consideration through certain differential equations. The latter allowed us to systematically resum NSV logarithms in Mellin N-space to all orders along with SV ones to obtain results at $\overline{\mathrm{N^nLL}}$, $n \geq 0$ accuracy. In order to distinguish between SV and SV + NSV resummed results, we denote the NSV included results by $\overline{\mathrm{N^nLL}}$. In this article, we study the numerical impact of NSV logarithms in the invariant mass distribution of a pair of leptons in DY process at the LHC up to $\overline{\mathrm{NNLL}}$ accuracy.

The paper is structured as follows. In Sect. 2, we briefly describe the theoretical framework for computing the invariant mass distribution of a pair of leptons in DY process, taking into account the NSV effects. Further in Sect. 3, we review the formalism given in [49] for computing the SV + NSV resummed cross section of di-lepton production in DY process. In addition, we also discuss different resummation prescriptions to explore the ambiguity involved in exponentiating the N-independent constants. In Sect. 4, we study the phenomenological aspects of NSV logarithms in great detail and present our findings and finally we conclude in Sect. 5.

2 Theoretical framework

In the QCD improved parton model, the invariant mass distribution of a pair of leptons produced in hadron colliders can be expressed as a convolution of perturbatively calculable coefficient functions (CFs), Δ_{ab}, and non-perturbative flux $\tilde{\Phi}_{ab}$. That is,

$$\frac{d\sigma}{dQ}(q^2,\tau) = \sigma^{(0)}_{DY} \int_\tau^1 \frac{dz}{z} \tilde{\Phi}_{ab}\left(\frac{\tau}{z}, \mu_F^2\right) \Delta_{ab}(q^2, \mu_F^2.z). \tag{1}$$

Here $a, b = q, \overline{q}, g$ refer to incoming partonic states and $\sigma^{(0)}_{DY}$ is the born cross section:

$$\sigma^{(0)}_{DY} = \frac{2\pi}{n_c}\left[\frac{Q}{S}\mathscr{F}^{(0)}\right], \tag{2}$$

with $Q = \sqrt{q^2}$ being the invariant mass of the lepton pairs and $n_c = 3$ in QCD. The factor $\mathscr{F}^{(0)}$ is found to be

$$\begin{aligned}\mathscr{F}^{(0)} = \frac{4\alpha^2}{3q^2}\Bigg[& Q_q^2 - \frac{2q^2(q^2-M_Z^2)}{\left((q^2-M_Z^2)^2+M_Z^2\Gamma_Z^2\right)c_w^2 s_w^2} Q_q g_e^V g_q^V \\ & + \frac{q^4}{\left((q^2-M_Z^2)^2+M_Z^2\Gamma_Z^2\right)c_w^4 s_w^4}\Big((g_e^V)^2 \\ & + (g_e^A)^2\Big)\Big((g_q^V)^2+(g_q^A)^2\Big)\Bigg].\end{aligned} \tag{3}$$

with α being the fine structure constant and c_w, s_w are respectively the sine and cosine of Weinberg angle. M_Z and Γ_Z are the mass and the decay width of the Z-boson. Also,

$$g_a^A = -\frac{1}{2}T_a^3, \qquad g_a^V = \frac{1}{2}T_a^3 - s_w^2 Q_a, \tag{4}$$

where Q_a being the electric charge and T_a^3 is the weak isospin of the electron or quarks. The flux $\tilde{\Phi}_{ab}$ is defined in terms of parton distribution functions (PDF) f_a, f_b of incoming partons a and b respectively at the factorisation scale μ_F:

$$\tilde{\Phi}_{ab}\left(\frac{\tau}{z}, \mu_F^2\right) = \int_{\frac{\tau}{z}}^1 \frac{dy}{y} f_a(y, \mu_F^2) f_b\left(\frac{\tau}{zy}, \mu_F^2\right) \tag{5}$$

where $\tau = q^2/S$ is the hadronic scaling variable with S being the square of hadronic center of mass energy. The fits of non-perturbative PDFs are available to NNLO level while the CFs are perturbatively calculable in powers of renormalized strong coupling constant, $a_s = g_s^2/16\pi^2$:

$$\Delta_{ab}(q^2, \mu_F^2, z) = \sum_{i=0}^{\infty} a_s^i(\mu_R^2)\Delta_{ab}^{(i)}(q^2, \mu_R^2, \mu_F^2, z) \tag{6}$$

where g_s is the QCD coupling constant and μ_R is the renormalisation scale. Higher order corrections from QCD are inevitable at hadron colliders as they are often large and they reduce uncertainties resulting from the scales μ_R, μ_F, the choice of PDFs and a_s. Note that DY predictions are stable with respect to factorization (μ_F) and renormalisation (μ_R) scales already at NNLO in QCD. One finds 2% uncertainty in the predictions at NNLO for a canonical variation of factorization and renormalisation scales compared to NLO where it is about 9.2%. Similarly, the K-factor increases marginally from 1.25 at NLO to 1.28 at NNLO. At third order, the scale uncertainties can be determined from previous order DY results. However, such estimates make sense only if we include the scale independent parts which originate genuinely at third order. The recent third order results [17] predict decrease in the cross section by less than 1% for $Q = 150$ GeV and the uncertainties from scales and from the choice of PDFs give about 2.5%. While this is a great improvement in the predictions, it is important to estimate other missing higher order effects.

2.1 Threshold expansion

Computing CFs beyond N^{3}LO is highly challenging, hence one can look for alternative approaches to identify the dominant contributions to the CFs. In the case of leptons with high invariant mass, the threshold expansion of CFs around $z \approx 1$ was observed to be a good alternative to exact computation. Here, z is the partonic scaling variable defined by $z = q^2/\hat{s}$, with $\hat{s}$ the square of partonic center of mass energy. At the threshold, we decompose the CFs as

$$\Delta_{ab}(q^2, \mu_F^2, z) = \delta_{ab}\Delta_{a\bar{a}}^{SV}(q^2, \mu_F^2, z) + \Delta_{ab}^{reg}(q^2, \mu_F^2, z). \tag{7}$$

Here $\Delta_{a\bar{a}}^{SV}$ denotes the soft-virtual (SV) corrections which comprises pure virtual contributions from $q + \overline{q} \to l^+l^-$ and leading threshold contributions from quark anti-quark initiated partonic channels with at least one emission of on-shell parton. The former depends on the scale z through $\delta(1-z)$ while the latter through both $\delta(1-z)$ and plus distributions $\mathscr{D}_k(z)$ defined by

$$\mathscr{D}_k(z) = \left(\frac{\ln^k(1-z)}{1-z}\right)_+, \tag{8}$$

and are integrable with any regular function $f(z)$:

$$\int_0^1 dz\, f(z)\left(\frac{\ln^k(1-z)}{1-z}\right)_+ = \int_0^1 dz\, \big(f(z) - f(1)\big) \times \left(\frac{\ln^k(1-z)}{1-z}\right). \tag{9}$$

The second term in (7), Δ_{ab}^{reg}, refers to regular CFs, which contain terms of the form $(1-z)^m \ln^k(1-z), m, k = 0, 1, \ldots, \infty$ with rational and irrational constants. Expanding both SV and regular CFs perturbatively in powers of a_s,

$$\Delta_{ab}^J(q^2, \mu_F^2, z) = \sum_{i=0}^{\infty} a_s^i(\mu_R^2)\Delta_{ab}^{J,(i)}(q^2, \mu_R^2, \mu_F^2, z), \quad J = SV, reg \tag{10}$$

we find

$$\Delta_{ab}^{SV,(i)}(z) = \delta_{ab}\left(\Delta_{a\bar{a},\delta}\,\delta(1-z) + \sum_{k=0}^{2i-1}\Delta_{a\bar{a},\mathscr{D}_k}^{(i)}\mathscr{D}_k(z)\right), \tag{11}$$

and

$$\Delta_{ab}^{reg,(i)}(z) = \sum_{k=0}^{2i-1}\sum_{l=0}^{\infty}\Delta_{ab,l,k}^{reg,(i)}(1-z)^l \ln^k(1-z). \tag{12}$$

The above expansion is called threshold expansion. The systematic threshold expansion of CFs in partonic scaling variable z will be useful provided the partonic flux $\tilde{\Phi}_{ab}(\tau/z)$ that multiplies them to give hadronic cross sections also dominates in the same region for a given hadronic scaling variable τ.

In general, the CFs in inclusive cross sections such as DY and Higgs productions, the energy scales q^2, μ_R^2 and μ_F^2 appear as logarithms, in addition to the partonic scaling variable z appearing through $\delta(1-z)$, plus distributions $\mathscr{D}_k(z)$ and regular functions of z. The coefficients of these terms are perturbatively computable and are controlled by set of differential equations that depend on the UV and IR anomalous dimensions. The solutions to these equations demonstrate rich universal structure which can be exploited to understand the structure of the coefficients to all orders in

perturbation theory. The IR structure of multi-loop amplitudes beyond two loops [50–53] (see [54,55] for a QFT with mixed gauge groups), of inclusive cross sections to third order [1,3,17,56–58] provide better understanding of CFs. For complete list of Higgs production in gluon fusion see [3,10–12,16,33,46,56,59–71] and [1–17] for Drell–Yan production.

Among the aforementioned terms that contribute to CFs, the SV terms are known for several observables. In particular for DY and Higgs productions beyond second order, see [10–13,15,21–24]. We obtain these results from process dependent pure virtual subprocesses and soft gluons from real emissions in the threshold region. The latter is a universal quantity in such a sense that they do not depend on the hard process under study, but only on the nature of incoming states. The soft and collinear modes in a scattering process can be captured at the Lagrangian level using effective theory approach. For example, soft-collinear effective theory (SCET) [72–74] provides a convenient framework to compute the SV results order by order in perturbation theory. In addition, the intrinsic scales in the theory can be used to set up renormalisation group equations whose solutions sum up large logarithms from threshold regions to all orders.

When SV terms are convoluted with the appropriate PDFs to obtain hadronic cross sections, one finds that they give large contributions at every order, questioning the reliability of the predictions from the truncated series. This was successfully resolved in the seminal works by Sterman [25] and Catani and Trentedue [26] through reorganisation of the large logarithms to all order in the perturbative series, called the threshold resummation. There is a vast literature on this which is applied to variety of processes, see [27,32,75–78] for Higgs production in gluon fusion, [79,80] for bottom quark annihilation, for DY [15,27–30] and for DIS and SIA of e^+e^- [81]. Threshold resummation is conveniently performed in Mellin space where the conjugate variable to z is N. In Mellin space, all the z-space convolutions become normal products. The threshold limit in Mellin space is when N goes large, which corresponds to $z \to 1$ in z-space. Due to smallness of $a_s(\mu_R^2)$, one finds that the exponent in the N-space at each order in $a_s(\mu_R^2)$ contains $\mathcal{O}(1)$ terms defined by $\omega = 2a_s(\mu_R^2)\beta_0 \ln N$. Such terms spoil the truncation of the perturbative series. Using renormalisation group improved solution to RG of a_s, one can reorganise the perturbative series in the exponent wherein ω terms are summed up at every order in a_s. Following [25,26] one finds that for $\Delta_{c\bar{c},N} = \int_0^1 dz z^{N-1} \Delta_{c\bar{c}}(z)$,

$$\lim_{N\to\infty} \ln \Delta^{SV}_{c\bar{c},N} = \ln \tilde{g}_0^c(a_s(\mu_R^2)) + \ln N g_1^c(\omega) + \sum_{i=0}^{\infty} a_s^i(\mu_R^2) g_{i+2}^c(\omega), \tag{13}$$

where $\tilde{g}_0^c(a_s(\mu_R^2))$ is N independent. Inclusion of successive terms in (13) predicts the leading-logarithms (LL), next-to-leading (NLL) etc. logarithms to all orders in a_s. The exponents $g_i^c(\omega)$ depend on process independent/universal IR anomalous dimensions while the constant $\tilde{g}_0^c$ depends on the specific hard process. Results for the resummation of threshold logarithms in N-space up to third order are available for variety of inclusive processes such as DY and Higgs productions to perform threshold resummation to next-to-next-to-next-to leading logarithmic ($\mathrm{N^3LL}$) accuracy [15,27,30,80]. Threshold resummation is also found to play important role for differential observables like rapidity [19,26,82–84]. Inclusion of these effects are shown to improve the fixed-order results.

2.2 Next-to SV

Perturbative predictions of beyond SV terms are available for partonic sub processes up to third order for a variety of hadronic cross sections, namely Drell–Yan production and bottom quark as well as gluon initiated Higgs boson productions at the hadron colliders. Like SV terms, these results not only play an important role to precisely predict the respective observables, but also shed light on the structure of beyond SV terms in the threshold expansion at higher orders. Among these, let us consider a class of leading terms:

$$\Delta_{ab}^{NSV}(z) = \sum_{i=0}^{\infty} a_s^i(\mu_R^2) \Delta_{ab}^{NSV,(i)}(z), \tag{14}$$

where $\Delta_{ab}^{NSV,(i)}(z)$ is defined by setting $l = 0$ in (12), i.e.,

$$\Delta_{ab}^{NSV,(i)}(z) = \sum_{k=0}^{2i-1} \Delta_{ab,0,k}^{reg,(i)} \ln^k(1-z). \tag{15}$$

These contributions are often called next-to SV (NSV) or next to leading power (NLP) contributions. There have been several studies to understand the NSV terms in inclusive processes [35,38–45]. The physical evolution equation was exploited earlier in the work by [36] to understand the effect of these terms. A remarkable development was made by Moch and Vogt in [37] (and [33,46]) using the physical evolution kernels (PEK) and the fixed-order results that are available for DIS, semi-inclusive e^+e^- annihilation and Drell–Yan production of a pair of leptons in hadron collisions. They found that in kernels that govern the physical equations, there is an enhancement of single-logarithms at large z up to third order. Conjecturing that it will hold true to all orders around $z = 1$, the logarithms were systematically resummed to all orders exactly like the way of SV resummation. In addition, absence of certain powers of $\ln(1-z)$ terms in the kernel at a given order in a_s can be used [37] to predict certain next-to SV logarithms at higher orders.

Recently, in [49], we investigated the structure of NSV terms present in the quark anti-quark initiated channels in the inclusive production of pair of leptons in Drell–Yan process and gluon/bottom anti-bottom initiated ones for Higgs boson production. We also analyzed the all-order perturbative structure of the NSV logarithms in the coefficient functions of deep inelastic scattering (DIS) and semi-inclusive e^+e^- annihilation (SIA) processes in [85]. The formalism is even extended in the context of rapidity distributions to study the all-order behaviour of the NSV terms in addition to the SV distributions in the aforementioned threshold processes, namely Drell–Yan and Higgs production through gluon fusion and bottom quark annihilation in [86]. We used the well known factorisation properties and renormalisation group invariance along with certain universal structure of real and virtual contributions obtained through Sudakov K + G equation. Like, SV terms, NSV terms do demonstrate rich perturbative structure with certain universal anomalous dimensions. We found that the NSV logarithms in Mellin space can also be resummed in a systematic fashion to all orders in perturbation theory. fixed-order results known up to third order for DY productions can be used to determine the threshold exponents from the NSV logarithms with third order logarithmic accuracy. The present article explores the numerical impact of these resummed results taking into account both SV and NSV logarithms in the quark anti-quark initiated channels for the DY process at the LHC.

3 Resummation of SV + NSV

In [49], some of us have developed a theoretical formalism to systematically resum the NSV contributions in the diagonal channels of inclusive cross sections of Drell–Yan and Higgs boson productions at the hadron colliders. For completeness, we briefly describe the formalism [49], which shows how the building blocks of perturbative results in the threshold region can be organised using their factorisation properties and the logarithmic structure. Thanks to a set of differential equations that govern these building blocks, it is possible to sum up certain class of threshold logarithms to all orders in perturbation theory. In particular, the solutions to such equations lead to a compact integral representation in z-space that captures SV and NSV terms of inclusive rates in these processes. The integral representation can be conveniently used in Mellin N-space to resum $\mathscr{O}(1)$ terms that show up in large SV and NSV contributions at every order to obtain reliable theoretical predictions at colliders.

We begin by defining Δ_q as a sum of SV and NSV contributions to diagonal channels:

$$\Delta_q(z) = \Delta_{q\bar{q}}^{SV}(z) + \Delta_{q\bar{q}}^{NSV}(z) \tag{16}$$

where the SV part is defined in (11) and NSV in (14). Using the mass factorisation that separates collinear singular part from the bare partonic cross sections and the UV and IR renormalisation group equations that various building blocks satisfy we can cast the CFs of inclusive cross sections in dimensional regularisation ($n = 4 + \varepsilon$) as

$$\Delta_q(q^2, \mu_R^2, \mu_F^2, z) = \mathscr{C} \exp\left(\Psi^q\left(q^2, \mu_R^2, \mu_F^2, z, \varepsilon\right)\right)\Big|_{\varepsilon=0}, \tag{17}$$

where Ψ^q is finite in the limit $\varepsilon \to 0$ and is given by

$$\begin{aligned}\Psi^q\left(q^2, \mu_R^2, \mu_F^2, z, \varepsilon\right) = &\left(\ln\left(Z_{UV,q}\left(\hat{a}_s, \mu^2, \mu_R^2, \varepsilon\right)\right)^2\right. \\ &\left. + \ln\left|\hat{F}_q\left(\hat{a}_s, \mu^2, -q^2, \varepsilon\right)\right|^2\right)\delta(1-z) \\ &+ 2\Phi_q\left(\hat{a}_s, \mu^2, q^2, z, \varepsilon\right) \\ &- 2\mathscr{C}\ln\Gamma_{qq}\left(\hat{a}_s, \mu^2, \mu_F^2, z, \varepsilon\right),\end{aligned} \tag{18}$$

where $Z_{UV,q}$ is the overall renormalisation constant which is unity for vector/axial vector interactions in quark anti-quark initiated channels. The bare strong coupling constant, $\hat{a}_s = \hat{g}_s^2/16\pi^2$, with $\hat{g}_s$ the bare QCD coupling constant and the scale μ results from dimensional regularisation. The square of the form factor (FF), $\hat{F}_q$, encodes pure virtual contributions to $q + \overline{q} \to l^+l^-$ while the soft-collinear function, Φ_q, contains contributions from remaining partonic subprocesses normalised by square of the form factor. Thanks to the fact that mass factorisation terms required for the SV and NSV contributions to diagonal channels depend only on diagonal kernels $\Gamma_{q\overline{q}}$ where we need to keep only diagonal splitting functions P_{qq}, the logarithm of these kernels completely decouples from the rest.

The symbol "$\mathscr{C}$" refers to convolution, which acting on any exponential of a function $f(z)$ takes the following expansion::

$$\mathscr{C}e^{f(z)} = \delta(1-z) + \frac{1}{1!}f(z) + \frac{1}{2!}(f \otimes f)(z) + \cdots \tag{19}$$

Since we have restricted ourselves to SV + NSV contributions to Δ_q, we keep only those terms that are proportional to SV distributions namely $\delta(1-z)$, $\mathscr{D}_i(z)$ and NSV terms $\ln^i(1-z)$ with $i = 0, 1, \ldots$ and drop rest of the terms resulting from the convolutions.

The form factor, soft-collinear function and Altarelli–Parisi (AP) kernels that contribute to Δ_q are computable order by order in a_s in perturbation theory. One finds that each of them demonstrates rich infrared structure through certain differential equations. For example, the form factor satisfies Sudakov's K + G differential equation while the mass factorisation kernels satisfy AP evolution equations.

In addition, they are independently renormalisation group invariants. These differential equations are controlled by universal UV and IR anomalous dimensions that are perturbatively calculable. Thanks to these differential equations and the fact that Δ_q is finite, one finds that soft-collinear function Φ_q also satisfies K + G like differential equation. The solution to the form factor is expressed in terms of cusp (A^q), soft (f^q), collinear (B^q) anomalous dimensions and process dependent constants, while for the mass factorisation kernels, one finds the solution in terms of diagonal AP splitting functions which contain only $\delta(1-z)$, $\mathscr{D}_0(z)$ and $\ln^j(1-z)$, $j = 0, 1$ terms. Unlike the form factor and AP kernels, the solution to Φ_q is hard to obtain without the knowledge of their kernels $\overline{\mathrm{K}}$ and $\overline{\mathrm{G}}$ (see [49]). The singular kernel $\overline{\mathrm{K}}$ can be determined from singular terms of FF and AP kernels while the finite part is obtained from the fixed-order results of Δ_q. We use the perturbative results known to third order to parametrise the kernels in terms of $\delta(1-z)$, plus distributions and $\ln(1-z)$ in dimensional regularisation. The resulting z dependent solution of Φ_q depends on process independent anomalous dimensions A^q, f^q, C^q and D^q and certain process dependent quantities. Combining the solutions from all the differential equations one obtains an all order exponentiation of SV and NSV contributions to Δ_q as given in (17). While each piece contains both UV and IR divergences as poles in ε, the divergences cancel among themselves when $\varepsilon \to 0$, leaving finite Ψ^q. In [49], an integral representation for the function Ψ^q in terms of z was obtained:

$$\Delta_q(q^2,\mu_R^2,\mu_F^2,z) = C_0^q(q^2,\mu_R^2,\mu_F^2) \times \mathscr{C}\exp\left(2\Psi_{\mathscr{D}}^q(q^2,\mu_F^2,z)\right), \tag{20}$$

where

$$\Psi_{\mathscr{D}}^q(q^2,\mu_F^2,z) = \frac{1}{2}\int_{\mu_F^2}^{q^2(1-z)^2}\frac{d\lambda^2}{\lambda^2}P'_{qq}(a_s(\lambda^2),z) + \mathscr{Q}^q(a_s(q^2(1-z)^2),z), \tag{21}$$

with

$$\mathscr{Q}^q(a_s(q^2(1-z)^2),z) = \left(\frac{1}{1-z}\overline{G}_{SV}^q(a_s(q^2(1-z)^2))\right)_+ + \varphi_{f,q}(a_s(q^2(1-z)^2),z). \tag{22}$$

The coefficient C_0^q is z independent and is expanded in powers of $a_s(\mu_R^2)$ as

$$C_0^q(q^2,\mu_R^2,\mu_F^2) = \sum_{i=0}^{\infty} a_s^i(\mu_R^2)C_{0i}^q(q^2,\mu_R^2,\mu_F^2), \tag{23}$$

The results for C_0^q can be found in [15] and the coefficients C_{0i}^q are given in Appendix C.1. The splitting function P'_{qq} is related to the AP splitting functions $P_{qq}\left(z,\mu_F^2\right)$. Expanding the latter around $z = 1$ and dropping those terms that do not contribute to SV + NSV, we find

$$P_{qq}\left(z,a_s(\mu_F^2)\right) = 2B^q(a_s(\mu_F^2))\delta(1-z) + P'_{qq}\left(z,a_s(\mu_F^2)\right), \tag{24}$$

where,

$$P'_{qq}\left(z,a_s(\mu_F^2)\right) = 2\Big[A^q(a_s(\mu_F^2))\mathscr{D}_0(z) + C^q(a_s(\mu_F^2))\ln(1-z) + D^q(a_s(\mu_F^2))\Big]. \tag{25}$$

The constants C^q and D^q can be obtained from the splitting functions P'_{qq} which are known to three loops in QCD [87,88] (see [87–96] for the lower order ones). The cusp, soft and the collinear anomalous dimensions and the constants C^q and D^q are expanded in powers of $a_s(\mu_F^2)$:

$$X^q(a_s(\mu_F^2)) = \sum_{i=1}^{\infty} a_s^i(\mu_F^2)X_i^q, \qquad X = A, f, B, C, D \tag{26}$$

where X_i^q to third order are available in [87,88] and are listed in Appendix A. The function $\overline{G}_{SV}^q\left(a_s(q^2(1-z)^2)\right)$ is related to the threshold exponent $\mathbf{D}^q\left(a_s(q^2(1-z)^2)\right)$ via Eq. (46) of [11] (see Appendix A). The function $\varphi_{f,q}$ in powers of a_s is given by

$$\varphi_{f,q}(a_s(q^2(1-z)^2),z) = \sum_{i=1}^{\infty} a_s^i(q^2(1-z)^2) \times \sum_{k=0}^{i}\varphi_{q,i}^{(k)}\ln^k(1-z). \tag{27}$$

The coefficients $\varphi_{q,i}^{(k)}$ are known to third order and are listed in Appendix B (see also [49]).

The resummation of threshold logarithms can be conveniently done in Mellin space, where $z \to 1$ translates to large N limit. In the latter, $\mathscr{O}(1)$ terms from $\omega = 2\beta_0 a_s(\mu_R^2)\ln N$ show up at every order in a_s spoiling the truncation of perturbative series in the exponent. This can be resolved by reorganising the series using the integral representation (21) and the resummed strong coupling constant. To include SV and NSV terms in the resummation in Mellin space, we need to keep $\ln N$ as well as $\mathscr{O}(1/N)$ terms in the large N limit. We find that (21) can correctly predict only SV and NSV terms while the predictions beyond the NSV terms namely $\mathscr{O}((1-z)^n\ln^j(1-z))$; $n, j \geq 0$ in z-space and terms of $\mathscr{O}(1/N^2)$ in N-space will not be correct!. The Mellin moment of Δ_q was obtained in [49] and is given by

$$\Delta_{q,N}(q^2,\mu_R^2,\mu_F^2) = C_0^q(q^2,\mu_R^2,\mu_F^2)\exp\left(\Psi_{q,N}^q(q^2,\mu_F^2)\right), \tag{28}$$

where

$$\Psi_{q,N}^q(q^2,\mu_F^2) = 2\int_0^1 dz z^{N-1}\Psi_{\mathscr{D}}^q(q^2,\mu_F^2,z). \tag{29}$$

Also, C_0^q are N-independent constants coming from FF and the $\delta(1-z)$ part of soft-collinear function and AP kernels. Note that the $\delta(1-z)$ pieces in z-space translates to N-independent pieces in Mellin space. And the Mellin transformation of the plus distributions, given in (29), give rise to $\ln N$ and N-independent constants. Hence expressing $\Psi_{q,N}^q$ as

$$\Psi_{q,N}^q = \Psi_{\mathrm{SV},N}^q + \Psi_{\mathrm{NSV},N}^q \tag{30}$$

where $\Psi_{\mathrm{SV},N}^q$ contains $\ln^j N, j = 0,1,\ldots$ terms and while $\Psi_{\mathrm{NSV},N}^q$ contains terms of the form $(1/N)\ln^j N, j = 0,1,\ldots$. We find that $\Psi_{\mathrm{SV},N}^q$ takes the form:

$$\Psi_{\mathrm{SV},N}^q = \ln(g_0^q(a_s(\mu_R^2))) + g_1^q(\omega)\ln N + \sum_{i=0}^{\infty} a_s^i(\mu_R^2) g_{i+2}^q(\omega). \tag{31}$$

Here the g_i^q coefficients are universal and they depend only on the initial partons. The constants $\ln g_0^q$ are the N-independent pieces obtained after Mellin transformation of $\Psi_{\mathscr{D}}^q$ and they satisfy the condition $\Psi_{\mathrm{SV},N}^q - \ln(g_0^q) = 0$ when $N = 1$. Expanding them in powers of a_s we get,

$$\ln g_0^q(a_s(\mu_R^2)) = \sum_{i=1}^{\infty} a_s^i(\mu_R^2)\, g_{0,i}^q. \tag{32}$$

These exponents agree with those given in [26,27,80], and they are listed in the Appendices C.2 and C.4. In standard N-approach we absorb the N-independent pieces $g_{0,i}^q$ into C_0^q and collectively define it as

$$\tilde{g}_0^q(q^2,\mu_R^2,\mu_F^2) = C_0^q(q^2,\mu_R^2,\mu_F^2)\, g_0^q(a_s(\mu_R^2)). \tag{33}$$

Thus the resulting quantity comprises of $\delta(1-z)$ contributions from the form factor, soft-collinear function, AP kernels and N-independent part of the Mellin moment of the distributions in $\Psi_{\mathscr{D}}^q(q^2,\mu_F^2,z)$.

The coefficients $\tilde{g}_{0,i}^q$ are listed in the Appendix C.3.

The function $\Psi_{\mathrm{NSV},N}^q$ in (30) is given by

$$\Psi_{\mathrm{NSV},N}^q = \frac{1}{N}\sum_{i=0}^{\infty} a_s^i(\mu_R^2)\left(\bar{g}_{i+1}^q(\omega) + h_i^q(\omega,N)\right), \tag{34}$$

with

$$h_i^q(\omega,N) = \sum_{k=0}^{i} h_{ik}^q(\omega)\ \ln^k N. \tag{35}$$

where $\bar{g}_i^q(\omega)$ and $h_{ik}^q(\omega)$ are presented in the Appendices C.5 and C.6 respectively. In each exponents, $g_i^q(\omega)$, $\overline{g}_i^q(\omega)$ and $h_{ik}^q(\omega)$, we resum $\mathscr{O}(1)$ term ω in Mellin space to all orders in perturbation theory. This is possible because of the argument in the coupling constant $a_s(q^2(1-z)^2)$ resulting the integrals and from the function $\mathscr{Q}^q$.

In the SV part of the resummed result, the intrinsic ambiguity that exists while dealing with what needs to be exponentiated gives scope to explore their impact. Among different prescriptions, the standard approach is to exponentiate only large-N pieces coming from the threshold region. Also, for large N, the expansion of Euler Gamma functions gives *Euler–Mascheroni* constant, γ_E and considering these large effects, one can exponentiate $\overline{N}$, which is defined as $\overline{N} = N\exp(\gamma_E)$, instead of N without disturbing the fixed-order predictions. Numerically, however this can make a difference at the leading logarithmic accuracy as was already seen in [97] where the perturbative convergence was shown to improve with $\overline{N}$ terms. In a different scheme, called *Soft exponentiation* one exponentiates the Mellin moment of soft-collinear function [11,21] which contains all the plus distributions and $\delta(1-z)$ terms. Alternatively, one can also exponentiate the complete form factor along with the soft-collinear function in the Mellin space. This approach was explored in [32,78] to study the inclusive Higgs boson production in gluon fusion. It was found to predict results that are less sensitive to the unphysical scales compared to the standard threshold approach. This approach is theoretically justified because the form factor satisfies the Sudakov K + G type equation [11,21,98–101] whose solution is an exponential of N independent constant. For the numerical study of DY production this approach was used in [102]. We give the expressions for different resummation schemes below.

– Standard N exponentiation: In this scheme, we exponentiate only the large-N pieces that contribute to the CFs and the exponent is devoid of N-independent pieces. Note that this will only change the $\Psi_{\mathrm{SV},N}^q$. The $\Psi_{\mathrm{NSV},N}^q$ will remain same as it contains only N-dependent terms. Hence we write:

$$\Delta_{q,N}(q^2,\omega) = \tilde{g}_0^q(q^2)\exp\left(G_{\mathrm{SV},N}^q(q^2,\omega) + \Psi_{\mathrm{NSV},N}^q(q^2,\omega)\right), \tag{36}$$

where NSV part is defined in (34). And the SV part is given as,

$$G^q_{\mathrm{SV},N}(q^2,\omega) = \Psi^q_{\mathrm{SV},N}(q^2,\omega) - \ln(g^q_0) \tag{37}$$

which can be obtained from the Mellin transformation of $\Psi^q_{\mathscr{D}}$ and keeping only those terms that vanish when $N = 1$. This is the standard approach adopted all along this paper and we compare other prescriptions with the N-exponentiation scheme in later sections.

– Standard $\bar{N}$ exponentiation: Here, the large logarithms are expressed in functions of $\bar{N}$ instead of N, where $\bar{N} = N\exp(\gamma_E)$. Hence along with large N-pieces, the γ_E terms are also taken into exponentiation as they also contribute to $\mathscr{O}(1)$ terms. The resulting exponent takes the form:

$$\Delta_{q,\overline{N}}(q^2,\mu_R^2,\mu_F^2) = \bar{\tilde{g}}^q_0(q^2,\mu_R^2,\mu_F^2)\exp\Big(G^q_{\mathrm{SV},\overline{N}}(q^2,\omega) + \Psi^q_{\mathrm{NSV},\overline{N}}(q^2,\omega)\Big). \tag{38}$$

Here the $\bar{\tilde{g}}^q_0(q^2,\mu_R^2,\mu_F^2)$ are given by

$$\bar{\tilde{g}}^q_0(q^2,\mu_R^2,\mu_F^2) = C^q_0(q^2,\mu_R^2,\mu_F^2)\,\bar{g}^q_0(a_s(\mu_R^2)), \tag{39}$$

where $\overline{g}^q_0$ results from the N-independent part of the Mellin transformation of the distributions and the γ_E's are all absorbed into the $\overline{N}$-dependent functions. In doing so, the $\overline{N}$-dependent part of SV, i.e., $G^q_{\mathrm{SV},\overline{N}}$, is obtained by setting $\Psi^q_{\mathrm{SV},\overline{N}} - \ln\overline{g}^q_0 = 0$ when $\overline{N} = 1$. Hence, $G^q_{\mathrm{SV},\overline{N}}$ and $\Psi^q_{\mathrm{NSV},\overline{N}}$ are given by

$$G^q_{\mathrm{SV},\overline{N}} = g^q_1(\overline{\omega})\ln\overline{N} + \sum_{i=0}^{\infty} a_s^i(\mu_R^2)\; g^q_{i+2}(\overline{\omega}), \tag{40}$$

$$\Psi^q_{\mathrm{NSV},\overline{N}} = \frac{1}{N}\sum_{i=0}^{\infty} a_s^i(\mu_R^2)\Big(\bar{g}^q_{i+1}(\overline{\omega}) + h^q_i(\overline{\omega},\overline{N})\Big), \tag{41}$$

with

$$h^q_i(\overline{\omega},\overline{N}) = \sum_{k=0}^{i} h^q_{ik}(\overline{\omega})\;\ln^k\overline{N}. \tag{42}$$

The expansion parameter $\overline{\omega} = 2\beta_0 a_s(\mu_R^2)\ln\overline{N}$. Numerically, this can make difference at every logarithmic accuracy. For the SV, the perturbative convergence was shown to improve with $\overline{N}$ terms in [30]. We will address the impact of the same in NSV case in next section.

– Soft exponentiation: Another scheme one can adopt is the *Soft exponentiation*, where we exponentiate the complete finite part of soft-collinear function Φ_{q}. This includes the N-independent pieces arising after the Mellin transformation of $\Psi^q_{\mathscr{D}}$, along with the N-dependent ones which we used in Standard N-exponentiation. For this scheme the resummed result takes the form:

$$\Delta_{q,N}(q^2,\omega) = \tilde{g}^{q,\mathrm{Soft}}_0(q^2)\exp\Big(\Psi^{q,\mathrm{Soft}}_{\mathrm{SV},N}(q^2,\omega) + \Psi^q_{\mathrm{NSV},N}(q^2,\omega)\Big). \tag{43}$$

with

$$\Psi^{q,\mathrm{Soft}}_{\mathrm{SV},N}(q^2,\omega) = \ln N\; g^{q,\mathrm{Soft}}_1(\omega) + \sum_{i=0}^{\infty} a_s^i g^{q,\mathrm{Soft}}_{i+2}(q^2,\omega). \tag{44}$$

Here the complete finite part coming from the soft-collinear function is absorbed into the resummed exponents, which thereby gives rise to the exponents, $g^{q,\mathrm{Soft}}_i$. The remaining N-independent terms coming from finite part of form factor and AP kernels contribute to $\tilde{g}^{q,\mathrm{Soft}}_0$, whose expansion in powers of a_s is given as:

$$\tilde{g}^{q,\mathrm{Soft}}_0(q^2) = 1 + \sum_{i=1}^{\infty} a_s^i\;\tilde{g}^{q,\mathrm{Soft}}_{0i}(q^2). \tag{45}$$

The N-independent constants $\tilde{g}^{q,\mathrm{Soft}}_{0i}(q^2)$ and the resummed exponents $g^{q,\mathrm{Soft}}_i(\omega)$ are listed in Appendix E.

– All exponentiation: In light of (17), which came out as a consequence to the first-order differential equations satisfied by each of the building blocks results in an all-order exponential structure for $\Delta_{q,N}$. Hence it is natural to study the numerical impact of entire contribution taken in to Mellin space, which is done in *All exponentiation* scheme. The resummed result then takes the form:

$$\Delta_{q,N}(q^2,\omega) = \exp\Big(\Psi^{q,\mathrm{All}}_{\mathrm{SV},N}(q^2,\omega) + \Psi^q_{\mathrm{NSV},N}(q^2,\omega)\Big), \tag{46}$$

where

$$\Psi^{q,\mathrm{All}}_{\mathrm{SV},N}(q^2,\omega) = \ln N\; g^{q,\mathrm{All}}_1(q^2) + \sum_{i=0}^{\infty} a_s^i g^{q,\mathrm{All}}_{i+2}(q^2,\omega). \tag{47}$$

The resummed exponents $g^{q,\mathrm{All}}_i(\omega)$ contain both N-dependent and independent terms and are listed in Appendix F. This scheme was explored in [32,78] to study the inclusive cross section for the production of Higgs boson in gluon fusion at the LHC. For similar study for the DY in DIS and $\overline{\mathrm{MS}}$ schemes, see [102].

In [30], we had studied how various schemes discussed so far can affect the predictions of invariant mass distribution of lepton pairs, inclusive Z and $W^{\pm}$ production rates. In the present paper we extend this analysis in the presence of resummed NSV exponent and study the numerical impact

on the production of a pair of leptons in DY process at the LHC. At NNLO level, we have the contributions from all the channels. Our numerical predictions are based on fixed-order NNLO results for the CFs and on parton distribution functions known to NNLO accuracy. The resummed results are matched to the fixed-order result in order to avoid any double counting of threshold logarithms. The resummed result at a given accuracy, say $\overline{\text{N}^{\text{n}}\text{LL}}$, is computed by taking the difference between the resummed result and the same truncated up to order a_s^n. Hence, it contains contributions from the SV and NSV terms to all orders in perturbation theory starting from a_s^{n+1}:

$$\sigma_N^{\text{N}^{\text{n}}\text{LO}+\overline{\text{N}^{\text{n}}\text{LL}}} = \sigma_N^{\text{N}^{\text{n}}\text{LO}} + \sigma^{(0)} \times \sum_{ab\in\{q,\bar{q}\}} \int_{c-i\infty}^{c+i\infty} \frac{dN}{2\pi i}(\tau)^{-N} \delta_{a\bar{b}} f_{a,N}(\mu_F^2) f_{b,N}(\mu_F^2) \times \left(\Delta_{q,N}\Big|_{\overline{\text{N}^{\text{n}}\text{LL}}} - \Delta_{q,N}\Big|_{tr\ \text{N}^{\text{n}}\text{LO}} \right), \tag{48}$$

where σ_N is the Mellin moment of $d\sigma/dQ$. The Mellin space PDF ($f_{i,N}$) can be evolved using QCD-PEGASUS [103]. Alternatively, we use the technique described in [26,66] to directly deal with PDFs in the z-space. The contour c in the Mellin inversion can be chosen according to *Minimal prescription* [75] procedure. In the above (48) the second term represents the resummed result truncated to N^nLO order. To distinguish between SV and SV + NSV resummation, all along the paper, we denote the former by N^nLL and the latter by $\overline{\text{N}^{\text{n}}\text{LL}}$ for the n^{th} level logarithmic accuracy.

In Tables 1 and 2, we list the resummed exponents which are required to predict the tower of SV and NSV logarithms respectively in $\Delta_{q,N}$ at a given logarithmic accuracy. Let us first review the predictions for the SV logarithms which are already known in the literature [15,25–30]. As can be seen from Table 1, using the first set of resummed exponents $\{\tilde{g}^q_{0,0}, g^q_1\}$ which constitute to the SV-LL resummation, we can predict the highest SV logarithm of $\Delta^{(i)}_{q,N}$ at every order in a_s in perturbation theory, i.e, L_N^{2i} at the order a_s^i for all $i > 1$. Similarly using the second set of resummed exponents $\{\tilde{g}^q_{0,1}, g^q_2\}$ along with the first set, one can predict the next-to-highest SV logarithms to all orders, i.e., two towers of logarithms namely $\{L_N^{(2i-1)}, L_N^{(2i-2)}\}$ in $\Delta^{(i)}_{q,N}$ for all $i > 2$. These towers of logarithms belong to the SV-NLL resummation. In general, using the n-th set $\{\tilde{g}^q_{0,n}, g^q_{n+1}\}$ along with the previous sets, we can predict the highest $(2n+1)$ towers of SV-logarithms, at every order in a_s^i for all $i > n+1$ with $n = 0, 1, 2\ldots$ and these towers constitute to the SV-$\text{N}^{\text{n}}\text{LL}$ resummation.

Now let us turn to the predictions for NSV logarithms present in $\Delta_{q,N}$. From Table 2, we can see that the first set of resummed exponents $\{\tilde{g}^q_{0,0}, g^q_1, \overline{g}^q_1, h^q_0\}$ which contributes to the $\overline{\text{LL}}$ resummation, facilitates the prediction of highest NSV logarithms of $\Delta^{(i)}_{q,N}$ to all orders in perturbation theory, i.e, $L_N^{(2i-1)}$ at a_s^i for all $i > 1$. Furthermore, the second set of resummed exponents $\{\tilde{g}^q_{0,1}, g^q_2, \overline{g}^q_2, h^q_1\}$ along with the first set, predicts the next-to-highest NSV logarithms besides the highest NSV logarithms to all orders, namely the tower of $L_N^{(2i-2)}$ for $\Delta^{(i)}_{q,N}$ with $i > 2$. This tower of logarithms belongs to the $\overline{\text{NLL}}$ resummation. In general, using the n-th set $\{\tilde{g}^q_{0,n}, g^q_{n+1}, \overline{g}^q_{n+1}, h^q_n\}$ along with the previous sets, we can predict the highest $(n+1)$ towers of NSV logarithms at every order in a_s^i for all $i > n+1$ with $n = 0, 1, 2\ldots$. These $n+1$ towers of NSV logarithms constitute to the $\overline{\text{N}^{\text{n}}\text{LL}}$ resummation. In summary, the predictive nature of SV and NSV logarithms start to differ from next-to-leading logarithmic accuracy (which is NLL for SV and $\overline{\text{NLL}}$ for NSV) onwards. For the SV case, beyond LL accuracy, we can predict additional two towers of logarithms at each logarithmic accuracy to all orders in a_s. On the other hand, for the NSV case, only one additional tower of logarithms can be predicted at each logarithmic accuracy. This implies that the NSV resummation is less predictive compared to the SV counterpart, however this is the inherent property of the subleading logarithms present in the NSV part.

In the following, we expand the resummed results in power series in a_s at various logarithmic accuracy and compare them against the known fixed-order results in the literature. Prior to this, we compare our result at $\overline{\text{LL}}$ accuracy against that of [104]. In [104] , within the framework of soft-collinear effective theory (SCET), the authors have obtained leading logarithmic terms at NSV for the quark–antiquark production channel of the DY process to all orders in a_s. This was achieved by extending the factorisation properties of the cross section to NSV level and using renormalisation group equations of NSV operators and soft functions. Using our N-space result, in the $\overline{\text{LL}}$ approximation, we have

$$\Delta^{\overline{\text{LL}}}_{q,N} = \tilde{g}^q_{0,0} \exp\left[\ln N\ g^q_1(\omega) + \frac{1}{N}\left(\overline{g}^q_1(\omega) + h^q_0(\omega, N) \right) \right]. \tag{49}$$

After expanding the exponents in powers of a_s and keeping only terms of $\mathcal{O}(1/N)$, we obtain

$$\Delta^{\overline{\text{LL}}}_{q,N} = \exp\left[8C_F a_s \left(\ln^2 N + \frac{\ln N}{N} \right) \right]. \tag{50}$$

The above N-space result can be Mellin inverted to z-space and it reads as

$$\Delta^{\overline{\text{LL}}}_{q,z} = \Delta^{\text{LL}}_{q,SV} - 16\ C_F\ a_s \exp\left[8C_F a_s \ln^2(1-z) \right] \ln(1-z). \tag{51}$$

Table 1 The set of resummed exponents $\left\{\tilde{g}^q_{0,n}, g^q_n(\omega)\right\}$ which is required to predict the tower of SV logarithms in $\Delta_{q,N}$ at a given logarithmic accuracy. Here $L^j = \ln^j N$

GIVEN	PREDICTIONS – SV Logarithms							Logarithmic accuracy
Resummed exponents	$\Delta^{(2)}_{q,N}$	$\Delta^{(3)}_{q,N}$	$\Delta^{(4)}_{q,N}$	$\Delta^{(5)}_{q,N}$	$\Delta^{(6)}_{q,N}$	$\cdots$	$\Delta^{(i)}_{q,N}$	
$\tilde{g}^q_{0,0}, g^q_1$	L^4	L^6	L^8	L^{10}	L^{12}	$\cdots$	L^{2i}	LL
$\tilde{g}^q_{0,1}, g^q_2$		$\{L^5, L^4\}$	$\{L^7, L^6\}$	$\{L^9, L^8\}$	$\{L^{11}, L^{10}\}$	$\cdots$	$\{L^{2i-1}, L^{2i-2}\}$	NLL
$\tilde{g}^q_{0,2}, g^q_3$			$\{L^5, L^4\}$	$\{L^7, L^6\}$	$\{L^9, L^8\}$	$\cdots$	$\{L^{2i-3}, L^{2i-4}\}$	NNLL

Table 2 The set of resummed exponents $\left\{\tilde{g}^q_{0,n}, g^q_n(\omega), \overline{g}^q_n(\omega), h^q_n(\omega)\right\}$ which is required to predict the tower of NSV logarithms in $\Delta_{q,N}$ at a given logarithmic accuracy. Here $L^j_N = \ln^j N/N$

GIVEN	PREDICTIONS – NSV Logarithms							Logarithmic accuracy
Resummed exponents	$\Delta^{(2)}_{q,N}$	$\Delta^{(3)}_{q,N}$	$\Delta^{(4)}_{q,N}$	$\Delta^{(5)}_{q,N}$	$\Delta^{(6)}_{q,N}$	$\cdots$	$\Delta^{(i)}_{q,N}$	
$\tilde{g}^q_{0,0}, g^q_1, \overline{g}^q_1, h^q_0$	L^3_N	L^5_N	L^7_N	L^9_N	L^{11}_N	$\cdots$	$L^{(2i-1)}_N$	$\overline{\text{LL}}$
$\tilde{g}^q_{0,1}, g^q_2, \overline{g}^q_2, h^q_1$		L^4_N	L^6_N	L^8_N	L^{10}_N	$\cdots$	$L^{(2i-2)}_N$	$\overline{\text{NLL}}$
$\tilde{g}^q_{0,2}, g^q_3, \overline{g}^q_3, h^q_2$			L^5_N	L^7_N	L^9_N	$\cdots$	$L^{(2i-3)}_N$	$\overline{\text{NNLL}}$

The above result agrees exactly with Eq. (4.2) of [104] for $\mu = Q$.

Next, we expand the resummed expression at $\overline{\text{LL}}$ accuracy given in (50) up to a_s^4 (N^{4}LO) and compare the predictions for leading NSV logarithms against those from fixed-order predictions. Note that, as can be seen from Table 2, the $\overline{\text{LL}}$ resummation which comprises of only one loop anomalous dimensions and SV + NSV coefficients from fixed-order NLO results, predicts the leading logarithms $\frac{\ln^3 N}{N}$, $\frac{\ln^5 N}{N}$, $\frac{\ln^7 N}{N}$ etc at a_s^2 (NNLO), a_s^3 (N^{3}LO), a_s^4 (N^{4}LO) and so on respectively.

For example, at a_s^2 (NNLO), in N-space, we obtain

$$\Delta^{(2)}_{q,N}|_{\overline{\text{LL}}} = \Delta^{SV,(2)}_{q,N}|_{\text{LL}} + \frac{\ln^3 N}{N}\left\{64 C_F^2\right\}, \tag{52}$$

and the Mellin inverted result in z-space is

$$\Delta^{(2)}_{q,z}|_{\overline{\text{LL}}} = \Delta^{SV,(2)}_{q,z}|_{\text{LL}} - \ln^3(1-z)\left\{128 C_F^2\right\}. \tag{53}$$

The above predictions at NNLO level agrees with the known results obtained in [1–3]. Our prediction at a_s^3 (N^{3}LO) in N and z-spaces are

$$\begin{aligned}\Delta^{(3)}_{q,N}|_{\overline{\text{LL}}} &= \Delta^{SV,(3)}_{q,N}|_{\text{LL}} + \frac{\ln^5 N}{N}\left\{256 C_F^3\right\},\\ \Delta^{(3)}_{q,z}|_{\overline{\text{LL}}} &= \Delta^{SV,(3)}_{q,z}|_{\text{LL}} - \ln^5(1-z)\left\{512 C_F^3\right\},\end{aligned} \tag{54}$$

and are agreement with the results given in [58]. Now at a_s^4 (N^{4}LO), our predictions in N and z-spaces read as

$$\begin{aligned}\Delta^{(4)}_{q,N}|_{\overline{\text{LL}}} &= \Delta^{SV,(4)}_{q,N}|_{\text{LL}} + \frac{\ln^7 N}{N}\left\{\frac{2048}{3} C_F^4\right\},\\ \Delta^{(4)}_{q,z}|_{\overline{\text{LL}}} &= \Delta^{SV,(4)}_{q,z}|_{\text{LL}} + \ln^7(1-z)\left\{-\frac{4096}{3} C_F^4\right\},\end{aligned} \tag{55}$$

and are found to be in agreement with the results obtained using the physical evolution kernels (PEK) approach by Moch and Vogt in [37]. In all of the above expressions, we have set $\mu_R^2 = \mu_F^2 = q^2$.

We now consider the predictions of resummed result at $\overline{\text{NLL}}$ and $\overline{\text{NNLL}}$ up to order a_s^4. At $\overline{\text{NLL}}$, the resummed expression takes the following form

$$\begin{aligned}\Delta^{\overline{\text{NLL}}}_{q,N} = (\tilde{g}^q_{0,0} + a_s\, \tilde{g}^q_{0,1})\, \exp\Bigg[&\ln N\, g^q_1(\omega) + g^q_2(\omega)\\ &+ \frac{1}{N}\Big(\overline{g}^q_1(\omega) + a_s\, \overline{g}^q_2(\omega) + h^q_0(\omega, N) + a_s\, h^q_1(\omega, N)\Big)\Bigg],\end{aligned} \tag{56}$$

where the resummed exponents can be found in the Appendices C.5 and C.6. Note that at $\overline{\text{NLL}}$ accuracy, we require anomalous dimensions up to two loops and second order SV + NSV coefficients obtained from NNLO results. Expanding the resummed result in powers of a_s, we obtain the next-to leading logarithms $\frac{\ln^4 N}{N}$, $\frac{\ln^6 N}{N}$ etc at a_s^3 (N^{3}LO), a_s^4 (N^{4}LO) and so on respectively. At a_s^3 (N^{3}LO), in N

and z-spaces, the predictions are given below by setting $\mu_R^2 = \mu_F^2 = q^2$.

$$\begin{aligned}
\Delta_{q,N}^{(3)}|_{\overline{\rm NLL}} &= \Delta_{q,N}^{(3)}|_{\overline{\rm LL}} + \Delta_{q,N}^{SV,(3)}|_{\rm NLL} + \frac{\ln^4 N}{N}\Big\{\frac{3520}{9}C_A C_F^2 \\
&\quad - \frac{640}{9}C_F^2 n_f + \Big(448 + 1280\,\gamma_E\Big)C_F^3\Big\}, \\
\Delta_{q,z}^{(3)}|_{\overline{\rm NLL}} &= \Delta_{q,z}^{(3)}|_{\overline{\rm LL}} + \Delta_{q,z}^{SV,(3)}|_{\rm NLL} + \ln^4(1-z)\Big\{\frac{7040}{9}C_A C_F^2 \\
&\quad - \frac{1280}{9}C_F^2 n_f + 1728 C_f^3\Big\}, \qquad (57)
\end{aligned}$$

where γ_E is the Euler–Mascheroni constant which arises due to the Mellin transformation in N-space. The above prediction agrees with the fixed-order result at order a_s^3 given in [58]. The predictions at a_s^4 (N^{4}LO) in N and z-spaces are as follows

$$\begin{aligned}
\Delta_{q,N}^{(4)}|_{\overline{\rm NLL}} &= \Delta_{q,N}^{(4)}|_{\overline{\rm LL}} + \Delta_{q,N}^{SV,(4)}|_{\rm NLL} \\
&\quad + \frac{\ln^6 N}{N}\Big\{\frac{19712}{9}C_A C_F^3 \\
&\quad - \frac{3584}{9}C_F^3 n_f + \Big(1792 + \frac{14336}{3}\,\gamma_E\Big)C_F^4\Big\}, \\
\Delta_{q,z}^{(4)}|_{\overline{\rm NLL}} &= \Delta_{q,z}^{(4)}|_{\overline{\rm LL}} + \Delta_{q,z}^{SV,(4)}|_{\rm NLL} \\
&\quad + \ln^6(1-z)\Big\{\frac{39424}{9}C_A C_F^3 \\
&\quad - \frac{7168}{9}C_F^3 n_f + \frac{19712}{3}C_F^4\Big\}, \qquad (58)
\end{aligned}$$

where we have set $\mu_R^2 = \mu_F^2 = q^2$. The above predictions at a_s^4 are found to be in agreement with the results computed using the physical evolution kernels (PEK) approach in [37].

Finally, using the $\overline{\rm NNLL}$ resummation, which further embeds the three loop anomalous dimensions and third order SV + NSV coefficients obtained from N^{3}LO results, we predict the next-to-next-to leading logarithms $\frac{\ln^5 N}{N}$ at a_s^4 (N^{4}LO), $\frac{\ln^7 N}{N}$ at a_s^5 (N^{5}LO) and so on. The resummed expression at $\overline{\rm NNLL}$ accuracy is given by

$$\begin{aligned}
\Delta_{q,N}^{\overline{\rm NNLL}} &= (\tilde{g}_{0,0}^q + a_s\,\tilde{g}_{0,1}^q + a_s^2\,\tilde{g}_{0,2}^q)\,\exp\Big[\ln N\, g_1^q(\omega) \\
&\quad + g_2^q(\omega) + a_s\, g_3^q(\omega) + \frac{1}{N}\Big(\overline{g}_1^q(\omega) + a_s\,\overline{g}_2^q(\omega) \\
&\quad + a_s^2\,\overline{g}_3^q(\omega) + h_0^q(\omega, N) + a_s\, h_1^q(\omega, N) \\
&\quad + a_s^2\, h_2^q(\omega, N)\Big)\Big]. \qquad (59)
\end{aligned}$$

The prediction for the next-to-next-to leading logarithm $\frac{\ln^5 N}{N}$ at a_s^4 (N^{4}LO) in N and z-spaces is provided below

$$\begin{aligned}
\Delta_{q,N}^{(4)}|_{\overline{\rm NNLL}} &= \Delta_{q,N}^{(4)}|_{\overline{\rm NLL}} + \Delta_{q,N}^{SV,(4)}|_{\rm NNLL} \\
&\quad + \frac{\ln^5 N}{N}\Big\{\frac{61952}{27}C_F^2 C_A^2 \\
&\quad + \Big(\frac{296192}{27} + \frac{39424}{3}\gamma_E - 1536\zeta_2\Big)C_F^3 C_A \\
&\quad + \Big(-4992 + 10752\gamma_E + 14336\gamma_E^2 + 4096\zeta_2\Big)C_F^4 \\
&\quad - \frac{22528}{27}n_f C_F^2 C_A + \Big(\frac{-51968}{27} - \frac{7168}{3}\gamma_E\Big)n_f C_F^3 \\
&\quad + \frac{2048}{27}n_f^2 C_F^2\Big\}, \\
\Delta_{q,z}^{(4)}|_{\overline{\rm NNLL}} &= \Delta_{q,z}^{(4)}|_{\overline{\rm NLL}} + \Delta_{q,z}^{SV,(4)}|_{\rm NNLL} \\
&\quad + \ln^5(1-z)\Big\{-\frac{123904}{27}C_F^2 C_A^2 - \Big(\frac{805376}{27} \\
&\quad - 3072\zeta_2\Big)C_F^3 C_A + \Big(9088 + 20480\zeta_2\Big)C_F^4 \\
&\quad + \frac{45056}{27}n_f C_F^2 C_A + \frac{139520}{27}n_f C_F^3 - \frac{4096}{27}n_f^2 C_F^2\Big\}, \qquad (60)
\end{aligned}$$

where we have set $\mu_R^2 = \mu_F^2 = q^2$. The above predictions at a_s^4 agree with those of [37] predicted using physical evolution equations. In the next section we present the numerical results of our predictions along with the scale uncertainties for the neutral DY process at the LHC.

4 Phenomenology

In this section, we perform a detailed numerical study on the impact of resummed soft virtual plus next-to-soft virtual (SV + NSV) results for the production of di-leptons in neutral DY process at the LHC. We include all the partonic channels at the Fixed-order (FO) up to NNLO with off-shell photon and Z boson intermediate states. We restrict ourselves to center of mass energy of 13 TeV at the LHC, however our analysis can be extended to other energies as well as to other colliders. We use the following electro-weak parameters for the vector boson masses and widths, Weinberg angle (θ_w) and the fine structure constant (α):

$$\begin{aligned}
&m_Z = 91.1876\ \text{GeV}, \quad \Gamma_Z = 2.4952\ \text{GeV}, \\
&\sin^2\theta_w = 0.22343, \quad \alpha = 1/128. \qquad (61)
\end{aligned}$$

The parton distribution functions are directly taken from the `lhapdf` [105] routine. All results are obtained using the `MMHT2014` [106] parton densities throughout. The strong coupling constant is evolved to the renormalisation scale μ_R using the three-loop QCD beta function in the $\overline{\rm MS}$-scheme with $n_f = 5$ active massless quark flavours.

We begin with a discussion on the relative contributions of SV and NSV terms in the fixed-order results at the hadronic level. We carry out this analysis in N-space as the resum-

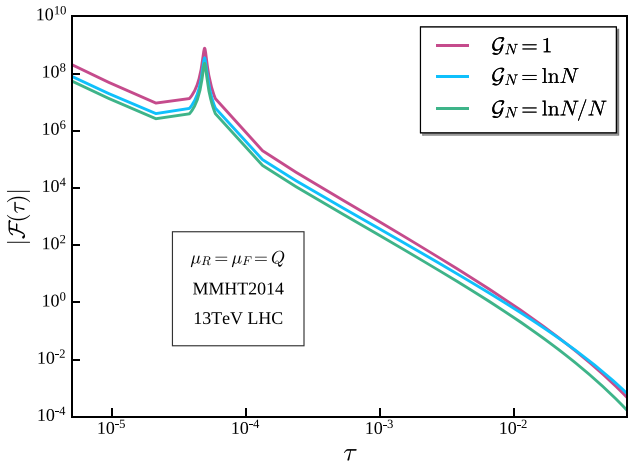

Fig. 1 Variation of SV and NSV functions with respect to $\tau = Q^2/S$

mation is performed in the N-space. The partonic coefficient function, Δ_q given in (16), comprises of functions namely, SV distributions, $\{\delta(1-z), \mathscr{D}_k(z)\}$ and NSV logarithms, $\ln^k(1-z)$ in z-space. After performing the Mellin transformation on Δ_q, the SV distributions and NSV logarithms transform to $\{1, \ln^k N, \frac{\ln^k N}{N}\}$ in the Mellin N-space. Here, '1' stands for the Mellin moment of the SV distribution $\delta(1-z)$. Before we present the corresponding contributions of SV and NSV terms to hadronic cross sections, we plot the following integral as a function of τ:

$$\mathscr{F}(\tau) = \int_\tau^1 \frac{dz}{z} \tilde{\Phi}_{q\bar{q}}\left(\frac{\tau}{z}\right) \mathscr{M}^{-1}[\mathscr{G}(N)],$$
$$\text{where} \quad \mathscr{G}(N) = \left\{1, \ln N, \frac{\ln N}{N}\right\}. \tag{62}$$

In the above expression, $\mathscr{M}^{-1}$ stands for the Mellin inversion. The plot given in Fig. 1 demonstrates the hierarchical behaviour of the terms in the threshold expansion at the numerical level, in particular, it reflects to the fact that at the threshold, $\mathscr{F}$ gets larger contribution from the SV terms $\{1, \ln N\}$ as compared to the subleading $\frac{\ln N}{N}$ terms. This hierarchy remains the same when the corresponding coefficients from the perturbative results of CFs are taken into account along with these functions. This is shown in Table 3 for $\Delta_q^{(2)}$, i.e., at NNLO, we find that the SV logarithms contribute to 34.5% of the Born contribution, whereas the NSV distributions give 7.87% in N-space. We notice that this trend is same at other known orders too. For example at NLO, the total SV contributions amount to 22% whereas NSV gives rise to a total of 6% of the Born contribution in N-space for $Q = 200$ GeV. Similarly Table 4 shows the contributions from SV and NSV logarithms at the N^{3}LO level. Although the contribution of NSV logarithms is subdominant to the SV counterpart in N-space up to N^{3}LO, it is still numerically sizeable and hence cannot be ignored.

Table 3 % contribution of SV distributions and NSV logarithms to the Born cross section at NNLO for $Q = 200$ GeV

$Q = \mu_R = \mu_F$ (GeV)	SV		NSV	
200	$\ln^4 N$	0.0144%	$\frac{\ln^4 N}{N}$	0%
	$\ln^3 N$	0.125%	$\frac{\ln^3 N}{N}$	0.05%
	$\ln^2 N$	2.70%	$\frac{\ln^2 N}{N}$	0.392%
	$\ln N$	6.07%	$\frac{\ln N}{N}$	4.08%
	$\ln^0 N$	17.7%	$\frac{1}{N}$	3.35%
Total		34.5%		7.87%

Table 4 % contribution of SV distributions and NSV logarithms to the Born cross section at N^{3}LO for $Q = 200$ GeV

$Q = \mu_R = \mu_F$ (GeV)	SV		NSV	
200	$\ln^6 N$	− 0.0025%	$\frac{\ln^6 N}{N}$	0%
	$\ln^5 N$	− 0.001%	$\frac{\ln^5 N}{N}$	0.0004%
	$\ln^4 N$	0.0244%	$\frac{\ln^4 N}{N}$	0.006%
	$\ln^3 N$	0.171%	$\frac{\ln^3 N}{N}$	0.1%
	$\ln^2 N$	2.85%	$\frac{\ln^2 N}{N}$	0.56%
	$\ln N$	6.23%	$\frac{\ln N}{N}$	4.31%
	$\ln^0 N$	18.3%	$\frac{1}{N}$	3.30%
Total		27.6%		8.28%

Having studied the numerical relevance of subleading NSV logarithms in the fixed-order results, we now turn to assess the impact of their resummation on the cross sections. Besides the theoretical motivation of resumming the large enhancements arising from these logarithms, it would be interesting to see how phenomenologically important the resummed NSV logarithms are, in addition to the well established SV resummation for the Drell–Yan cross section. We begin the analysis by addressing the following questions:

- In comparison to the fixed-order corrections, how large are the SV + NSV resummed effects on the cross sections?
- How do the resummed NSV terms change the predictions of SV resummed result?
- What are the impacts of different schemes on the SV + NSV resummation?

We will discuss each of these questions in great detail in subsequent sections. To begin with, let us look at the impact of SV + NSV resummed results in comparison to the fixed-order results, which is the topic of the next section.

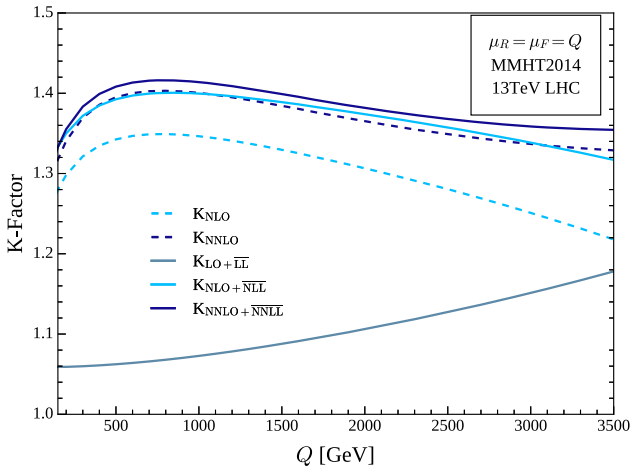

Fig. 2 K-factors till NNLO + $\overline{\text{NNLL}}$ level at the central scale $Q = \mu_R = \mu_F$

4.1 Fixed-order vs resummed results

In the following we study how the inclusion of SV+NSV resummation modifies the predictions from fixed-order results for inclusive DY di-lepton pair production. For this purpose, we get the matched predictions by appropriately including the leading, the next-to-leading and the next-to-next-to-leading resummed results with the corresponding fixed-order results. By investigating how sensitive is the SV + NSV resummed cross section to the choices of factorisation (μ_F) and renormalisation (μ_R) scales, we study their perturbative uncertainties. The quantitative impact of higher order effects can be obtained using "K-factor" defined by

$$\mathrm{K}(Q) = \frac{\frac{d\sigma}{dQ}(\mu_R = \mu_F = Q)}{\frac{d\sigma^{\mathrm{LO}}}{dQ}(\mu_R = \mu_F = Q)} \tag{63}$$

where we have set renormalisation (μ_R) and factorisation (μ_F) scales at Q. The K-factor for NLO + $\overline{\text{NLL}}$ and NNLO+$\overline{\text{NNLL}}$ are depicted in Fig. 2 along with the corresponding fixed-order ones.

In Table 5 we present the K factors resulting from both fixed as well as resummed contributions at three different values of Q, namely $Q = 500, 1000, 2000$ GeV. We find that there is an increment of $\{39.5\%, 36.5\%\}$ in the cross section when we go from LO to NNLO for the Q values $\{500, 2000\}$ GeV respectively. The inclusion of the resummed results, for the same values of Q, increases, the LO by $\{6.2\%, 10.62\%\}$ when we include $\overline{\text{LL}}$, the NLO by $\{3.7\%, 5.2\%\}$ due to $\overline{\text{NLL}}$ and the NNLO by $\{0.94\%, 1.2\%\}$ due to $\overline{\text{NNLL}}$. This is reflected in Fig. 2, where the resummed curves can be found to lie above their corresponding fixed-order ones signifying the enhancement due to the resummed corrections.

Interestingly, we can also see from Table 5, that the K factors at NLO + $\overline{\text{NLL}}$ are closer to those of NNLO hinting that $\overline{\text{NLL}}$ from quark part mimics the contributions from entire second order. The resummed curves at NLO + $\overline{\text{NLL}}$ and NNLO + $\overline{\text{NNLL}}$ are closer compared to the fixed-order ones, namely NLO and NNLO. This accounts for the fact that the addition of resummed effect improves the reliability of perturbative predictions. The K factors at NNLO and NNLO + $\overline{\text{NNLL}}$ are more closer than those at NLO and NLO + $\overline{\text{NLL}}$. This is attributed to the fact that the resummed correction decreases as we go for higher order resummed contributions.

7-point scale uncertainties of the resummed results

Both fixed-order as well as resummed results contain renormalisation and factorisation scales which are unphysical. We now turn to assess the impact of these scales on our predictions. The dependence on these scales quantifies the corresponding errors due to their presence. The standard approach to estimate this error is to use the canonical 7-point variation, where $\mu = \{\mu_F, \mu_R\}$ is varied in the range $\frac{1}{2} \leq \frac{\mu}{Q} \leq 2$, keeping the ratio μ_R/μ_F not larger than 2 and smaller than 1/2.

The left panel of Fig. 3 contains the invariant mass distributions obtained using fixed-order CFs as a function of τ and the bands are due to 7-point scale variation, while the right panel is obtained using resummed results at various logarithmic accuracy. We find that the width of the resummed band at NLO + $\overline{\text{NLL}}$ is lesser than that of the corresponding fixed-order ones from $Q = 1000$ GeV onwards but the width of the NNLO+$\overline{\text{NNLL}}$ doesn't show much improvement against the fixed-order ones. The reason for this large scale uncertainty can be attributed to the fact that the resummed predictions lack the off-diagonal counter part. We will discuss more on this point in detail in subsequent analysis while considering the effect of both the scales independently.

In Table 6 we quote both fixed-order and resummed predictions at various logarithmic accuracies along with asymmetric errors resulting from 7-point scale variation for two values of Q, namely $Q = 1000$ GeV and $Q = 2000$ GeV. We find that there is a systematic enhancement of the cross sections as we increase the order of perturbation. For example, there is an increment of 24.2% when going from LO + $\overline{\text{LL}}$ to NLO + $\overline{\text{NLL}}$ accuracy, which further improves by 0.58% at NNLO + $\overline{\text{NNLL}}$ for $Q = 2000$ GeV. In addition, the scale uncertainty gets reduced significantly while going from LO + $\overline{\text{LL}}$ to NNLO + $\overline{\text{NNLL}}$. This is also reflected in Fig. 3 (right panel), where one finds the uncertainty band of NNLO + $\overline{\text{NNLL}}$ is contained within the NLO + $\overline{\text{NLL}}$ band throughout the considered Q-range. This was not the case for the fixed-order predictions, where NNLO band was found to differ from the NLO one at high energies. This hints

Table 5 The K-factor values for resummed result in comparison to the fixed-order ones

$\mu_R = \mu_F = Q$(GeV)	LO + $\overline{\text{LL}}$	NLO	NLO + $\overline{\text{NLL}}$	NNLO	NNLO + $\overline{\text{NNLL}}$
500	1.0624	1.3425	1.3925	1.3950	1.4082
1000	1.0728	1.3464	1.3995	1.4004	1.4138
2000	1.1062	1.3064	1.3739	1.3652	1.3818

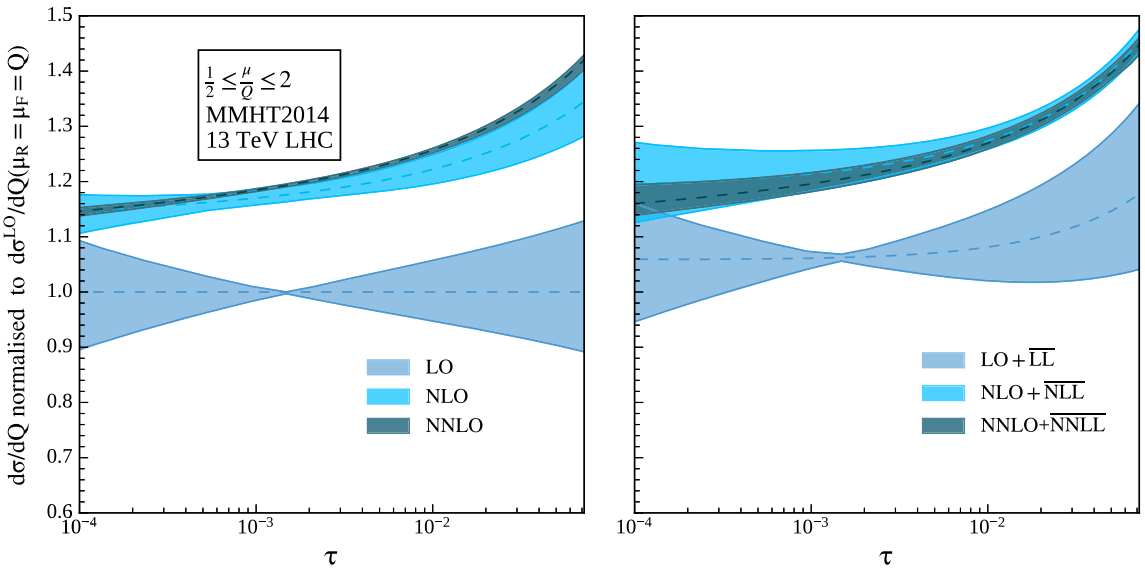

Fig. 3 7-point scale variation of the resummed result against fixed-order around the central scale choice $(\mu_R, \mu_F) = (1, 1)Q$ for 13 TeV LHC. The dashed lines refer to the corresponding central scale $Q = \mu_R = \mu_F$ at each order

Table 6 Values of resummed cross section in 10^{-5} pb/GeV at various orders in comparison to the fixed-order results at different central scales $Q = \mu_R = \mu_F = 1000$ and 2000 GeV for 13 TeV LHC

Q	LO	LO + $\overline{\text{LL}}$	NLO	NLO + $\overline{\text{NLL}}$	NNLO	NNLO + $\overline{\text{NNLL}}$
1000	$2.3476^{+4.10\%}_{-3.92\%}$	$2.5184^{+4.49\%}_{-4.25\%}$	$3.1609^{+1.79\%}_{-1.69\%}$	$3.2857^{+2.08\%}_{-1.18\%}$	$3.2876^{+0.20\%}_{-0.31\%}$	$3.3191^{+1.13\%}_{-0.86\%}$
2000	$0.0501^{+8.50\%}_{-7.46\%}$	$0.0554^{+9.10\%}_{-7.91\%}$	$0.0654^{+2.83\%}_{-2.98\%}$	$0.0688^{+1.43\%}_{-1.23\%}$	$0.0684^{+0.37\%}_{-0.62\%}$	$0.0692^{+0.89\%}_{-0.78\%}$

to the notable NSV contributions coming from the resummation effects in diagonal channels. These conclusions might change if we include resummed effects from off-diagonal channels which are currently not available.

In the above analysis, fixed-order results used for the numerical predictions contained all the partonic channels while the resummed contributions are only from quark anti-quark initiated channels. In the absence of resummed contributions, under the 7-point scale variations, the scale dependence is expected to go down as we increase the order of perturbation. However, this may not be the case if we include resummed effects only in quark anti-quark initiated channels. The quark gluon and gluon gluon initiated channels are also important as they contribute significantly to the cross section and more importantly they improve the stability of perturbative predictions under the scale variations. In order to understand the role of these partonic contributions, we drop them in the previous analysis restricting to quark anti-quark initiated contributions and then compare the outcomes given in Fig. 4 and in Table 7 against Fig. 3 and the Table 6. We find that there is a systematic enhancement of 28.19% when going from LO + $\overline{\text{LL}}$ to NLO$_{q\bar{q}}$ + $\overline{\text{NLL}}$ and 2.08% from NLO$_{q\bar{q}}$ + $\overline{\text{NLL}}$ to NNLO$_{q\bar{q}}$ + $\overline{\text{NNLL}}$ for $Q = 2000$ GeV. These increments are more compared to those in the case where all the channels are included in the fixed-order part. This stems from the fact that the cancellation which results due to the inclusion of other channels, in particular the qg-channel, is not considered here. As a result of which the error bands in Fig. 4 of NNLO$_{q\bar{q}}$ + $\overline{\text{NNLL}}$ is wider than that of NLO$_{q\bar{q}}$ + $\overline{\text{NLL}}$ in comparison to the resummed curves shown in Fig. 3 (left panel).

Hence in the 7-point variation, we find that the resummed result shows a systematic enhancement of the cross section as well as reduction of the uncertainties with the inclusion of each logarithmic corrections. But the scale uncertainties of the resummed result shows much improvement at the NLO+

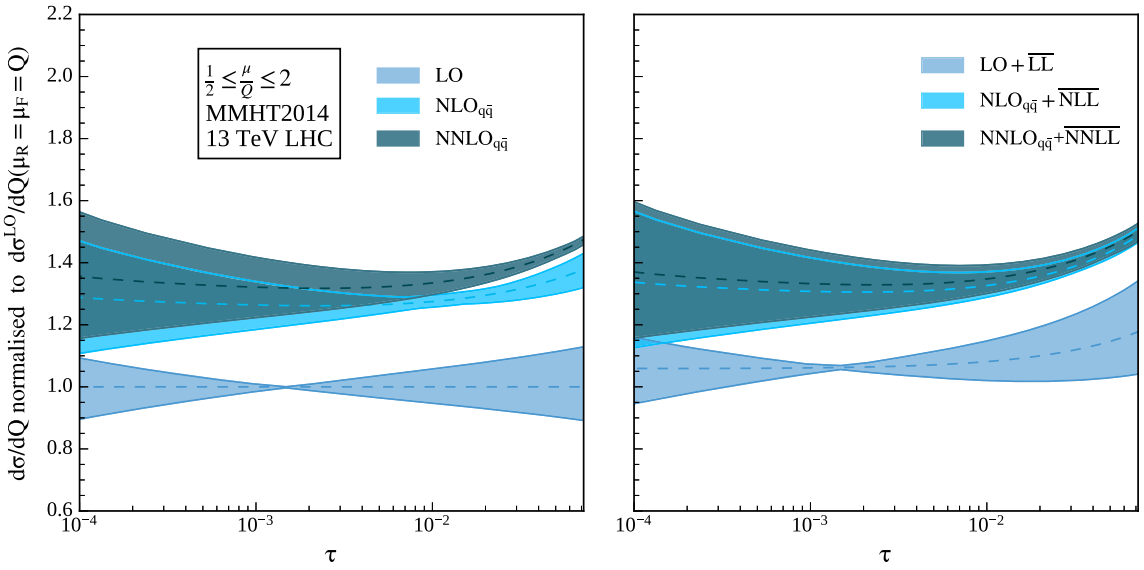

Fig. 4 7-point scale variation of the resummed result against fixed-order around the central scale choice $(\mu_R, \mu_F) = (1, 1)Q$ for $q\bar{q}$ channel

Table 7 Values of resummed cross section at various orders in comparison to the fixed-order results in 10^{-5} pb/GeV for $q\bar{q}$ channel at different central scales $Q = \mu_R = \mu_F = 1000$ and 2000 GeV for 13 TeV LHC

$Q = \mu_R = \mu_F$(GeV)	$NLO_{q\bar{q}}$	$NLO_{q\bar{q}} + \overline{NLL}$	$NNLO_{q\bar{q}}$	$NNLO_{q\bar{q}} + \overline{NNLL}$
1000	$3.3204^{+1.91\%}_{-2.00\%}$	$3.4452^{+4.18\%}_{-3.71\%}$	$3.5260^{+3.46\%}_{-3.63\%}$	$3.5576^{+4.16\%}_{-4.24\%}$
2000	$0.0676^{+1.65\%}_{-2.17\%}$	$0.07102^{+2.33\%}_{-1.71\%}$	$0.0717^{+1.63\%}_{-1.76\%}$	$0.0725^{+2.37\%}_{-2.47\%}$

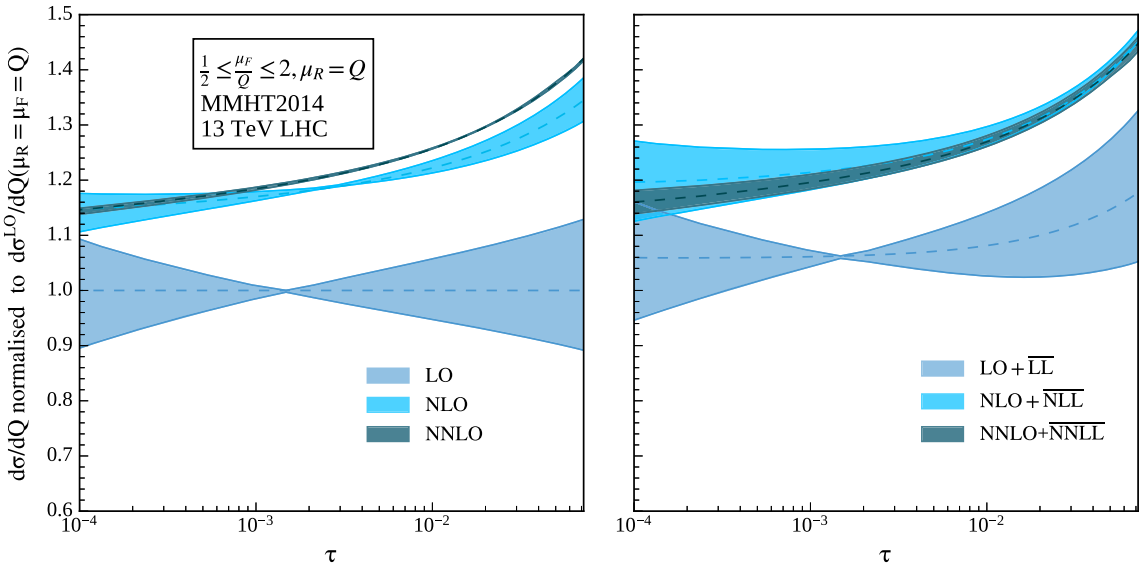

Fig. 5 μ_F scale variation of the resummed results against the fixed-order with the scale μ_R held fixed at Q for 13 TeV LHC

$\overline{\text{NLL}}$ than at the NNLO + $\overline{\text{NNLL}}$ level. To understand this and also the cause of the uncertainties better we now turn to analyze the effect of each scale individually on the resummed result.

Uncertainties of the resummed results with respect to μ_R and μ_F

So far, we have studied the importance of both fixed-order as well as resummed contributions using the K factor and the uncertainties arising from unphysical scales μ_R and μ_F. The numbers in the Table 5 demonstrate the importance of not only the fixed-order contributions but also the effects coming from the resummed ones. The resummed results comprises of both SV and NSV logarithms and the importance of large coefficients of the NSV terms was illustrated for the case of fixed-order corrections in Table 3. From the analysis of 7-point variation, we have shown that inclusion of leading, next-to-leading and next-to-next-to-leading collinear logarithms, in addition to the SV distributions, from the $q\bar{q}$ channel, to all orders in perturbation theory through resummation significantly enhances the cross section. But this enhancement comes with a price, namely the uncertainties resulting from unphysical scales. As we have seen in Fig. 3 that while the width of the resummed band at NLO + $\overline{\text{NLL}}$ is less than that of the corresponding fixed-order ones from $Q = 1000$ GeV onwards, the width of the NNLO + $\overline{\text{NNLL}}$ doesn't show much improvement even at higher values of Q as against the fixed-order result. In order to understand the reason behind this we aim to study the impact of the two scales separately. This is our next task.

The dependence of the cross section on μ_F is plotted in Fig. 5, as a function of τ with μ_R held fixed at Q. The bands are obtained by varying the scale μ_F by a factor of two up and down around the central scale $\mu_R = \mu_F = Q$. Here, the resummed bands look similar to that of Fig. 3 (right panel), however the width of NLO + $\overline{\text{NLL}}$ and NNLO + $\overline{\text{NNLL}}$ bands become slightly thinner as compared to the 7-point scale variation. This suggest that the contribution to the width of the bands in Fig. 3 mainly comes from the uncertainties arising from the μ_F variations. For instance, the uncertainty at NLO + $\overline{\text{NLL}}$ with respect to μ_F variation is $^{+1.44\%}_{-0.52\%}$ whereas the uncertainties arising from the 7-point variation is $^{+1.43\%}_{-1.23\%}$ for $Q = 2000$ GeV. Similarly at NNLO + $\overline{\text{NNLL}}$, the uncertainty arising from μ_F variation is $^{+0.79\%}_{-0.63\%}$ and from 7-point variation is $^{+0.89\%}_{-0.78\%}$ for the same value of Q. Now let us compare the μ_F uncertainty of the resummed result with respect to their fixed-order. We find that the width of the NLO band decreases with the inclusion of $\overline{\text{NLL}}$ from $Q = 1600$ GeV on wards. But the μ_F uncertainty for NNLO increases at NNLO + $\overline{\text{NNLL}}$. The reason behind this stems from the contribution coming from qg-channel. The one-loop correction from the $q\bar{q}$-channel is 22.09% of the NLO cross section, whereas the correction at the same order from the qg-channel is about −5.04% of the NLO cross section. Now at NLO + $\overline{\text{NLL}}$, we sum up the collinear logarithms from the diagonal channel which is also the dominating channel at NLO and hence the improvement through resummation. But the scenario is different at NNLO level. The a_s^2 corrections from $q\bar{q}$ and qg-channel contribute to 4.86% and −2.47% respectively to the NNLO cross section along with the other sub-dominating channels. However the sources of collinear logarithms at the threshold limit is only from $q\bar{q}$ and qg-channels. Hence at NNLO there is a bigger cancellation between $q\bar{q}$ and qg-channels than that at NLO. The cancellation at NNLO + $\overline{\text{NNLL}}$ is not matched due to the unavailability of the qg resummed collinear logarithms. Thus the μ_F variation in Fig. 5 reflects the role of the other channels and the need for qg resummation for betterment of the result.

Let us try to understand why the inclusion of resummed contributions in quark gluon initiated channels is important. Note that in the above analysis, we had taken all the partonic channels for the fixed-order part and only quark anti-quark initiated channels for the resummed part. We found that in the fixed-order, the μ_F dependence from the PDFs and from quark anti-quark initiated as well as from the quark-gluon initiated processes are expected to compensate each other according to renormalisation group equation with respect to factorisation scale. However, in the resummed part, this will not happen due the absence of resummed quark gluon counter part and this is the reason why one gets larger μ_F dependence in the predictions at NNLO + $\overline{\text{NNLL}}$ level. A symmetric analysis where we keep only quark anti-quark initiated channels both in fixed and resummed contributions can demonstrate this better and hence the Fig. 6. As one can see easily, the bands in both fixed-order and resummed predictions are wider compared to those in the Fig. 5 indicating the importance of quark gluon initiated channel both in fixed as well as resummed parts.

Figure 7 shows the dependence of the cross section on μ_R keeping μ_F fixed at Q. The bands are obtained by varying the scale μ_R by a factor of two up and down around the central scale $\mu_R = \mu_F = Q$. We observe that at NNLO + $\overline{\text{NNLL}}$ the error band becomes substantially thinner as compared to Fig. 5. This is because each partonic channel is invariant under μ_R variation when taken to all orders and hence inclusion of more corrections within a channel is expected to reduce the uncertainty. We find that the μ_R uncertainty at NLO + $\overline{\text{NLL}}$ ranges between $^{+1.35\%}_{-1.23\%}$ whereas for NLO it is between $^{+1.46\%}_{-1.28\%}$ for $Q = 2000$ GeV. And at NNLO + $\overline{\text{NNLL}}$ the uncertainty is found to be $^{+0.02\%}_{-0.23\%}$ and for NNLO it is $^{+0.37\%}_{-0.46\%}$ for the same value of Q. Hence from Fig. 7 one can see that μ_R dependence goes down for $Q = 800$ GeV on wards.

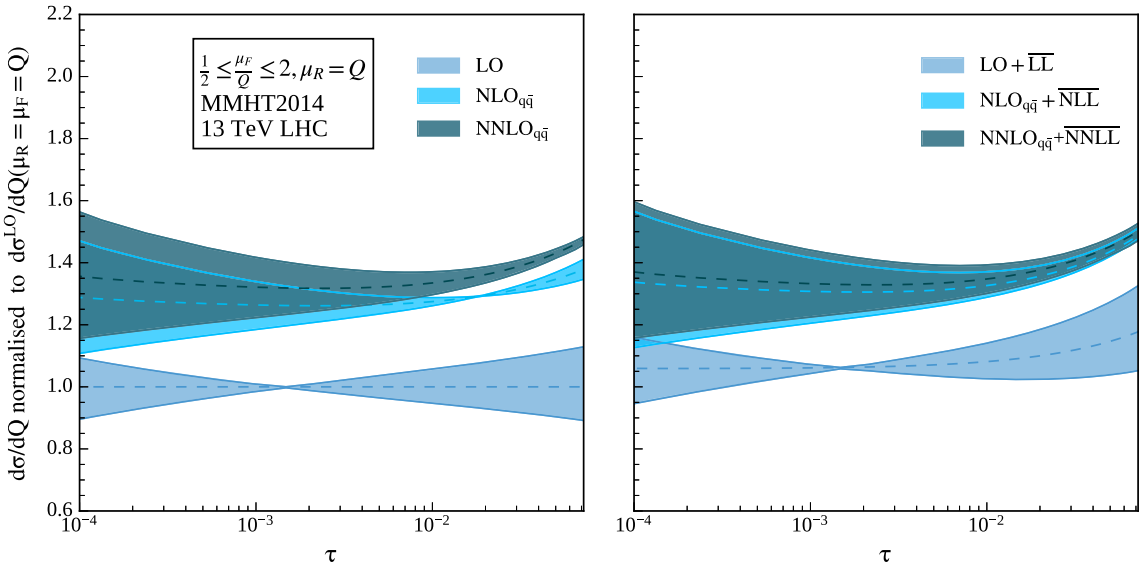

Fig. 6 μ_F scale variation of the resummed results against the fixed-order with the scale μ_R held fixed at Q for $q\bar{q}$-channel for 13 TeV LHC

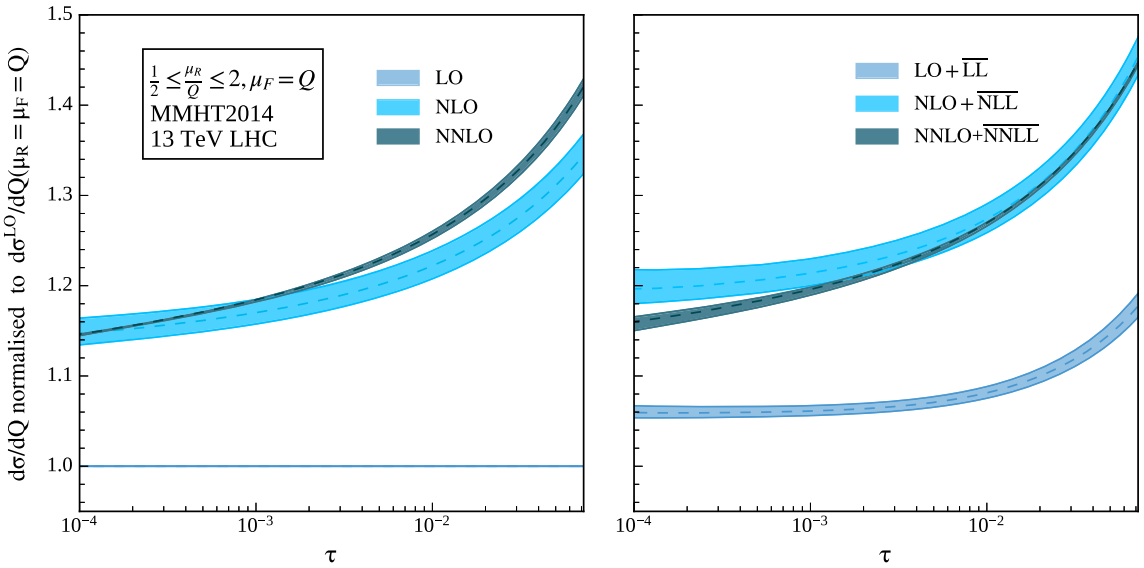

Fig. 7 μ_R scale variation of the resummed results against the fixed-order with the scale μ_F held fixed at Q for 13 TeV LHC

Since different partonic channels do not mix under the variation of μ_R, the symmetric analysis of keeping only quark anti-quark initiated channels will have similar behaviour as that of the case where other partonic channels are included in the fixed-order, which is given in Fig. 8. The μ_R uncertainty is significantly decreased as we go from NLO to NLO + $\overline{\text{NLL}}$ to NNLO to NNLO + $\overline{\text{NNLL}}$. We find the uncertainty at NNLO $^{+0.48\%}_{-0.57\%}$ gets improved to $^{+0.006\%}_{-0.20\%}$ for $Q = 1000$ GeV. And this improvement continues to grow even for higher values of Q. Therefore the inclusion of resummed result reduces the μ_R uncertainly remarkably as compared to the fixed-order ones.

Hence in conclusion to this section, we find that the uncertainty, which earlier manifested in the 7-point variation, shown in Fig. 3, was largely due to the μ_F uncertainty. Now as we know that different partonic channels mix under the variation of factorisation scale μ_F and so any uncertainty arising due to its variation only hints towards the "uncompensated" contributions from other channels. The fact that the resummed result at NLO + $\overline{\text{NLL}}$ shows improvement as compared to the fixed-order, emphasizes the importance of the resummed NSV logarithms. Similarly at the NNLO + $\overline{\text{NNLL}}$ level the large cancellation between different channels, mainly $q\bar{q}$ and qg, equally hints towards the importance of the collinear logarithms of the qg channel. Similarly for the μ_R variation, where the dependency is supposed to get better with the inclusion of more corrections within a

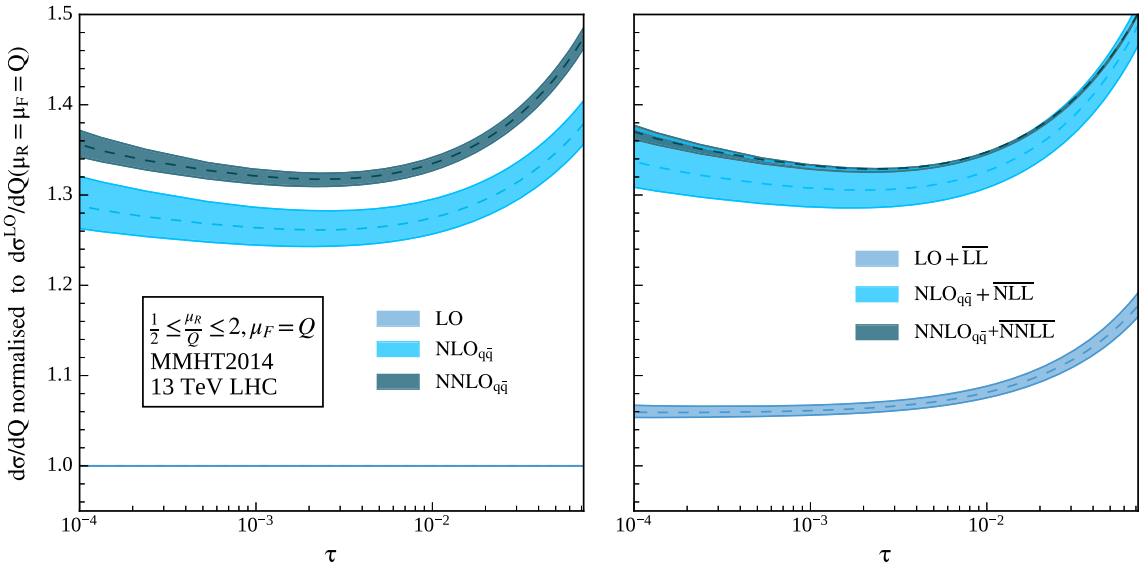

Fig. 8 μ_R scale variation of the resummed results against the fixed-order with the scale μ_F held fixed at Q for $q\bar{q}$-channel for 13 TeV LHC

partonic channel, we see a substantial improvement due to SV + NSV resummation in comparison to the fixed-order result. But now that we have seen the effect of the combined resummed result on the fixed-order let us analyze which part of the SV + NSV resummation, i.e., whether its the resummation of the distribution or of the NSV logarithms, plays the dominant role in any kind of improvement discussed so far.

4.2 SV resummation vs SV + NSV resummation

In the earlier section we have made a quantitative comparison of SV + NSV resummed results against the fixed-order ones. We found that there is a significant enhancement of the cross section and the μ_R scale uncertainty gets substantially improved with the inclusion of the resummed corrections. We also found that the uncertainties related to the μ_F variation shows betterment at NLO + $\overline{\text{NLL}}$ for higher Q values but not at the NNLO+$\overline{\text{NNLL}}$ level. Now, in this section we turn to a detailed analysis on the inclusion of NSV resummation over SV resummation so as to estimate the effect of resummed collinear logarithms from the $q\bar{q}$-channel.

We begin with the K-factor, which is presented in Table 8, to examine the impact of resummed NSV logarithms. Keeping all the partonic channels in the fixed-order, we find that the inclusion of the resummed NSV logarithms enhances the SV resummed corrections significantly throughout the considered Q range. In particular, for $Q = 2000$ GeV, there is a considerable amount of increment of 2.08% when we go from NLL to $\overline{\text{NLL}}$ and 0.64% from NNLL to $\overline{\text{NNLL}}$.

Figure 9 demonstrates this for a wider range of Q values. We can also observe that the curves corresponding to SV + NSV resummed results at NLO + $\overline{\text{NLL}}$ and NNLO + $\overline{\text{NNLL}}$ are closer compared to the SV counter parts, accounting for the perturbative convergence when NSV effects are taken into consideration. It also shows that the resummed correction decreases when we go to higher logarithmic accuracy as the resummed curves at the second order are closer than that of the first order ones.

We now analyze the scale uncertainties of the SV + NSV resummed results in comparison to the SV resummation. In Fig. 10 we plot the SV and SV + NSV resummed results at various logarithmic accuracy as a function of τ taking into account the respective 7-point scale variations. Note that the SV + NSV resummed predictions are more sensitive to the scales compared to the SV ones. For instance, for $Q = 2000$ GeV, we find the scale uncertainty of SV resummed results, which was in between $^{+0.32\%}_{-0.27\%}$, is enhanced to $^{+0.89\%}_{-0.78\%}$ when the resummed NSV corrections are added. This further hints towards our earlier findings in Sect. 4.1, that the absence of complete resummation of collinear logarithms, which includes both diagonal as well as off-diagonal contributions, causes the SV + NSV resummed predictions to be more sensitive to the unphysical scales.

However the SV resummation, which gets contributions only from the diagonal channel, shows improvement in 7-point scale uncertainties for higher values of Q. Similar findings are observed even if we restrict ourselves to only diagonal $(q\bar{q})$ channel as shown in right panel of Fig. 10. For comparison, we present the SV and SV + NSV resummed results along with the fixed-order predictions for $Q = 1000, 2000$ GeV with their respective percentage scale uncertainties in Table 9 at the second order.

The width of the band is expected to reduce when we fix the factorisation scale and vary only the renormalisation

Table 8 The K-factor values for NSV resummed result in comparison to the SV resummed predictions at various logarithmic accuracy

$Q = \mu_R = \mu_F$	NLO + NLL	NLO + $\overline{\text{NLL}}$	NNLO + NNLL	NNLO + $\overline{\text{NNLL}}$
1000	1.3711	1.3995	1.4053	1.4138
2000	1.3459	1.3739	1.3729	1.3818

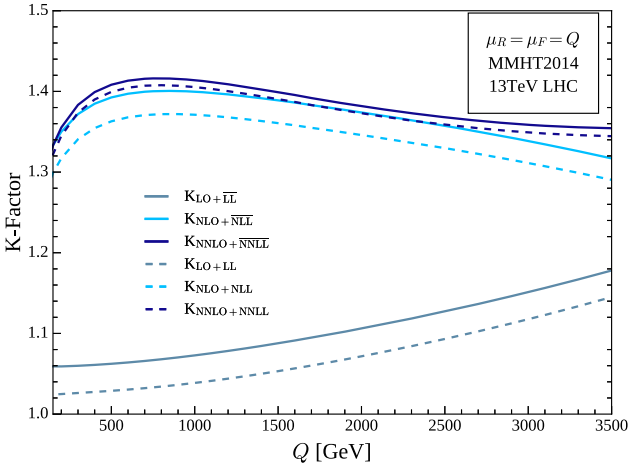

Fig. 9 A comparison of the K-factors of both SV and SV + NSV resummation for 13 TeV LHC

scale, since the effect of latter gets cancelled within a given partonic channel. Hence we now turn to analyze the effect of each these scales separately on the resummed result.

As seen in Sect. 4.1, the large uncertainties in the 7-point variations were mostly from the μ_F variation and hence we compare in Fig. 11 the μ_F sensitivity of SV and SV + NSV resummed cross sections as a function of τ, keeping μ_R fixed at Q. Note here that the bands are obtained by varying only μ_F by a factor of 2 up and down around the central scale $\mu_R = \mu_F = Q$. We find, that where the μ_F band of fixed-order, i.e., at NLO, starts widening for higher values of Q, the resummed bands i.e., at NLO + NLL and NLO + $\overline{\text{NLL}}$, shows a systematic reduction in the width for the same range of Q. But there is larger reduction in the SV resummed case in comparison to the SV + NSV. On the other hand the μ_F band of NNLO is better than both SV and SV + NSV for the considered Q range. This clearly hints towards the level of cancellation between different partonic channels. At NNLO there is a significant cancellation between $q\bar{q}$ and qg-channel which leads to the reduction of the μ_F width from NLO to NNLO and the SV resummation, which resums the distributions present only in the diagonal channel, doesn't require any compensation from other channels. But when it comes to SV + NSV resummation there is a compensation required from the other partonic channels to enhance the μ_F stability. Note that in all these analysis, we studied the impact of fixed-order and resummed CFs using same PDF sets to desired logarithmic accuracy for both of them. For studies related to μ_F variations, it is worthwhile to consider resummed PDFs if they are available.

However, this is not the case if we keep the μ_F intact and study the sensitivity due to μ_R variation as the latter effects are supposed to cancel within a partonic channel. This is depicted in Fig. 12, where we vary the μ_R dependence of cross section as a function of τ with μ_F held fixed at Q. As can be seen from the plot, the width of the μ_R band is significantly reduced in case of resummed bands in comparison to the fixed-order band, leading to a reliable predictions from the resummation. And among the resummed bands, the uncertainty of SV + NSV resummed results are comparable to those of SV resummation. For instance, for $Q = 1000$ GeV, the uncertainty is $^{+1.26\%}_{-1.11\%}$ at NLO + NLL whereas it is $^{+1.28\%}_{-1.15\%}$ at NLO + $\overline{\text{NLL}}$. Similarly, the uncertainty at NNLO + NNLL is $^{+0.0\%}_{-0.12\%}$ whereas at NNLO+$\overline{\text{NNLL}}$ is it found to be $^{+0.01\%}_{-0.30\%}$ for the same value of Q.

In order to see the NSV effects more clearly, let us focus on the sensitivity of the predictions to the choice of the scale μ_R within the $q\bar{q}$ channel as a function of τ, which is depicted in Fig. 13. Interestingly, the behaviour of $\text{NNLO}_{q\bar{q}} + \overline{\text{NNLL}}$ is significantly improved from the corresponding SV results, $\text{NNLO}_{q\bar{q}}$ + NNLL, for a wide range of Q. There is a large increment in the central value, in addition to the significant reduction of the μ_R uncertainty. To see this quantitatively, we quote in Table 10 both the fixed-order and SV and SV + NSV resummed predictions along with asymmetric errors resulting from μ_R variation with μ_F held fixed at Q, say $Q = 1000$ and 2000 GeV. The uncertainties, in Table 10, are obtained with respect to the μ_R scale variation with μ_F held fixed at Q. This evidently shows that there is a considerable improvement when adding NSV resummation over the existing SV results and hence leading to more reliable predictions.

To summarise, our analysis on the sensitivity of hadronic results to μ_F and μ_R scales where the resummed parts from $q\bar{q}$ channel is taken into account, helps us to understand the role of various channels as well as on the PDFs that contribute. As far as the μ_R scale is concerned, inclusion of SV as well as NSV resummed contributions in CFs alone helps to reduce the sensitive to this scale. However, this is not the case for μ_F as our numerical study shows the need for resummed NSV contributions to CFs of qg-channel as well as the resummed PDFs.

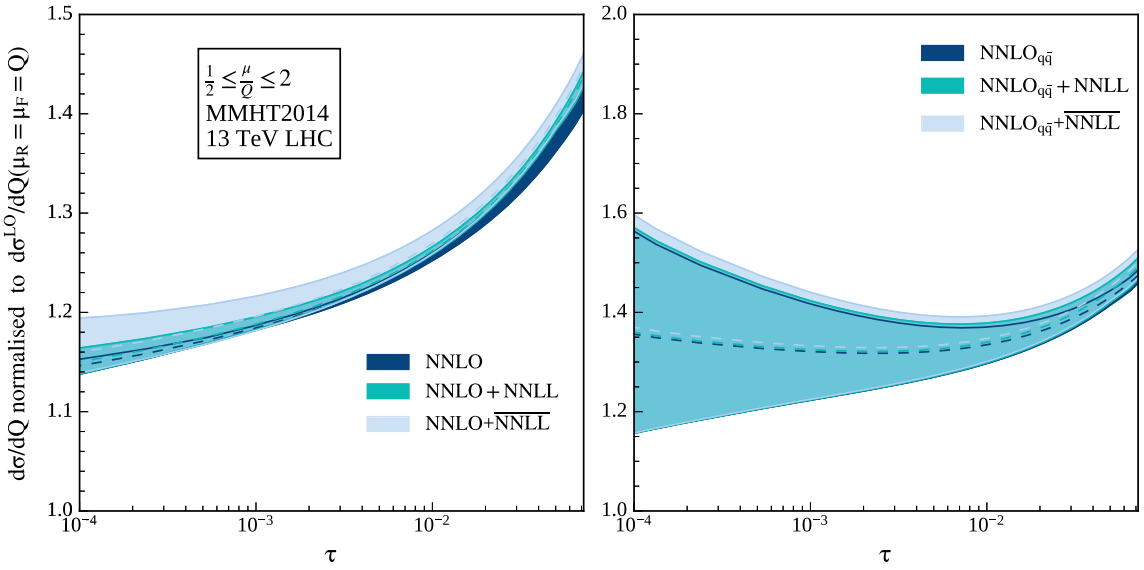

Fig. 10 7-point scale variations of NNLL and $\overline{\text{NNLL}}$ matched to NNLO for all-channels (left panel) and $q\bar{q}$-channel (right panel)

Table 9 Values of SV and SV + NSV resummed cross section in 10^{-5} pb/GeV at second logarithmic accuracy in comparison to the fixed-order results at different central scales

$Q = \mu_R = \mu_F$	NNLO	NNLO + NNLL	NNLO + $\overline{\text{NNLL}}$
1000	$3.2876^{+0.20\%}_{-0.31\%}$	$3.2993^{+0.36\%}_{-0.29\%}$	$3.3191^{+1,13\%}_{-0.86\%}$
2000	$0.0684^{+0.37\%}_{-0.62\%}$	$0.0687^{+0.32\%}_{-0.27\%}$	$0.0692^{+0.89\%}_{-0.78\%}$

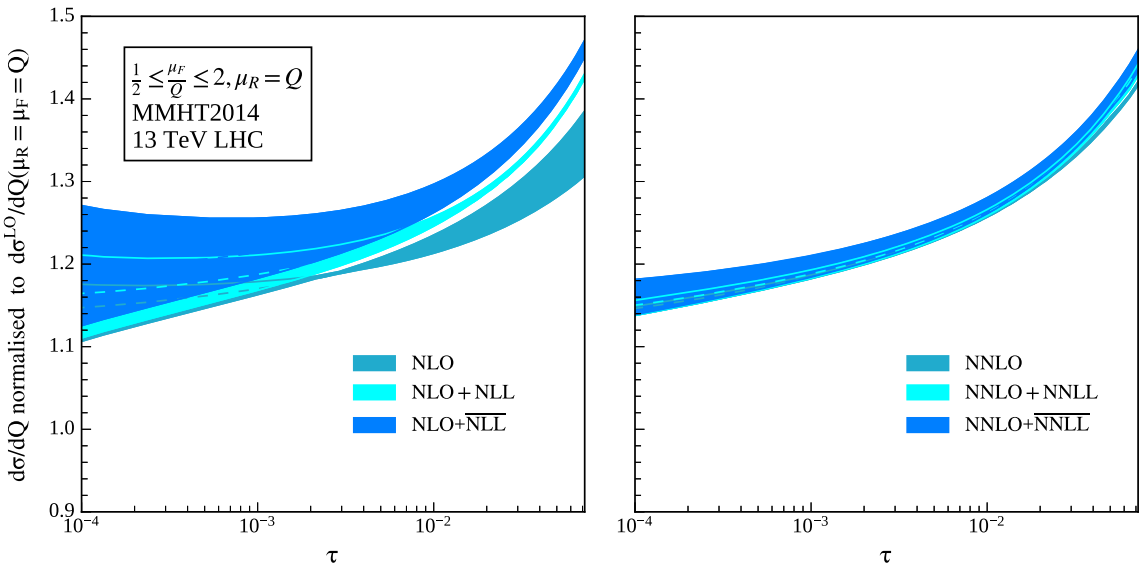

Fig. 11 μ_F variation between SV and SV + NSV resummed results matched to NLO (left panel) and NNLO (right panel) with the scale μ_R held fixed at Q

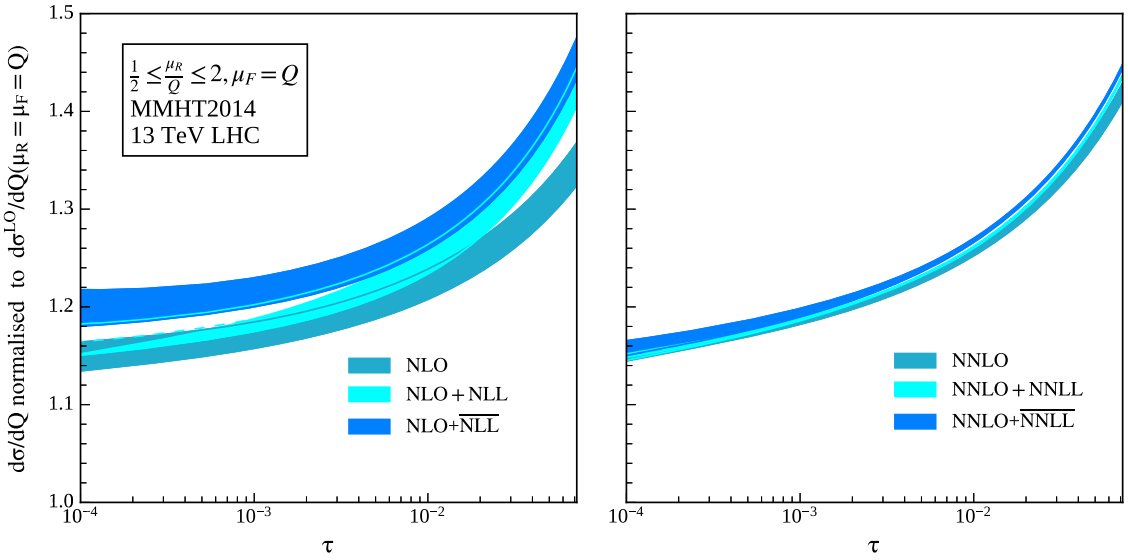

Fig. 12 μ_R variation between SV and SV + NSV resummed results matched to NLO (left panel) and NNLO (right panel) with the scale μ_F held fixed at Q

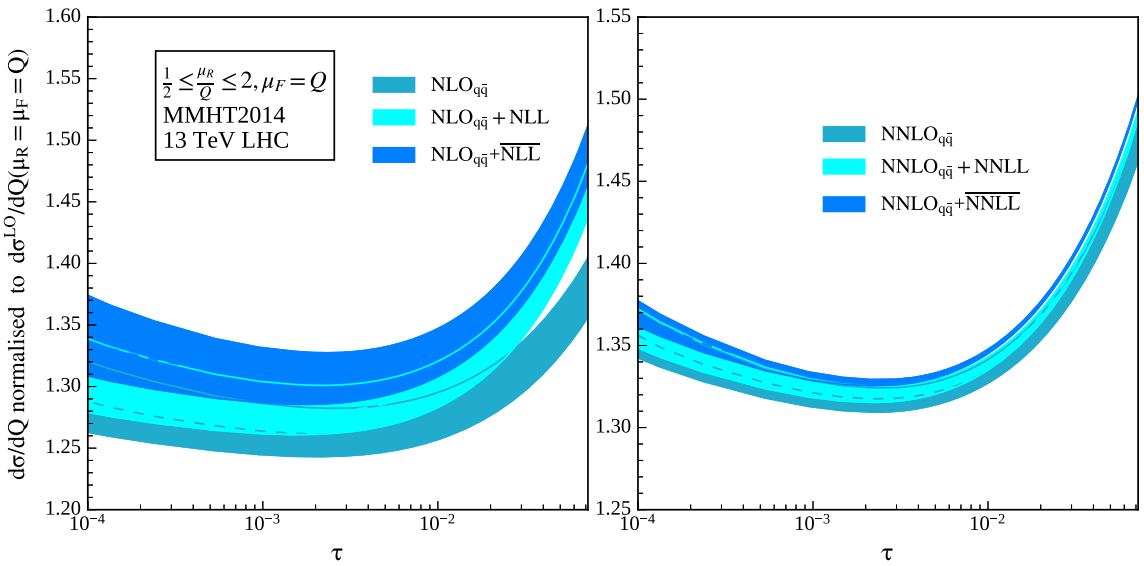

Fig. 13 μ_R variation between SV and SV + NSV matched to NNLO$_{q\bar{q}}$ with the scale μ_F held fixed at Q in $q\bar{q}$-channel

4.3 SV + NSV resummation in different schemes

This section is devoted to the study of SV + NSV resummation effects in different schemes, namely N and $\overline{N}$ exponentiations. The details of both the schemes are discussed in Sect. 3 and here we illustrate their numerical impact. The main point of difference between these two scheme arises from the "additional" resummation of γ_E, i.e., in $\overline{N}$. We resum γ_E terms along with $\ln N$ whereas for N exponentiation we only resum the $\ln N$ terms. The effect of this "additional" resummation of γ_E has shown better convergence for SV resummation, now here it would be interesting to see what changes does SV + NSV resummation bring to the observations made earlier in [30].

At first we begin with the analysis of K factor which is defined in (63). To differentiate between these two scheme we denote K for N and $\overline{\text{K}}$[1] for $\overline{N}$ exponentiation as given in Fig. 14. Earlier in Sect. 4.1, we found that the K factor for N exponentiation shows certain hierarchy which grows from LO + $\overline{\text{LL}}$ to NLO + $\overline{\text{NLL}}$ to NNLO + $\overline{\text{NNLL}}$. Now for $\overline{N}$ we find, that the $\overline{\text{K}}_{\text{NLO+}\overline{\text{NLL}}}$ is greater than $\overline{\text{K}}_{\text{NNLO+}\overline{\text{NNLL}}}$. However at NNLO + $\overline{\text{NNLL}}$, we observe a striking feature,

[1] It is to be noted that both K and $\overline{\text{K}}$ follows the same definition as given in (63).

Table 10 Comparison of SV and SV + NSV resummed cross section in 10^{-5} pb/GeV for $q\bar{q}$-channel at different central scales

$Q = \mu_R = \mu_F$	$\text{NNLO}_{q\bar{q}}$	$\text{NNLO}_{q\bar{q}} + \text{NNLL}$	$\text{NNLO}_{q\bar{q}} + \overline{\text{NNLL}}$
1000	$3.5260^{+0.49\%}_{-0.58\%}$	$3.5376^{+0.25\%}_{-0.39\%}$	$3.5576^{+0.006\%}_{-0.20\%}$
2000	$0.0717^{+0.54\%}_{-0.62\%}$	$0.0721^{+0.19\%}_{-0.33\%}$	$0.0725^{+0.0\%}_{-0.15\%}$

namely the K factors for both N and $\overline{N}$ exactly overlap on each other for the considered Q range. To quantify the overlap at NNLO + $\overline{\text{NNLL}}$, we quote that for $\overline{N}$ at $Q = 2000$ GeV, the $\overline{\text{K}}$ factor is 1.3823 while for N it is 1.3818 (see Table 5). This implies that the correction at NNLO + $\overline{\text{NNLL}}$ is independent of any schemes.

Moreover, like N exponentiation, we see an overall increment in the cross section for $\overline{N}$ with the inclusion of higher order logarithmic corrections. For instance at $Q = 2000$ GeV, the LO prediction is enhanced by 27.34%, the NLO by 6.88% and similarly the NNLO by 1.31%. As a whole the resummed result at NNLO + $\overline{\text{NNLL}}$ increases the LO prediction by 38.32% for the same value of Q. And the perturbative convergence between resummed curves in $\overline{N}$ is better than N exponentiation by a very small margin as can be seen from Fig. 14.

Now we proceed to study the uncertainties resulting from μ_R and μ_F for both N and $\overline{N}$. This is presented in Fig. 15. We find that there is a systematic enhancement in the cross section and in scale reduction for both the schemes. However, in contrast to N exponentiation, studied in sec. 4.1, we find that the bands of NNLO + $\overline{\text{NNLL}}$ is not contained within the band of NLO + $\overline{\text{NLL}}$ in $\overline{N}$-scheme, as the enhancement from NLO + $\overline{\text{NLL}}$ to NNLO + $\overline{\text{NNLL}}$ is negative. For instance, there is an increment of 9.6% from LO +LL to NLO + $\overline{\text{NLL}}$ accuracy, which decreases by −0.85% at NNLO + $\overline{\text{NNLL}}$ for $Q = 2000$ GeV. This can also be seen from Fig. 14. Although the width of NNLO + $\overline{\text{NNLL}}$ band is smaller than that of NLO + $\overline{\text{NLL}}$ yet the uncertainties associated with these two bands are more than N exponentiation (see Table 11). Hence in summary, we find that when we go from LO+LL to NNLO+$\overline{\text{NNLL}}$, the cross section increases more in N scheme compared to $\overline{N}$ and the uncertainty in N scheme is smaller compared to $\overline{N}$. Interestingly at NNLO+$\overline{\text{NNLL}}$ level, their central values are very close to each other compared to previous order hinting better scheme independence as we increase the order of perturbation.

Besides N and $\overline{N}$ there are two other schemes as we discussed in Sect. 3, which are *Soft* and *All exponentiation*. While in *Soft* -scheme, we exponentiate only the Mellin moment of complete soft-collinear function, in *All* -scheme, the form factor contributions are also taken into exponentiation, additionally. We have explored the NSV resummation under these two schemes along with the N- and $\overline{N}$-schemes for two different Q-values, namely $Q = 1000$ GeV and 2000 GeV and the results are enlisted in Table 11

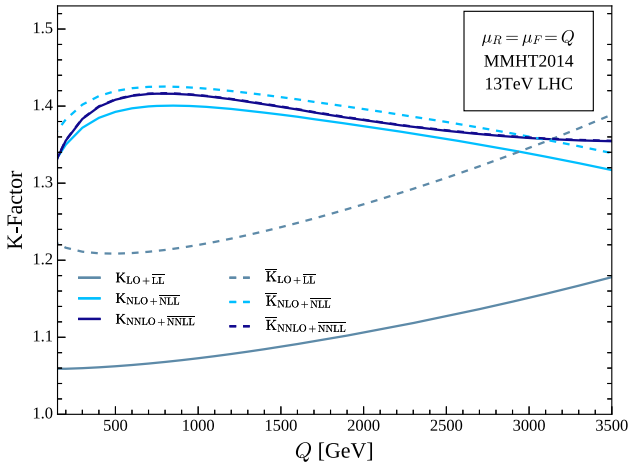

Fig. 14 Comparison between the K-factors for the N and $\overline{N}$ exponentiation at the central scale $Q = \mu_R = \mu_F$

for different logarithmic accuracies. Noting various values, we find that at LO+$\overline{\text{LL}}$ and NLO + $\overline{\text{NLL}}$, the $\overline{N}$ scheme gives the large corrections, say 0.0638×10^{-5} pb/GeV and 0.0699×10^{-5} pb/GeV respectively at $Q = 2000$ GeV, whereas, at NNLO+$\overline{\text{NNLL}}$ i.e., after adding more logarithmic corrections, the large contributions are arising from *All* -scheme. However, the uncertainties coming from μ_R and μ_F variation are found to be least in N and *All exponentiation* at any logarithmic accuracy for the considered Q-*range.*

4.4 Numerical results for different collider energies

In Tables 12, 13 and 14, we summarise the results for different collider energies and different values of the invariant mass of di-leptons. We estimate the theoretical uncertainty by independently varying the scales $\mu = \{\mu_F, \mu_R\}$ up and down, by a factor of two i.e. $\frac{1}{2} \leq \frac{\mu}{Q} \leq 2$. We find that the inclusion of SV NNLL increases the NNLO distribution by 0.24–0.55% whereas the inclusion of NSV at $\overline{\text{NNLL}}$ increases it by 0.72–1.65%, in the considered collider energies and the Q range.

5 Discussion and conclusions

Production of pair of leptons in Drell–Yan process is one of the cleanest processes at the LHC, also well studied both in SM and beyond SM. The perturbative predictions taking into account radiative corrections from strong and elec-

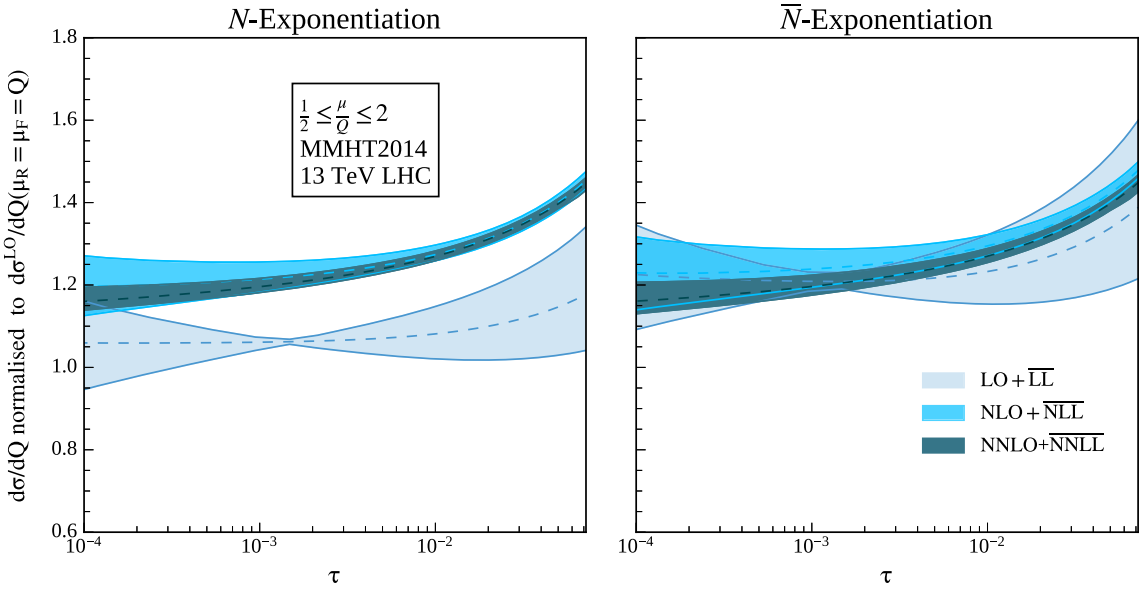

Fig. 15 A comparison between 7-point scale variation in both N and $\overline{N}$ exponentiation around the central scale choice $(\mu_R, \mu_F) = (1, 1)Q$ for 13 TeV LHC

Table 11 A comparison of resummed cross-sections in 10^{-5} pb/GeV between different resummation schemes up to NNLO + $\overline{\text{NNLL}}$

Order	$Q = \mu_R = \mu_F$ (GeV)	N-Exp	$\overline{N}$-Exp	Soft-Exp	All-Exp
LO + $\overline{\text{LL}}$	1000	$2.5184^{+4.49\%}_{-4.25\%}$	$2.8636^{+5.53\%}_{-5.07\%}$	$2.5184^{+4.49\%}_{-4.25\%}$	$2.5184^{+4.49\%}_{-4.25\%}$
	2000	$0.0554^{+9.10\%}_{-7.92\%}$	$0.0638^{+10.21\%}_{-8.73\%}$	$0.0554^{+9.10\%}_{-7.92\%}$	$0.0554^{+9.10\%}_{-7.92\%}$
NLO + $\overline{\text{NLL}}$	1000	$3.2857^{+2.08\%}_{-1.18\%}$	$3.3418^{+2.41\%}_{-2.13\%}$	$3.3027^{+2.12\%}_{-1.74\%}$	$3.3101^{+1.89\%}_{-1.24\%}$
	2000	$0.0688^{+1.44\%}_{-1.24\%}$	$0.0699^{+1.69\%}_{-1.51\%}$	$0.0691^{+1.59\%}_{-1.16\%}$	$0.0693^{+1.44\%}_{-1.31\%}$
NNLO + $\overline{\text{NNLL}}$	1000	$3.3191^{+1.13\%}_{-0.87\%}$	$3.3204^{+1.58\%}_{-1.29\%}$	$3.3222^{+1.32\%}_{-0.91\%}$	$3.3264^{+1.13\%}_{-0.91\%}$
	2000	$0.0692^{+0.89\%}_{-0.79\%}$	$0.0693^{+1.28\%}_{-1.15\%}$	$0.0693^{+1.04\%}_{-0.82\%}$	$0.0694^{+0.89\%}_{-0.82\%}$

Table 12 Resummed results for invariant mass distribution of di-lepton pair against fixed-order (in pb/GeV) at different centre of mass energies at the LHC for $Q = 200$ GeV

$\sqrt{S}$	NNLO	NNLO + NNLL	NNLO + $\overline{\text{NNLL}}$
7 TeV	$2.56 \times 10^{-2}{}^{+0.29\%}_{-0.28\%}$	$2.57 \times 10^{-2}{}^{+0.82\%}_{-0.62\%}$	$2.59 \times 10^{-2}{}^{+2.19\%}_{-1.38\%}$
8 TeV	$3.06 \times 10^{-2}{}^{+0.29\%}_{-0.32\%}$	$3.07 \times 10^{-2}{}^{+0.86\%}_{-0.65\%}$	$3.09 \times 10^{-2}{}^{+2.25\%}_{-1.41\%}$
13 TeV	$5.63 \times 10^{-2}{}^{+0.41\%}_{-0.45\%}$	$5.65 \times 10^{-2}{}^{+0.99\%}_{-0.76\%}$	$5.69 \times 10^{-2}{}^{+2.43\%}_{-1.49\%}$
14 TeV	$6.16 \times 10^{-2}{}^{+0.43\%}_{-0.47\%}$	$6.18 \times 10^{-2}{}^{+1.00\%}_{-0.78\%}$	$6.22 \times 10^{-2}{}^{+2.45\%}_{-1.50\%}$
100 TeV	$5.13 \times 10^{-1}{}^{+0.62\%}_{-1.18\%}$	$5.15 \times 10^{-1}{}^{+1.16\%}_{-1.44\%}$	$5.18 \times 10^{-1}{}^{+2.79\%}_{-2.09\%}$

Table 13 Resummed results for invariant mass distribution of di-lepton pair against fixed-order (in pb/GeV) at different centre of mass energies at the LHC for $Q = 500$ GeV

$\sqrt{S}$	NNLO	NNLO + NNLL	NNLO + $\overline{\text{NNLL}}$
7 TeV	$3.25 \times 10^{-4}{}^{+0.22\%}_{-0.35\%}$	$3.26 \times 10^{-4}{}^{+0.404\%}_{-0.33\%}$	$3.28 \times 10^{-4}{}^{+1.36\%}_{-1.02\%}$
8 TeV	$4.13 \times 10^{-4}{}^{+0.19\%}_{-0.32\%}$	$4.14 \times 10^{-4}{}^{+0.412\%}_{-0.347\%}$	$4.17 \times 10^{-4}{}^{+1.40\%}_{-1.03\%}$
13 TeV	$9.04 \times 10^{-4}{}^{+0.21\%}_{-0.207\%}$	$9.07 \times 10^{-4}{}^{+0.546\%}_{-0.40\%}$	$9.13 \times 10^{-4}{}^{+1.56\%}_{-1.08\%}$
14 TeV	$10.09 \times 10^{-4}{}^{+0.213\%}_{-0.19\%}$	$10.13 \times 10^{-4}{}^{+0.565\%}_{-0.409\%}$	$10.19 \times 10^{-4}{}^{+1.59\%}_{-1.09\%}$
100 TeV	$1.214 \times 10^{-2}{}^{+0.35\%}_{-0.43\%}$	$1.217 \times 10^{-2}{}^{+0.787\%}_{-0.650\%}$	$1.223 \times 10^{-2}{}^{+1.94\%}_{-1.23\%}$

Table 14 Resummed results for invariant mass distribution of di-lepton pair against fixed-order (in pb/GeV) at different centre of mass energies at the LHC for $Q = 1000$ GeV

$\sqrt{S}$	NNLO	NNLO + NNLL	NNLO + $\overline{\text{NNLL}}$
7 TeV	$7.55 \times 10^{-6}{}^{+0.42\%}_{-0.704\%}$	$7.59 \times 10^{-6}{}^{+0.32\%}_{-0.26\%}$	$7.65 \times 10^{-6}{}^{+0.99\%}_{-0.87\%}$
8 TeV	$1.092 \times 10^{-5}{}^{+0.36\%}_{-0.57\%}$	$1.098 \times 10^{-5}{}^{+0.33\%}_{-0.27\%}$	$1.11 \times 10^{-5}{}^{+1.02\%}_{-0.86\%}$
13 TeV	$3.29 \times 10^{-5}{}^{+0.28\%}_{-0.32\%}$	$3.30 \times 10^{-5}{}^{+0.36\%}_{-0.29\%}$	$3.32 \times 10^{-5}{}^{+1.135\%}_{-0.87\%}$
14 TeV	$3.79 \times 10^{-5}{}^{+0.19\%}_{-0.29\%}$	$3.81 \times 10^{-5}{}^{+0.36\%}_{-0.30\%}$	$3.83 \times 10^{-5}{}^{+1.15\%}_{-0.87\%}$
100 TeV	$6.96 \times 10^{-4}{}^{+0.21\%}_{-0.19\%}$	$6.98 \times 10^{-4}{}^{+0.59\%}_{-0.39\%}$	$7.01 \times 10^{-4}{}^{+1.50\%}_{-0.94\%}$

troweak interactions are known to unprecedented accuracy. Third order perturbative results in QCD improved with the SV enhanced resummed contributions and with partial second order results in electroweak sector have already played important role in our understanding of the underlying dynamics and in addition, these results have set stringent constraints on the parameters of various beyond the SM scenarios. In this article we have improved the predictions by including next-to-SV enhanced resummed contributions from strong interactions. We have used the recent formalism that systematically resums such next-to-SV logarithms to all orders. We have restricted ourselves to the production mechanism where only neutral gauge bosons such photon and Z boson produce leptons. For our study, we have included fixed-order results from QCD upto NNLO and resummed results upto $\overline{\text{NNLL}}$ level. The latter contains both resummed threshold SV contributions as well as next-to-SV resumed ones. Using the so called matched results, we study the impact of resummed NSV contributions on the invariant mass of the pair of leptons. As the fixed-order predictions have already indicated that NSV logarithms dominate over SV distributions, the inclusion of resummed NSV terms along with the SV resumed predictions are expected to show appreciable numerical effects that can not be ignored. We have studied their impact over a wide range of Q values, i.e., 100 to 3500 GeV for 13 TeV LHC. We find that about 6–11% increase when we go from LO to LO + $\overline{\text{LL}}$ while at second order it stabilises to 1% when we include $\overline{\text{NNLL}}$ to NNLO. These predictions were obtained by setting both renormalisation μ_R and factorisation μ_F scales at Q. The sensitivity of our predictions with respect to these scales can be studied using 7-point scale variation and single scale variation. In the seven point scale variation, we find that the inclusion of resummed $\overline{\text{LL}}$, $\overline{\text{NLL}}$ and $\overline{\text{NNLL}}$ terms to fixed-order LO, NLO and NNLO contributions increases the sensitivity of the predictions to these scales. A detailed investigation reveals that the resumed results are more sensitive to factorisation scale compared to renormalisation scale and in particular we find that NSV part of the resumed result is largely responsible for this. The reason for this is the absence of NSV resummed terms from quark gluon initiated processes in our analysis. These contributions would provide right logarithms of μ_F to compensate against those from the PDFs at the hadronic level. Note that different partonic channels mix under factorisation scale variations when they are convoluted with appropriate PDFs. Hence, absence of any partonic channel at any given order can increase the sensitivity to μ_F at the hadronic level. We have also noticed that the μ_F sensitivity is large at second order compared to lower orders. This is easy to understand if we observe that the quark gluon initiated channels give larger negative contribution at NNLO level compared to NLO level. In order to understand the role of quark-gluon initiated channel in the context of unphysical scales, we have computed both SV and NSV resummed contributions with and without qg-channels and performed 7-point and single scale variations. We find that at a_s^2, the corrections from $q\bar{q}$ and qg-channel are 4.86% and -2.47% respectively to the NNLO cross section along with the other sub-dominating channels. As these corrections are closer to each other at the fixed-order level, we expect that resumed NSV from qg-channel is as important as the one from $q\overline{q}$ channel.

Unlike in the case of μ_F, different channels that contribute do not mix under the variation of μ_R as each of them is renormalisation group invariant with respect to μ_R. Hence, we expect that the predictions based on single scale variation should be less sensitive to μ_R as we increase the order of perturbation. Our numerical study confirms this both for fixed-order as well as for resummed predictions.

We have also investigated the role of resummed NSV terms in the resummed predictions in comparison to the known SV resummation. We find that there is about 2% increment when we go from NLL to $\overline{\text{NLL}}$ and about 0.64% from NNLL to $\overline{\text{NNLL}}$ demonstrating the importance of resummed NSV contributions from quark anti-quark initiated channels. The 7-point scale variation gives larger scale uncertainty if we add resummed contributions from NSV terms. This stems from the scale μ_F as resummed NSV part lack contributions from qg channel. The single scale variations where we keep one scale fixed and vary the other scale confirms our interpretation.

One finds that the SV part of the resummed predictions depends on how one treats the N-independent part of the resummed results. Such terms come from both form factors

and SV part of the soft-collinear function. Different schemes are adopted to deal with such terms and they give different numerical predictions. We consider four schemes and study their numerical impact on the predictions taking into account NSV terms. Interestingly we find that the difference in predictions from N and $\overline{N}$ schemes gets reduced as we increase the logarithmic accuracy signaling the scheme independence. Finally, we conclude our detailed numerical analysis by presenting predictions for invariant mass distributions at scales $Q = 1000, 2000$ GeV for different hadronic center of mass energies along with uncertainties resulting from unphysical scales.

In summary, our analysis provides the precise numerical predictions from resummed NSV terms upto NNLO+$\overline{\text{NNLL}}$ level for the first time to the invariant mass distribution of a pair of leptons produced at the LHC.

Acknowledgements We thank Claude Duhr and Moch for useful discussion throughout this project. We also thank Claude Duhr and Bernhard Mistlberger for providing third order results for the inclusive reactions. We would like to thank L. Magnea and E. Laenen for their encouragement to work on this area. In addition we would also like to thank the computer administrative unit of IMSc for their help and support.

Data Availability Statement This manuscript has no associated data or the data will not be deposited. [Authors' comment: There are no associated data available.]

Funded by SCOAP[3].

Appendix A: Anomalous dimensions

Here we present all the anomalous dimensions used in performing the resummation.

A.1 Cusp anomalous dimensions A_i^q

In the following we list the cusp anomalous dimensions A_i^q till four-loop level:

$$A_1^q = 4\,C_F, \tag{A.1}$$

$$A_2^q = C_F\,n_f\left(-\frac{40}{9}\right) + C_F\,C_A\left(\frac{268}{9} - 8\,\zeta_2\right), \tag{A.2}$$

$$A_3^q = C_F\,n_f^2\left(-\frac{16}{27}\right) + C_F\,C_A\,n_f\left(-\frac{836}{27} - \frac{112}{3}\,\zeta_3 + \frac{160}{9}\,\zeta_2\right) + C_F\,C_A^2\left(\frac{490}{3} + \frac{88}{3}\,\zeta_3 - \frac{1072}{9}\,\zeta_2 + \frac{176}{5}\,\zeta_2^2\right) + C_F^2\,n_f\left(-\frac{110}{3} + 32\,\zeta_3\right), \tag{A.3}$$

$$\begin{aligned} A_4^q = {} & C_F\frac{d_F^{abcd}d_A^{abcd}}{N_A}\left(\frac{7040}{3}\zeta_5 + \frac{256}{3}\zeta_3 - 768\zeta_3^2 - 256\zeta_2 - \frac{15872}{35}\zeta_2^3\right) \\ & + C_F n_f\frac{d_F^{abcd}d_F^{abcd}}{N_A}\left(-\frac{2560}{3}\zeta_5 - \frac{512}{3}\zeta_3 + 512\zeta_2\right) \\ & + C_F n_f^3\left(-\frac{32}{81} + \frac{64}{27}\zeta_3\right) + C_F^2 n_f^2\left(\frac{2392}{81} - \frac{640}{9}\zeta_3 + \frac{64}{5}\zeta_2^2\right) + C_F^3 n_f\left(\frac{572}{9} - 320\zeta_5 + \frac{592}{3}\zeta_3\right) \\ & + C_A C_F n_f^2\left(\frac{923}{81} + \frac{2240}{27}\zeta_3 - \frac{608}{81}\zeta_2 - \frac{224}{15}\zeta_2^2\right) \\ & + C_A C_F^2 n_f\left(-\frac{34066}{81} + 160\zeta_5 + \frac{3712}{9}\zeta_3 + \frac{440}{3}\zeta_2 - 128\zeta_2\zeta_3 - \frac{352}{5}\zeta_2^2\right) + C_A^2 C_F n_f\left(-\frac{24137}{81} + \frac{2096}{9}\zeta_5 - \frac{23104}{27}\zeta_3 + \frac{20320}{81}\zeta_2 + \frac{448}{3}\zeta_2\zeta_3 - \frac{352}{15}\zeta_2^2\right) \\ & + C_A^3 C_F\left(\frac{84278}{81} - \frac{3608}{9}\zeta_5 + \frac{20944}{27}\zeta_3 - 16\zeta_3^2 - \frac{88400}{81}\zeta_2 - \frac{352}{3}\zeta_2\zeta_3 + \frac{3608}{5}\zeta_2^2 - \frac{20032}{105}\zeta_2^3\right), \end{aligned} \tag{A.4}$$

where n_f is the number of active quark flavours in the theory. The quadratic Casimirs C_F and C_A are given by $\frac{n_c^2-1}{2\,nc}$ and n_c respectively. The quartic Casimirs are given by

$$\begin{aligned} \frac{d_F^{abcd}d_A^{abcd}}{N_A} &= \frac{n_c(n_c^2+6)}{48}, \\ \frac{d_F^{abcd}d_F^{abcd}}{N_A} &= \frac{(n_c^4 - 6n_c^2 + 18)}{96n_c^2}, \end{aligned} \tag{A.5}$$

with $N_A = n_c^2 - 1$ and $N_F = n_c$ where $n_c = 3$ for QCD.

A.2 Collinear anomalous dimensions B_i^q

The collinear anomalous dimensions B_i^q are given till three-loop as,

$$B_1^q = 3\,C_F, \tag{A.6}$$

$$B_2^q = C_F\,n_f\left(-\frac{1}{3} - \frac{8}{3}\,\zeta_2\right) + C_F\,C_A\left(\frac{17}{6} - 12\,\zeta_3\right.$$

$$+\frac{44}{3}\,\zeta_2\Big)+C_F^2\,\Big(\frac{3}{2}+24\,\zeta_3-12\,\zeta_2\Big), \tag{A.7}$$

$$\begin{aligned}B_3^q=&\,C_F\,n_f^2\,\Big(-\frac{17}{9}-\frac{16}{9}\,\zeta_3+\frac{80}{27}\,\zeta_2\Big)+C_F\,C_A\,n_f\,\Big(20\\&+\frac{200}{9}\,\zeta_3-\frac{1336}{27}\,\zeta_2+\frac{4}{5}\,\zeta_2^2\Big)+C_F\,C_A^2\,\Big(-\frac{1657}{36}\\&+40\,\zeta_5-\frac{1552}{9}\,\zeta_3+\frac{4496}{27}\,\zeta_2-2\,\zeta_2^2\Big)+C_F^2\,n_f\\&\times\Big(-23-\frac{136}{3}\,\zeta_3+\frac{20}{3}\,\zeta_2+\frac{232}{15}\,\zeta_2^2\Big)+C_F^2\,C_A\,\Big(\frac{151}{4}\\&+120\,\zeta_5+\frac{844}{3}\,\zeta_3-\frac{410}{3}\,\zeta_2+16\,\zeta_2\,\zeta_3-\frac{988}{15}\,\zeta_2^2\Big)\\&+C_F^3\,\Big(\frac{29}{2}-240\,\zeta_5+68\,\zeta_3+18\,\zeta_2-32\,\zeta_2\,\zeta_3\\&+\frac{288}{5}\,\zeta_2^2\Big).\end{aligned} \tag{A.8}$$

A.3 Soft anomalous dimensions f_i^q

The soft anomalous dimensions f_i^q till three-loop are given as

$$f_1^q=0, \tag{A.9}$$

$$f_2^q=C_F\,n_f\,\Big(-\frac{112}{27}+\frac{4}{3}\,\zeta_2\Big)+C_F\,C_A\,\Big(\frac{808}{27}-28\,\zeta_3-\frac{22}{3}\,\zeta_2\Big), \tag{A.10}$$

$$\begin{aligned}f_3^q=&\,C_F\,n_f^2\,\Big(-\frac{2080}{729}+\frac{112}{27}\,\zeta_3-\frac{40}{27}\,\zeta_2\Big)\\&+C_F\,C_A\,n_f\,\Big(-\frac{11842}{729}+\frac{728}{27}\,\zeta_3+\frac{2828}{81}\,\zeta_2-\frac{96}{5}\,\zeta_2^2\Big)\\&+C_F\,C_A^2\,\Big(\frac{136781}{729}+192\,\zeta_5-\frac{1316}{3}\,\zeta_3\\&-\frac{12650}{81}\,\zeta_2+\frac{176}{3}\,\zeta_2\,\zeta_3+\frac{352}{5}\,\zeta_2^2\Big)\\&+C_F^2\,n_f\,\Big(-\frac{1711}{27}+\frac{304}{9}\,\zeta_3+4\,\zeta_2+\frac{32}{5}\,\zeta_2^2\Big).\end{aligned} \tag{A.11}$$

A.4 NSV anomalous dimensions C_i^q & D_i^q

The NSV anomalous dimensions C_i^q and D_i^q till three-loop are given as

$$C_1^q=0, \tag{A.12}$$

$$C_2^q=16C_F^2, \tag{A.13}$$

$$C_3^q=C_F^2C_A\Big(\frac{2144}{9}-64\zeta_2\Big)+n_fC_F^2\Big(-\frac{320}{9}\Big). \tag{A.14}$$

$$D_1^q=-4C_F, \tag{A.15}$$

$$D_2^q=12C_F^2+C_AC_F\Big(\frac{-400}{9}+8\zeta_2\Big)+C_Fn_f\Big(\frac{64}{9}\Big), \tag{A.16}$$

$$\begin{aligned}D_3^q=&\,C_FC_A^2\Big(-\frac{8582}{27}-\frac{88}{3}\zeta_3+\frac{1336}{9}\zeta_2-\frac{176}{5}\zeta_2^2\Big)\\&+C_F^2C_A\Big(\frac{302}{3}-48\zeta_3+\frac{104}{3}\zeta_2\Big)\\&+C_F^3\Big(6+96\zeta_3-48\zeta_2\Big)\\&+n_fC_FC_A\Big(\frac{724}{9}+\frac{112}{3}\zeta_3-\frac{208}{9}\zeta_2\Big)\\&+n_fC_F^2\Big(30-32\zeta_3-\frac{32}{3}\zeta_2\Big)\\&+n_f^2C_F\Big(-\frac{64}{27}\Big).\end{aligned} \tag{A.17}$$

A.5 SV threshold exponents

The function $\overline{G}_{SV}^q\big(a_s(q^2(1-z)^2),\varepsilon\big)$ given in (22) is related to the threshold exponent $\mathbf{D}^q\big(a_s(q^2(1-z)^2),\varepsilon\big)$ via Eq. (46) of [11] where the universal $\mathbf{D}_i^q$ coefficients, till three-loop, are given as,

$$\mathbf{D}_1^q=0, \tag{A.18}$$

$$\mathbf{D}_2^q=C_Fn_f\Big(\frac{224}{27}-\frac{32}{3}\zeta_2\Big)+C_A\Big(-\frac{1616}{27}+56\zeta_3+\frac{176}{3}\zeta_2\Big), \tag{A.19}$$

$$\begin{aligned}\mathbf{D}_3^q=&\,C_F{n_f}^2\Big(-\frac{3712}{729}+\frac{320}{27}\zeta_3+\frac{640}{27}\zeta_2\Big)+C_Fn_f\Big(\frac{3422}{27}\\&-\frac{608}{9}\zeta_3-32\zeta_2-\frac{64}{5}\zeta_2^2\Big)+C_An_f\Big(\frac{125252}{729}-\frac{2480}{9}\zeta_3\\&-\frac{29392}{81}\zeta_2+\frac{736}{15}\zeta_2^2\Big)+C_A^2\Big(-\frac{594058}{729}-384\zeta_5\\&+\frac{40144}{27}\zeta_3+\frac{98224}{81}\zeta_2-\frac{352}{3}\zeta_2\zeta_3-\frac{2992}{15}\zeta_2^2\Big).\end{aligned} \tag{A.20}$$

Appendix B: NSV coefficients

Here we present all the NSV coefficients $\varphi_{q,i}^{(k)}$ given in (27).

$$\begin{aligned}\varphi_{q,1}^{(0)}&=4C_F,\\ \varphi_{q,1}^{(1)}&=0,\\ \varphi_{q,2}^{(0)}&=C_FC_A\Big(\frac{1402}{27}-28\zeta_3-\frac{112}{3}\zeta_2\Big)+C_F^2(-32\zeta_2)\\&\quad+n_fC_F\Big(-\frac{328}{27}+\frac{16}{3}\zeta_2\Big),\\ \varphi_{q,2}^{(1)}&=10C_FC_A-10C_F^2,\\ \varphi_{q,2}^{(2)}&=-4C_F^2,\end{aligned}$$

$$\varphi_{q,3}^{(0)} = C_F C_A^2\left(\frac{727211}{729} + 192\zeta_5 - \frac{29876}{27}\zeta_3 - \frac{82868}{81}\zeta_2 + \frac{176}{3}\zeta_2\zeta_3 + 120\zeta_2^2\right) + C_F^2 C_A\left(-\frac{5143}{27} - \frac{2180}{9}\zeta_3 - \frac{11584}{27}\zeta_2 + \frac{2272}{15}\zeta_2^2\right) + C_F^3\left(23 + 48\zeta_3 - \frac{32}{3}\zeta_2 - \frac{448}{15}\zeta_2^2\right) + n_f C_F C_A\left(-\frac{155902}{729} + \frac{1292}{9}\zeta_3 + \frac{26312}{81}\zeta_2 - \frac{368}{15}\zeta_2^2\right) + n_f C_F^2\left(-\frac{1309}{9} + \frac{496}{3}\zeta_3 + \frac{2536}{27}\zeta_2 + \frac{32}{5}\zeta_2^2\right) + n_f^2 C_F\left(\frac{12656}{729} - \frac{160}{27}\zeta_3 - \frac{704}{27}\zeta_2\right),$$

$$\varphi_{q,3}^{(1)} = C_F C_A^2\left(\frac{244}{9} + 24\zeta_3 - \frac{8}{9}\zeta_2\right) + C_F^2 C_A\left(-\frac{18436}{81} + \frac{544}{3}\zeta_3 + \frac{964}{9}\zeta_2\right) + C_F^3\left(-\frac{64}{3} - 64\zeta_3 + \frac{80}{3}\zeta_2\right) + n_f C_F C_A\left(-\frac{256}{9} - \frac{28}{9}\zeta_2\right) + n_f C_F^2\left(\frac{3952}{81} - \frac{160}{9}\zeta_2\right),$$

$$\varphi_{q,3}^{(2)} = C_F C_A^2\left(34 - \frac{10}{3}\zeta_2\right) + C_F^2 C_A\left(-96 + \frac{52}{3}\zeta_2\right) + C_F^3\left(\frac{16}{3}\right) + n_f C_F C_A\left(-\frac{10}{3}\right) + n_f C_F^2\left(\frac{40}{3}\right),$$

$$\varphi_{q,3}^{(3)} = C_F^2 C_A\left(-\frac{176}{27}\right) + n_f C_F^2\left(\frac{32}{27}\right). \tag{B.21}$$

Appendix C: Resummation coefficients for the N exponentiation

C.1 The N-independent coefficients C_0^q

The N-independent coefficients C_{0i}^q in Eq. (23), till three-loop, are given by

$$C_{00}^q = 1, \tag{C.22}$$

$$C_{01}^q = C_F\left\{-16 + 8\zeta_2 + 6L_{qr} - 6L_{fr}\right\}, \tag{C.23}$$

$$C_{02}^q = C_F n_f\left\{\frac{127}{6} + 8\zeta_3 - \frac{112}{9}\zeta_2 - \frac{34}{3}L_{qr} + 2L_{qr}^2 + \frac{2}{3}L_{fr} + \frac{16}{3}L_{fr}\zeta_2 - 2L_{fr}^2\right\} + C_F C_A\left\{-\frac{1535}{12} + 28\zeta_3 + \frac{592}{9}\zeta_2 - \frac{12}{5}\zeta_2^2 + \frac{193}{3}L_{qr} - 24L_{qr}\zeta_3 - 11L_{qr}^2 - \frac{17}{3}L_{fr} + 24L_{fr}\zeta_3 - \frac{88}{3}L_{fr}\zeta_2 + 11L_{fr}^2\right\} + C_F^2\left\{\frac{511}{4} - 60\zeta_3 - 70\zeta_2 + \frac{72}{5}\zeta_2^2 - 93L_{qr} + 48L_{qr}\zeta_3 + 24L_{qr}\zeta_2 + 18L_{qr}^2 + 93L_{fr} - 48L_{fr}\zeta_3 - 24L_{fr}\zeta_2 - 36L_{fr}L_{qr} + 18L_{fr}^2\right\}, \tag{C.24}$$

$$C_{03}^q = C_F N_4 n_{fv}\left\{8 - \frac{160}{3}\zeta_5 + \frac{28}{3}\zeta_3 + 20\zeta_2 - \frac{4}{5}\zeta_2^2\right\} + C_F n_f^2\left\{-\frac{7081}{243} - \frac{1264}{81}\zeta_3 + \frac{2416}{81}\zeta_2 + \frac{128}{27}\zeta_2^2 + \frac{220}{9}L_{qr} + \frac{64}{9}L_{qr}\zeta_3 - \frac{32}{3}L_{qr}\zeta_2 - \frac{68}{9}L_{qr}^2 + \frac{8}{9}L_{qr}^3 + \frac{34}{9}L_{fr} + \frac{32}{9}L_{fr}\zeta_3 - \frac{160}{27}L_{fr}\zeta_2 + \frac{4}{9}L_{fr}^2 + \frac{32}{9}L_{fr}^2\zeta_2 - \frac{8}{9}L_{fr}^3\right\} + C_F C_A n_f\left\{\frac{110651}{243} - 8\zeta_5 - \frac{6016}{81}\zeta_3 - \frac{28132}{81}\zeta_2 + \frac{208}{3}\zeta_2\zeta_3 - \frac{5756}{135}\zeta_2^2 - \frac{3052}{9}L_{qr} + \frac{208}{9}L_{qr}\zeta_3 + \frac{320}{3}L_{qr}\zeta_2 - \frac{8}{5}L_{qr}\zeta_2^2 + \frac{850}{9}L_{qr}^2 - 16L_{qr}^2\zeta_3 - \frac{88}{9}L_{qr}^3 - 40L_{fr} - \frac{400}{9}L_{fr}\zeta_3 + \frac{2672}{27}L_{fr}\zeta_2 - \frac{8}{5}L_{fr}\zeta_2^2 - \frac{146}{9}L_{fr}^2 + 16L_{fr}^2\zeta_3 - \frac{352}{9}L_{fr}^2\zeta_2 + \frac{88}{9}L_{fr}^3\right\} + C_F C_A^2\left\{-\frac{1505881}{972} - 204\zeta_5 + \frac{82385}{81}\zeta_3 - \frac{400}{3}\zeta_3^2 + 843\zeta_2 - \frac{884}{3}\zeta_2\zeta_3 + \frac{14611}{135}\zeta_2^2 + \frac{13264}{315}\zeta_2^3 + \frac{3082}{3}L_{qr} + 80L_{qr}\zeta_5 - \frac{4952}{9}L_{qr}\zeta_3 - 240L_{qr}\zeta_2 + \frac{68}{5}L_{qr}\zeta_2^2 - \frac{2429}{9}L_{qr}^2 + 88L_{qr}^2\zeta_3 + \frac{242}{9}L_{qr}^3 + \frac{1657}{18}L_{fr} - 80L_{fr}\zeta_5 + \frac{3104}{9}L_{fr}\zeta_3 - \frac{8992}{27}L_{fr}\zeta_2 + 4L_{fr}\zeta_2^2 + \frac{493}{9}L_{fr}^2 - 88L_{fr}^2\zeta_3 + \frac{968}{9}L_{fr}^2\zeta_2 - \frac{242}{9}L_{fr}^3\right\} + C_F^2 n_f\left\{-\frac{421}{3} - \frac{608}{9}\zeta_5 + \frac{6952}{27}\zeta_3 + \frac{2632}{27}\zeta_2 - \frac{896}{9}\zeta_2\zeta_3 - \frac{3568}{135}\zeta_2^2 + 230L_{qr} - \frac{368}{3}L_{qr}\zeta_3 - \frac{176}{3}L_{qr}\zeta_2 + \frac{112}{15}L_{qr}\zeta_2^2 - 92L_{qr}^2 + 32L_{qr}^2\zeta_3 + 12L_{qr}^3 - \frac{275}{3}L_{fr} + \frac{128}{3}L_{fr}\zeta_3 - \frac{56}{3}L_{fr}\zeta_2 + \frac{176}{15}L_{fr}\zeta_2^2 + 72L_{fr}L_{qr} + 32L_{fr}L_{qr}\zeta_2 - 12L_{fr}L_{qr}^2 + 20L_{fr}^2 - 32L_{fr}^2\zeta_3 - 32L_{fr}^2\zeta_2 - 12L_{fr}^2L_{qr} + 12L_{fr}^3\right\} + C_F^2 C_A\left\{\frac{74321}{36} - \frac{5512}{9}\zeta_5 - \frac{34612}{27}\zeta_3 + \frac{592}{3}\zeta_3^2 - \frac{13186}{27}\zeta_2 + \frac{3392}{9}\zeta_2\zeta_3\right.$$

$$+\frac{24064}{135}\zeta_2^2-\frac{36944}{315}\zeta_2^3-\frac{3439}{2}L_{qr}+240L_{qr}\zeta_5$$
$$+\frac{4664}{3}L_{qr}\zeta_3+\frac{632}{3}L_{qr}\zeta_2-160L_{qr}\zeta_2\zeta_3-\frac{256}{15}L_{qr}\zeta_2^2$$
$$+551L_{qr}^2-320L_{qr}^2\zeta_3-66L_{qr}^3+\frac{2348}{3}L_{fr}-240L_{fr}\zeta_5$$
$$-\frac{3344}{3}L_{fr}\zeta_3+\frac{908}{3}L_{fr}\zeta_2+160L_{fr}\zeta_2\zeta_3$$
$$-\frac{1328}{15}L_{fr}\zeta_2^2-420L_{fr}L_{qr}+288L_{fr}L_{qr}\zeta_3$$
$$-176L_{fr}L_{qr}\zeta_2+66L_{fr}L_{qr}^2-131L_{fr}^2+32L_{fr}^2\zeta_3$$
$$+176L_{fr}^2\zeta_2+66L_{fr}^2L_{qr}-66L_{fr}^3\Big\}+C_F^3\Big\{-\frac{5599}{6}$$
$$+1328\zeta_5-460\zeta_3+32\zeta_3^2-\frac{130}{3}\zeta_2+80\zeta_2\zeta_3$$
$$-\frac{612}{5}\zeta_2^2+\frac{25696}{315}\zeta_2^3+\frac{1495}{2}L_{qr}-480L_{qr}\zeta_5$$
$$-992L_{qr}\zeta_3+24L_{qr}\zeta_2+320L_{qr}\zeta_2\zeta_3+\frac{48}{5}L_{qr}\zeta_2^2$$
$$-270L_{qr}^2+288L_{qr}^2\zeta_3+36L_{qr}^3-\frac{1495}{2}L_{fr}$$
$$+480L_{fr}\zeta_5+992L_{fr}\zeta_3-24L_{fr}\zeta_2-320L_{fr}\zeta_2\zeta_3$$
$$-\frac{48}{5}L_{fr}\zeta_2^2+540L_{fr}L_{qr}-576L_{fr}L_{qr}\zeta_3-108L_{fr}L_{qr}^2$$
$$-270L_{fr}^2+288L_{fr}^2\zeta_3+108L_{fr}^2L_{qr}-36L_{fr}^3\Big\}. \quad \text{(C.25)}$$

In the aforementioned equations, n_{fv} is proportional to the charge weighted sum of the quark flavours and $N_4=(n_c^2-4)/n_c$ [107]. Here $L_{qr}=\ln\left(\frac{q^2}{\mu_R^2}\right)$ and $L_{fr}=\ln\left(\frac{\mu_F^2}{\mu_R^2}\right)$.

C.2 The N-independent coefficients $g_{0,i}^q$

The N-independent coefficients $g_{0,i}^q$ in Eq. (32), till three-loop, are given by

$$g_{0,0}^q=0, \quad \text{(C.26)}$$
$$g_{0,1}^q=C_F\Big\{8\zeta_2-8\gamma_E L_{qr}+8\gamma_E L_{fr}+8\gamma_E^2\Big\}, \quad \text{(C.27)}$$
$$g_{0,2}^q=C_F n_f\Big\{-\frac{64}{9}\zeta_3-\frac{80}{9}\zeta_2+\frac{16}{3}L_{qr}\zeta_2-\frac{224}{27}\gamma_E$$
$$+\frac{80}{9}\gamma_E L_{qr}-\frac{8}{3}\gamma_E L_{qr}^2-\frac{80}{9}\gamma_E L_{fr}+\frac{8}{3}\gamma_E L_{fr}^2-\frac{80}{9}\gamma_E^2$$
$$+\frac{16}{3}\gamma_E^2 L_{qr}-\frac{32}{9}\gamma_E^3\Big\}+C_F C_A\Big\{\frac{352}{9}\zeta_3+\frac{536}{9}\zeta_2$$
$$-16\zeta_2^2-\frac{88}{3}L_{qr}\zeta_2+\frac{1616}{27}\gamma_E-56\gamma_E\zeta_3$$
$$-\frac{536}{9}\gamma_E L_{qr}+16\gamma_E L_{qr}\zeta_2$$
$$+\frac{44}{3}\gamma_E L_{qr}^2+\frac{536}{9}\gamma_E L_{fr}-16\gamma_E L_{fr}\zeta_2-\frac{44}{3}\gamma_E L_{fr}^2$$
$$+\frac{536}{9}\gamma_E^2-16\gamma_E^2\zeta_2-\frac{88}{3}\gamma_E^2 L_{qr}+\frac{176}{9}\gamma_E^3\Big\}, \quad \text{(C.28)}$$

$$g_{0,3}^q=C_F n_f^2\Big\{\frac{1280}{81}\zeta_3+\frac{800}{81}\zeta_2-\frac{64}{45}\zeta_2^2-\frac{256}{27}L_{qr}\zeta_3$$
$$-\frac{320}{27}L_{qr}\zeta_2+\frac{32}{9}L_{qr}^2\zeta_2+\frac{3712}{729}\gamma_E+\frac{64}{9}\gamma_E\zeta_3$$
$$-\frac{800}{81}\gamma_E L_{qr}+\frac{160}{27}\gamma_E L_{qr}^2-\frac{32}{27}\gamma_E L_{qr}^3-\frac{32}{27}\gamma_E L_{fr}$$
$$-\frac{160}{27}\gamma_E L_{fr}^2+\frac{32}{27}\gamma_E L_{fr}^3+\frac{800}{81}\gamma_E^2-\frac{320}{27}\gamma_E^2 L_{qr}$$
$$+\frac{32}{9}\gamma_E^2 L_{qr}^2+\frac{640}{81}\gamma_E^3-\frac{128}{27}\gamma_E^3 L_{qr}+\frac{64}{27}\gamma_E^4\Big\}$$
$$+C_F C_A n_f\Big\{-\frac{18496}{81}\zeta_3-\frac{16408}{81}\zeta_2+\frac{256}{9}\zeta_2\zeta_3$$
$$+\frac{256}{5}\zeta_2^2+\frac{2816}{27}L_{qr}\zeta_3+\frac{4624}{27}L_{qr}\zeta_2-\frac{64}{3}L_{qr}\zeta_2^2$$
$$-\frac{352}{9}L_{qr}^2\zeta_2-\frac{125252}{729}\gamma_E+\frac{1808}{27}\gamma_E\zeta_3+\frac{1648}{81}\gamma_E\zeta_2$$
$$-\frac{32}{5}\gamma_E\zeta_2^2+\frac{16408}{81}\gamma_E L_{qr}-\frac{320}{9}\gamma_E L_{qr}\zeta_2$$
$$-\frac{2312}{27}\gamma_E L_{qr}^2+\frac{32}{3}\gamma_E L_{qr}^2\zeta_2+\frac{352}{27}\gamma_E L_{qr}^3$$
$$-\frac{1672}{27}\gamma_E L_{fr}-\frac{224}{3}\gamma_E L_{fr}\zeta_3+\frac{320}{9}\gamma_E L_{fr}\zeta_2$$
$$+\frac{2312}{27}\gamma_E L_{fr}^2-\frac{32}{3}\gamma_E L_{fr}^2\zeta_2-\frac{352}{27}\gamma_E L_{fr}^3-\frac{16408}{81}\gamma_E^2$$
$$+\frac{320}{9}\gamma_E^2\zeta_2+\frac{4624}{27}\gamma_E^2 L_{qr}-\frac{64}{3}\gamma_E^2 L_{qr}\zeta_2-\frac{352}{9}\gamma_E^2 L_{qr}^2$$
$$-\frac{9248}{81}\gamma_E^3+\frac{128}{9}\gamma_E^3\zeta_2+\frac{1408}{27}\gamma_E^3 L_{qr}-\frac{704}{27}\gamma_E^4\Big\}$$
$$+C_F C_A^2\Big\{\frac{56960}{81}\zeta_3+\frac{62012}{81}\zeta_2-\frac{4576}{9}\zeta_2\zeta_3$$
$$-\frac{12656}{45}\zeta_2^2+\frac{352}{5}\zeta_2^3-\frac{7744}{27}L_{qr}\zeta_3-\frac{14240}{27}L_{qr}\zeta_2$$
$$+\frac{352}{3}L_{qr}\zeta_2^2+\frac{968}{9}L_{qr}^2\zeta_2+\frac{594058}{729}\gamma_E+384\gamma_E\zeta_5$$
$$-\frac{24656}{27}\gamma_E\zeta_3-\frac{12784}{81}\gamma_E\zeta_2+\frac{352}{3}\gamma_E\zeta_2\zeta_3$$
$$-\frac{176}{5}\gamma_E\zeta_2^2-\frac{62012}{81}\gamma_E L_{qr}+352\gamma_E L_{qr}\zeta_3$$
$$+\frac{2144}{9}\gamma_E L_{qr}\zeta_2-\frac{352}{5}\gamma_E L_{qr}\zeta_2^2+\frac{7120}{27}\gamma_E L_{qr}^2$$
$$-\frac{176}{3}\gamma_E L_{qr}^2\zeta_2-\frac{968}{27}\gamma_E L_{qr}^3+\frac{980}{3}\gamma_E L_{fr}$$
$$+\frac{176}{3}\gamma_E L_{fr}\zeta_3-\frac{2144}{9}\gamma_E L_{fr}\zeta_2+\frac{352}{5}\gamma_E L_{fr}\zeta_2^2$$
$$-\frac{7120}{27}\gamma_E L_{fr}^2+\frac{176}{3}\gamma_E L_{fr}^2\zeta_2+\frac{968}{27}\gamma_E L_{fr}^3$$
$$+\frac{62012}{81}\gamma_E^2-352\gamma_E^2\zeta_3-\frac{2144}{9}\gamma_E^2\zeta_2+\frac{352}{5}\gamma_E^2\zeta_2^2$$
$$-\frac{14240}{27}\gamma_E^2 L_{qr}+\frac{352}{3}\gamma_E^2 L_{qr}\zeta_2+\frac{968}{9}\gamma_E^2 L_{qr}^2$$
$$+\frac{28480}{81}\gamma_E^3-\frac{704}{9}\gamma_E^3\zeta_2-\frac{3872}{27}\gamma_E^3 L_{qr}+\frac{1936}{27}\gamma_E^4\Big\}$$
$$+C_F^2 n_f\Big\{-\frac{64}{3}\zeta_3-\frac{220}{3}\zeta_2+64\zeta_2\zeta_3+16L_{qr}\zeta_2$$
$$-\frac{3422}{27}\gamma_E+\frac{608}{9}\gamma_E\zeta_3$$
$$+\frac{64}{5}\gamma_E\zeta_2^2+\frac{220}{3}\gamma_E L_{qr}-64\gamma_E L_{qr}\zeta_3$$

$$- 8\gamma_E L_{qr}^2 - \frac{220}{3}\gamma_E L_{fr} + 64\gamma_E L_{fr}\zeta_3 + 8\gamma_E L_{fr}^2 - \frac{220}{3}\gamma_E^2 + 64\gamma_E^2\zeta_3 + 16\gamma_E^2 L_{qr} - \frac{32}{3}\gamma_E^3\Bigg\}. \tag{C.29}$$

Here, γ_E is the Euler–Mascheroni constant.

C.3 The N-independent coefficients $\tilde{g}_0^q$

The N-independent coefficients $\tilde{g}_{0,i}^q$ in Eq. (33), till three-loop, are given by

$$\tilde{g}_{0,0}^q = 1, \tag{C.30}$$

$$\tilde{g}_{0,1}^q = C_F\Bigg\{-16 + 16\zeta_2 + 6L_{qr} - 6L_{fr} - 8\gamma_E L_{qr} + 8\gamma_E L_{fr} + 8\gamma_E^2\Bigg\}, \tag{C.31}$$

$$\begin{aligned}
\tilde{g}_{0,2}^q = {} & C_F n_f\Bigg\{\frac{127}{6} + \frac{8}{9}\zeta_3 - \frac{64}{3}\zeta_2 - \frac{34}{3}L_{qr} + \frac{16}{3}L_{qr}\zeta_2 \\
& + 2L_{qr}^2 + \frac{2}{3}L_{fr} + \frac{16}{3}L_{fr}\zeta_2 - 2L_{fr}^2 - \frac{224}{27}\gamma_E \\
& + \frac{80}{9}\gamma_E L_{qr} - \frac{8}{3}\gamma_E L_{qr}^2 - \frac{80}{9}\gamma_E L_{fr} + \frac{8}{3}\gamma_E L_{fr}^2 - \frac{80}{9}\gamma_E^2 \\
& + \frac{16}{3}\gamma_E^2 L_{qr} - \frac{32}{9}\gamma_E^3\Bigg\} + C_F C_A\Bigg\{-\frac{1535}{12} + \frac{604}{9}\zeta_3 \\
& + \frac{376}{3}\zeta_2 - \frac{92}{5}\zeta_2^2 + \frac{193}{3}L_{qr} - 24L_{qr}\zeta_3 - \frac{88}{3}L_{qr}\zeta_2 \\
& - 11L_{qr}^2 - \frac{17}{3}L_{fr} + 24L_{fr}\zeta_3 - \frac{88}{3}L_{fr}\zeta_2 + 11L_{fr}^2 \\
& + \frac{1616}{27}\gamma_E - 56\gamma_E\zeta_3 - \frac{536}{9}\gamma_E L_{qr} + 16\gamma_E L_{qr}\zeta_2 \\
& + \frac{44}{3}\gamma_E L_{qr}^2 + \frac{536}{9}\gamma_E L_{fr} - 16\gamma_E L_{fr}\zeta_2 - \frac{44}{3}\gamma_E L_{fr}^2 \\
& + \frac{536}{9}\gamma_E^2 - 16\gamma_E^2\zeta_2 - \frac{88}{3}\gamma_E^2 L_{qr} + \frac{176}{9}\gamma_E^3\Bigg\} + C_F^2\Bigg\{ \\
& + \frac{511}{4} - 60\zeta_3 - 198\zeta_2 + \frac{552}{5}\zeta_2^2 - 93L_{qr} + 48L_{qr}\zeta_3 \\
& + 72L_{qr}\zeta_2 + 18L_{qr}^2 + 93L_{fr} - 48L_{fr}\zeta_3 - 72L_{fr}\zeta_2 \\
& - 36L_{fr}L_{qr} + 18L_{fr}^2 + 128\gamma_E L_{qr} - 128\gamma_E L_{qr}\zeta_2 \\
& - 48\gamma_E L_{qr}^2 - 128\gamma_E L_{fr} + 128\gamma_E L_{fr}\zeta_2 + 96\gamma_E L_{fr}L_{qr} \\
& - 48\gamma_E L_{fr}^2 - 128\gamma_E^2 + 128\gamma_E^2\zeta_2 + 48\gamma_E^2 L_{qr} + 32\gamma_E^2 L_{qr}^2 - 48\gamma_E^2 L_{fr} \\
& - 64\gamma_E^2 L_{fr}L_{qr} + 32\gamma_E^2 L_{fr}^2 - 64\gamma_E^3 L_{qr} + 64\gamma_E^3 L_{fr} + 32\gamma_E^4\Bigg\},
\end{aligned} \tag{C.32}$$

$$\begin{aligned}
\tilde{g}_{0,3}^q = {} & C_F N_4 n_{fv}\Bigg\{8 - \frac{160}{3}\zeta_5 + \frac{28}{3}\zeta_3 + 20\zeta_2 - \frac{4}{5}\zeta_2^2\Bigg\} \\
& + C_F n_f^2\Bigg\{-\frac{7081}{243} + \frac{16}{81}\zeta_3 + \frac{1072}{27}\zeta_2 + \frac{448}{135}\zeta_2^2 \\
& + \frac{220}{9}L_{qr} - \frac{64}{27}L_{qr}\zeta_3 - \frac{608}{27}L_{qr}\zeta_2 - \frac{68}{9}L_{qr}^2 \\
& + \frac{32}{9}L_{qr}^2\zeta_2 + \frac{8}{9}L_{qr}^3 + \frac{34}{9}L_{fr} + \frac{32}{9}L_{fr}\zeta_3 - \frac{160}{27}L_{fr}\zeta_2 \\
& + \frac{4}{9}L_{fr}^2 + \frac{32}{9}L_{fr}^2\zeta_2 - \frac{8}{9}L_{fr}^3 + \frac{3712}{729}\gamma_E + \frac{64}{9}\gamma_E\zeta_3 \\
& - \frac{800}{81}\gamma_E L_{qr} + \frac{160}{27}\gamma_E L_{qr}^2 - \frac{32}{27}\gamma_E L_{qr}^3 - \frac{160}{27}\gamma_E L_{fr}^2 \\
& + \frac{32}{27}\gamma_E L_{fr}^3 + \frac{800}{81}\gamma_E^2 - \frac{320}{27}\gamma_E^2 L_{qr} + \frac{32}{9}\gamma_E^2 L_{qr}^2 \\
& + \frac{640}{81}\gamma_E^3 - \frac{128}{27}\gamma_E^3 L_{qr} + \frac{64}{27}\gamma_E^4\Bigg\} + C_F C_A n_f\Bigg\{\frac{110651}{243} \\
& - 8\zeta_5 - \frac{24512}{81}\zeta_3 - \frac{44540}{81}\zeta_2 + \frac{880}{9}\zeta_2\zeta_3 + \frac{1156}{135}\zeta_2^2 \\
& - \frac{3052}{9}L_{qr} + \frac{3440}{27}L_{qr}\zeta_3 + \frac{7504}{27}L_{qr}\zeta_2 - \frac{344}{15}L_{qr}\zeta_2^2 \\
& + \frac{850}{9}L_{qr}^2 - 16L_{qr}^2\zeta_3 - \frac{352}{9}L_{qr}^2\zeta_2 - \frac{88}{9}L_{qr}^3 - 40L_{fr} \\
& - \frac{400}{9}L_{fr}\zeta_3 + \frac{2672}{27}L_{fr}\zeta_2 - \frac{8}{5}L_{fr}\zeta_2^2 - \frac{146}{9}L_{fr}^2 \\
& + 16L_{fr}^2\zeta_3 - \frac{352}{9}L_{fr}^2\zeta_2 + \frac{88}{9}L_{fr}^3 - \frac{125252}{729}\gamma_E \\
& + \frac{1808}{27}\gamma_E\zeta_3 + \frac{1648}{81}\gamma_E\zeta_2 - \frac{32}{5}\gamma_E\zeta_2^2 + \frac{16408}{81}\gamma_E L_{qr} \\
& - \frac{320}{9}\gamma_E L_{qr}\zeta_2 - \frac{2312}{27}\gamma_E L_{qr}^2 + \frac{32}{3}\gamma_E L_{qr}^2\zeta_2 \\
& + \frac{352}{27}\gamma_E L_{qr}^3 - \frac{1672}{27}\gamma_E L_{fr} - \frac{224}{3}\gamma_E L_{fr}\zeta_3 \\
& + \frac{320}{9}\gamma_E L_{fr}\zeta_2 + \frac{2312}{27}\gamma_E L_{fr}^2 - \frac{32}{3}\gamma_E L_{fr}^2\zeta_2 \\
& - \frac{352}{27}\gamma_E L_{fr}^3 - \frac{16408}{81}\gamma_E^2 + \frac{320}{9}\gamma_E^2\zeta_2 + \frac{4624}{27}\gamma_E^2 L_{qr} \\
& - \frac{64}{3}\gamma_E^2 L_{qr}\zeta_2 - \frac{352}{9}\gamma_E^2 L_{qr}^2 - \frac{9248}{81}\gamma_E^3 + \frac{128}{9}\gamma_E^3\zeta_2 \\
& + \frac{1408}{27}\gamma_E^3 L_{qr} - \frac{704}{27}\gamma_E^4\Bigg\} + C_F C_A^2\Bigg\{-\frac{1505881}{972} \\
& - 204\zeta_5 + \frac{139345}{81}\zeta_3 - \frac{400}{3}\zeta_3^2 + \frac{130295}{81}\zeta_2 \\
& - \frac{7228}{9}\zeta_2\zeta_3 - \frac{23357}{135}\zeta_2^2 + \frac{7088}{63}\zeta_2^3 + \frac{3082}{3}L_{qr} \\
& + 80L_{qr}\zeta_5 - \frac{22600}{27}L_{qr}\zeta_3 - \frac{20720}{27}L_{qr}\zeta_2 \\
& + \frac{1964}{15}L_{qr}\zeta_2^2 - \frac{2429}{9}L_{qr}^2 + 88L_{qr}^2\zeta_3 + \frac{968}{9}L_{qr}^2\zeta_2 \\
& + \frac{242}{9}L_{qr}^3 + \frac{1657}{18}L_{fr} - 80L_{fr}\zeta_5 + \frac{3104}{9}L_{fr}\zeta_3 \\
& - \frac{8992}{27}L_{fr}\zeta_2 + 4L_{fr}\zeta_2^2 + \frac{493}{9}L_{fr}^2 - 88L_{fr}^2\zeta_3 \\
& + \frac{968}{9}L_{fr}^2\zeta_2 - \frac{242}{9}L_{fr}^3 + \frac{594058}{729}\gamma_E + 384\gamma_E\zeta_5 \\
& - \frac{24656}{27}\gamma_E\zeta_3 - \frac{12784}{81}\gamma_E\zeta_2 + \frac{352}{3}\gamma_E\zeta_2\zeta_3 \\
& - \frac{176}{5}\gamma_E\zeta_2^2 - \frac{62012}{81}\gamma_E L_{qr} + 352\gamma_E L_{qr}\zeta_3 \\
& + \frac{2144}{9}\gamma_E L_{qr}\zeta_2 - \frac{352}{5}\gamma_E L_{qr}\zeta_2^2 + \frac{7120}{27}\gamma_E L_{qr}^2 \\
& - \frac{176}{3}\gamma_E L_{qr}^2\zeta_2 - \frac{968}{27}\gamma_E L_{qr}^3 + \frac{980}{3}\gamma_E L_{fr} + \frac{176}{3}\gamma_E L_{fr}\zeta_3 \\
& - \frac{2144}{9}\gamma_E L_{fr}\zeta_2 + \frac{352}{5}\gamma_E L_{fr}\zeta_2^2 - \frac{7120}{27}\gamma_E L_{fr}^2 \\
& + \frac{176}{3}\gamma_E L_{fr}^2\zeta_2 + \frac{968}{27}\gamma_E L_{fr}^3 \\
& + \frac{62012}{81}\gamma_E^2 - 352\gamma_E^2\zeta_3 - \frac{2144}{9}\gamma_E^2\zeta_2 + \frac{352}{5}\gamma_E^2\zeta_2^2 \\
& - \frac{14240}{27}\gamma_E^2 L_{qr} + \frac{352}{3}\gamma_E^2 L_{qr}\zeta_2 + \frac{968}{9}\gamma_E^2 L_{qr}^2 \\
& + \frac{28480}{81}\gamma_E^3 - \frac{704}{9}\gamma_E^3\zeta_2 - \frac{3872}{27}\gamma_E^3 L_{qr} + \frac{1936}{27}\gamma_E^4\Bigg\}
\end{aligned}$$

$$
\begin{aligned}
&+ C_F^2 n_f \Big\{ - \frac{421}{3} - \frac{608}{9}\zeta_5 + \frac{9448}{27}\zeta_3 + \frac{9064}{27}\zeta_2 \\
&- \frac{256}{3}\zeta_2\zeta_3 - \frac{36208}{135}\zeta_2^2 + 230 L_{qr} - \frac{496}{3} L_{qr}\zeta_3 \\
&- 272 L_{qr}\zeta_2 + \frac{464}{5} L_{qr}\zeta_2^2 - 92 L_{qr}^2 + 32 L_{qr}^2\zeta_3 \\
&+ 48 L_{qr}^2\zeta_2 + 12 L_{qr}^3 - \frac{275}{3} L_{fr} + \frac{256}{3} L_{fr}\zeta_3 + 40 L_{fr}\zeta_2 \\
&+ \frac{272}{5} L_{fr}\zeta_2^2 + 72 L_{fr} L_{qr} - 12 L_{fr} L_{qr}^2 + 20 L_{fr}^2 \\
&- 32 L_{fr}^2\zeta_3 - 48 L_{fr}^2\zeta_2 - 12 L_{fr}^2 L_{qr} + 12 L_{fr}^3 + 6\gamma_E \\
&+ \frac{608}{9}\gamma_E\zeta_3 - \frac{3584}{27}\gamma_E\zeta_2 + \frac{64}{5}\gamma_E\zeta_2^2 - 288\gamma_E L_{qr} \\
&- \frac{640}{9}\gamma_E L_{qr}\zeta_3 + \frac{2816}{9}\gamma_E L_{qr}\zeta_2 + \frac{536}{3}\gamma_E L_{qr}^2 \\
&- \frac{256}{3}\gamma_E L_{qr}^2\zeta_2 - 32\gamma_E L_{qr}^3 + 288\gamma_E L_{fr} + \frac{640}{9}\gamma_E L_{fr}\zeta_3 \\
&- \frac{2816}{9}\gamma_E L_{fr}\zeta_2 - \frac{608}{3}\gamma_E L_{fr} L_{qr} + 32\gamma_E L_{fr} L_{qr}^2 \\
&+ 24\gamma_E L_{fr}^2 + \frac{256}{3}\gamma_E L_{fr}^2\zeta_2 + 32\gamma_E L_{fr}^2 L_{qr} - 32\gamma_E L_{fr}^3 \\
&+ \frac{2144}{9}\gamma_E^2 + \frac{640}{9}\gamma_E^2\zeta_3 - \frac{2816}{9}\gamma_E^2\zeta_2 - \frac{3968}{27}\gamma_E^2 L_{qr} \\
&+ 128\gamma_E^2 L_{qr}\zeta_2 - \frac{208}{9}\gamma_E^2 L_{qr}^2 + \frac{64}{3}\gamma_E^2 L_{qr}^3 - \frac{208}{27}\gamma_E^2 L_{fr} \\
&+ \frac{128}{3}\gamma_E^2 L_{fr}\zeta_2 + \frac{992}{9}\gamma_E^2 L_{fr} L_{qr} - \frac{64}{3}\gamma_E^2 L_{fr} L_{qr}^2 \\
&- \frac{784}{9}\gamma_E^2 L_{fr}^2 - \frac{64}{3}\gamma_E^2 L_{fr}^2 L_{qr} + \frac{64}{3}\gamma_E^2 L_{fr}^3 - \frac{544}{27}\gamma_E^3 \\
&- \frac{512}{9}\gamma_E^3\zeta_2 + \frac{1088}{9}\gamma_E^3 L_{qr} - 64\gamma_E^3 L_{qr}^2 - \frac{1088}{9}\gamma_E^3 L_{fr} \\
&+ \frac{128}{3}\gamma_E^3 L_{fr} L_{qr} + \frac{64}{3}\gamma_E^3 L_{fr}^2 - \frac{640}{9}\gamma_E^4 + \frac{640}{9}\gamma_E^4 L_{qr} \\
&- \frac{256}{9}\gamma_E^4 L_{fr} - \frac{256}{9}\gamma_E^5 \Big\} + C_F^2 C_A \Big\{ + \frac{74321}{36} \\
&- \frac{5512}{9}\zeta_5 - \frac{51508}{27}\zeta_3 + \frac{592}{3}\zeta_3^2 - \frac{66544}{27}\zeta_2 \\
&+ \frac{3680}{3}\zeta_2\zeta_3 + \frac{258304}{135}\zeta_2^2 - \frac{123632}{315}\zeta_2^3 - \frac{3439}{2} L_{qr} \\
&+ 240 L_{qr}\zeta_5 + \frac{5368}{3} L_{qr}\zeta_3 + 1552 L_{qr}\zeta_2 - 352 L_{qr}\zeta_2\zeta_3 \\
&- \frac{2912}{5} L_{qr}\zeta_2^2 + 551 L_{qr}^2 - 320 L_{qr}^2\zeta_3 - 264 L_{qr}^2\zeta_2 \\
&- 66 L_{qr}^3 + \frac{2348}{3} L_{fr} - 240 L_{fr}\zeta_5 - \frac{4048}{3} L_{fr}\zeta_3 \\
&- 100 L_{fr}\zeta_2 + 352 L_{fr}\zeta_2\zeta_3 - \frac{1136}{5} L_{fr}\zeta_2^2 \\
&- 420 L_{fr} L_{qr} + 288 L_{fr} L_{qr}\zeta_3 + 66 L_{fr} L_{qr}^2 - 131 L_{fr}^2 \\
&+ 32 L_{fr}^2\zeta_3 + 264 L_{fr}^2\zeta_2 + 66 L_{fr}^2 L_{qr} - 66 L_{fr}^3 \\
&- \frac{25856}{27}\gamma_E + 896\gamma_E\zeta_3 + \frac{25856}{27}\gamma_E\zeta_2 - 896\gamma_E\zeta_2\zeta_3 \\
&+ \frac{7006}{3}\gamma_E L_{qr} - \frac{7856}{9}\gamma_E L_{qr}\zeta_3 - \frac{19904}{9}\gamma_E L_{qr}\zeta_2 \\
&+ \frac{2016}{5}\gamma_E L_{qr}\zeta_2^2 - \frac{3320}{3}\gamma_E L_{qr}^2 + 192\gamma_E L_{qr}^2\zeta_3 \\
&+ \frac{1696}{3}\gamma_E L_{qr}^2\zeta_2 + 176\gamma_E L_{qr}^3 - \frac{7006}{3}\gamma_E L_{fr} \\
&+ \frac{7856}{9}\gamma_E L_{fr}\zeta_3 + \frac{19904}{9}\gamma_E L_{fr}\zeta_2 - \frac{2016}{5}\gamma_E L_{fr}\zeta_2^2 \\
&+ \frac{3824}{3}\gamma_E L_{fr} L_{qr} - 384\gamma_E L_{fr} L_{qr}\zeta_3 - 192\gamma_E L_{fr} L_{qr}\zeta_2 \\
&- 176\gamma_E L_{fr} L_{qr}^2 - 168\gamma_E L_{fr}^2 + 192\gamma_E L_{fr}^2\zeta_3 \\
&- \frac{1120}{3}\gamma_E L_{fr}^2\zeta_2 - 176\gamma_E L_{fr}^2 L_{qr} + 176\gamma_E L_{fr}^3 \\
&- \frac{17786}{9}\gamma_E^2 + \frac{4832}{9}\gamma_E^2\zeta_3 + \frac{19904}{9}\gamma_E^2\zeta_2 - \frac{2016}{5}\gamma_E^2\zeta_2^2 \\
&+ \frac{23288}{27}\gamma_E^2 L_{qr} + 256\gamma_E^2 L_{qr}\zeta_3 - 800\gamma_E^2 L_{qr}\zeta_2 \\
&+ \frac{1912}{9}\gamma_E^2 L_{qr}^2 - 128\gamma_E^2 L_{qr}^2\zeta_2 - \frac{352}{3}\gamma_E^2 L_{qr}^3 \\
&+ \frac{2056}{27}\gamma_E^2 L_{fr} - 256\gamma_E^2 L_{fr}\zeta_3 - \frac{416}{3}\gamma_E^2 L_{fr}\zeta_2 \\
&- \frac{6992}{9}\gamma_E^2 L_{fr} L_{qr} + 256\gamma_E^2 L_{fr} L_{qr}\zeta_2 + \frac{352}{3}\gamma_E^2 L_{fr} L_{qr}^2 \\
&+ \frac{5080}{9}\gamma_E^2 L_{fr}^2 - 128\gamma_E^2 L_{fr}^2\zeta_2 + \frac{352}{3}\gamma_E^2 L_{fr}^2 L_{qr} \\
&- \frac{352}{3}\gamma_E^2 L_{fr}^3 + \frac{4480}{27}\gamma_E^3 - 448\gamma_E^3\zeta_3 + \frac{2816}{9}\gamma_E^3\zeta_2 \\
&- \frac{7520}{9}\gamma_E^3 L_{qr} + 256\gamma_E^3 L_{qr}\zeta_2 + 352\gamma_E^3 L_{qr}^2 \\
&+ \frac{7520}{9}\gamma_E^3 L_{fr} - 256\gamma_E^3 L_{fr}\zeta_2 - \frac{704}{3}\gamma_E^3 L_{fr} L_{qr} \\
&- \frac{352}{3}\gamma_E^3 L_{fr}^2 + \frac{4288}{9}\gamma_E^4 - 128\gamma_E^4\zeta_2 - \frac{3520}{9}\gamma_E^4 L_{qr} \\
&+ \frac{1408}{9}\gamma_E^4 L_{fr} + \frac{1408}{9}\gamma_E^5 \Big\} + C_F^3 \Big\{ - \frac{5599}{6} + 1328\zeta_5 \\
&- 460\zeta_3 + 32\zeta_3^2 + \frac{2936}{3}\zeta_2 - 400\zeta_2\zeta_3 - \frac{5972}{5}\zeta_2^2 \\
&+ \frac{169504}{315}\zeta_2^3 + \frac{1495}{2} L_{qr} - 480 L_{qr}\zeta_5 - 992 L_{qr}\zeta_3 \\
&- 720 L_{qr}\zeta_2 + 704 L_{qr}\zeta_2\zeta_3 + \frac{1968}{5} L_{qr}\zeta_2^2 - 270 L_{qr}^2 \\
&+ 288 L_{qr}^2\zeta_3 + 144 L_{qr}^2\zeta_2 + 36 L_{qr}^3 - \frac{1495}{2} L_{fr} \\
&+ 480 L_{fr}\zeta_5 + 992 L_{fr}\zeta_3 + 720 L_{fr}\zeta_2 - 704 L_{fr}\zeta_2\zeta_3 \\
&- \frac{1968}{5} L_{fr}\zeta_2^2 + 540 L_{fr} L_{qr} - 576 L_{fr} L_{qr}\zeta_3 - 288 L_{fr} L_{qr}\zeta_2 \\
&- 108 L_{fr} L_{qr}^2 - 270 L_{fr}^2 \\
&+ 288 L_{fr}^2\zeta_3 + 144 L_{fr}^2\zeta_2 + 108 L_{fr}^2 L_{qr} \\
&- 36 L_{fr}^3 - 1022\gamma_E L_{qr} \\
&+ 480\gamma_E L_{qr}\zeta_3 + 1584\gamma_E L_{qr}\zeta_2 - \frac{4416}{5}\gamma_E L_{qr}\zeta_2^2 \\
&+ 744\gamma_E L_{qr}^2 - 384\gamma_E L_{qr}^2\zeta_3 - 576\gamma_E L_{qr}^2\zeta_2 - 144\gamma_E L_{qr}^3 \\
&+ 1022\gamma_E L_{fr} - 480\gamma_E L_{fr}\zeta_3 - 1584\gamma_E L_{fr}\zeta_2 \\
&+ \frac{4416}{5}\gamma_E L_{fr}\zeta_2^2 - 1488\gamma_E L_{fr} L_{qr} + 768\gamma_E L_{fr} L_{qr}\zeta_3 \\
&+ 1152\gamma_E L_{fr} L_{qr}\zeta_2 + 432\gamma_E L_{fr} L_{qr}^2 + 744\gamma_E L_{fr}^2 \\
&- 384\gamma_E L_{fr}^2\zeta_3 - 576\gamma_E L_{fr}^2\zeta_2 - 432\gamma_E L_{fr}^2 L_{qr} \\
&+ 144\gamma_E L_{fr}^3 + 1022\gamma_E^2 - 480\gamma_E^2\zeta_3 - 1584\gamma_E^2\zeta_2 \\
&+ \frac{4416}{5}\gamma_E^2\zeta_2^2 - 744\gamma_E^2 L_{qr} + 384\gamma_E^2 L_{qr}\zeta_3 \\
&+ 576\gamma_E^2 L_{qr}\zeta_2 - 368\gamma_E^2 L_{qr}^2 + 512\gamma_E^2 L_{qr}^2\zeta_2 + 192\gamma_E^2 L_{qr}^3 \\
&+ 744\gamma_E^2 L_{fr} - 384\gamma_E^2 L_{fr}\zeta_3 - 576\gamma_E^2 L_{fr}\zeta_2 \\
&+ 736\gamma_E^2 L_{fr} L_{qr} - 1024\gamma_E^2 L_{fr} L_{qr}\zeta_2 - 576\gamma_E^2 L_{fr} L_{qr}^2 \\
&- 368\gamma_E^2 L_{fr}^2 + 512\gamma_E^2 L_{fr}^2\zeta_2 + 576\gamma_E^2 L_{fr}^2 L_{qr} \\
&- 192\gamma_E^2 L_{fr}^3 + 1024\gamma_E^3 L_{qr} - 1024\gamma_E^3 L_{qr}\zeta_2 - 384\gamma_E^3 L_{qr}^2 \\
&- \frac{256}{3}\gamma_E^3 L_{qr}^3 - 1024\gamma_E^3 L_{fr} + 1024\gamma_E^3 L_{fr}\zeta_2
\end{aligned}
$$

$$+768\gamma_E^3 L_{fr} L_{qr} + 256\gamma_E^3 L_{fr} L_{qr}^2 - 384\gamma_E^3 L_{fr}^2 - 256\gamma_E^3 L_{fr}^2 L_{qr} + \frac{256}{3}\gamma_E^3 L_{fr}^3 - 512\gamma_E^4 + 512\gamma_E^4\zeta_2 + 192\gamma_E^4 L_{qr} + 256\gamma_E^4 L_{qr}^2 - 192\gamma_E^4 L_{fr} - 512\gamma_E^4 L_{fr} L_{qr} + 256\gamma_E^4 L_{fr}^2 - 256\gamma_E^5 L_{qr} + 256\gamma_E^5 L_{fr} + \frac{256}{3}\gamma_E^6\Big\}. \quad \text{(C.33)}$$

C.4 The SV resummed exponent g_i^q

The resummation exponents g_i^q in Eq. (31), till three-loop, are given by

$$g_1^q = \frac{1}{\beta_0} C_F \left\{ 8 + \frac{8}{\omega} L_\omega - 8 L_\omega \right\}, \quad \text{(C.34)}$$

$$g_2^q = \frac{\beta_1}{\beta_0^3} C_F \left\{ 4\omega + 4L_\omega + 2L_\omega^2 \right\} + \frac{1}{\beta_0^2} C_F n_f \left\{ \frac{40}{9}\omega + \frac{40}{9} L_\omega \right\} + \frac{1}{\beta_0^2} C_F C_A \left\{ -\frac{268}{9}\omega + 8\omega\zeta_2 - \frac{268}{9} L_\omega + 8 L_\omega \zeta_2 \right\} + \frac{1}{\beta_0} C_F \left\{ 4\omega L_{fr} + 4 L_\omega L_{qr} - 8 L_\omega \gamma_E \right\}, \quad \text{(C.35)}$$

$$g_3^q = \frac{1}{(1-\omega)} \Bigg[\frac{\beta_1^2}{\beta_0^4} C_F \left\{ 2\omega^2 + 4L_\omega\omega + 2L_\omega^2 \right\} + \frac{\beta_2}{\beta_0^3} C_F \left\{ 4\omega - 2\omega^2 \right\} + \frac{\beta_1}{\beta_0^3} C_F n_f \left\{ \frac{40}{9}\omega + \frac{20}{9}\omega^2 + \frac{40}{9} L_\omega \right\} + \frac{\beta_1}{\beta_0^3} C_F C_A \left\{ -\frac{268}{9}\omega + 8\omega\zeta_2 - \frac{134}{9}\omega^2 + 4\omega^2\zeta_2 - \frac{268}{9} L_\omega + 8 L_\omega \zeta_2 \right\} + \frac{1}{\beta_0^2} C_F n_f^2 \left\{ -\frac{8}{27} \right\} + \frac{1}{\beta_0^2} C_F C_A n_f \left\{ -\frac{418}{27} - \frac{56}{3}\zeta_3 + \frac{80}{9}\zeta_2 \right\} + \frac{1}{\beta_0^2} C_F C_A^2 \times \left\{ \frac{245}{3} + \frac{44}{3}\zeta_3 - \frac{536}{9}\zeta_2 + \frac{88}{5}\zeta_2^2 \right\} + \frac{1}{\beta_0^2} C_F^2 n_f \left\{ -\frac{55}{3} + 16\zeta_3 \right\} + \frac{\beta_1}{\beta_0^2} C_F \left\{ 4\omega L_{qr} - 8\omega\gamma_E + 4 L_\omega L_{qr} - 8 L_\omega \gamma_E \right\} + \frac{1}{\beta_0} C_F n_f \left\{ -\frac{112}{27} + \frac{4}{3}\zeta_2 + \frac{40}{9} L_{qr} - \frac{80}{9}\gamma_E \right\} + \frac{1}{\beta_0} C_F C_A \left\{ \frac{808}{27} - 28\zeta_3 - \frac{22}{3}\zeta_2 - \frac{268}{9} L_{qr} + 8 L_{qr}\zeta_2 + \frac{536}{9}\gamma_E - 16\gamma_E\zeta_2 \right\} + C_F \left\{ 2\zeta_2 + 2L_{qr}^2 - 8\gamma_E L_{qr} + 8\gamma_E^2 \right\} \Bigg] + C_F \left\{ -2\zeta_2 - 2L_{qr}^2 + 8\gamma_E L_{qr} - 8\gamma_E^2 - 2\omega L_{fr}^2 \right\} + \frac{\beta_2}{\beta_0^3} C_F \left\{ 4 L_\omega \right\} + \frac{1}{\beta_0} C_F n_f \left\{ \frac{112}{27} - \frac{4}{3}\zeta_2 - \frac{40}{9} L_{qr} + \frac{80}{9}\gamma_E - \frac{40}{9}\omega L_{fr} \right\} + \frac{1}{\beta_0} C_F C_A \left\{ -\frac{808}{27} + 28\zeta_3 + \frac{22}{3}\zeta_2 + \frac{268}{9} L_{qr} - 8 L_{qr}\zeta_2 - \frac{536}{9}\gamma_E + 16\gamma_E\zeta_2 + \frac{268}{9}\omega L_{fr} - 8\omega L_{fr}\zeta_2 \right\} + \frac{1}{\beta_0^2} C_F^2 n_f \left\{ \frac{55}{3} - 16\zeta_3 + \frac{55}{3}\omega - 16\omega\zeta_3 \right\} + \frac{1}{\beta_0^2} C_F n_f^2 \left\{ \frac{8}{27} + \frac{8}{27}\omega \right\} + \frac{1}{\beta_0^2} C_F C_A n_f \left\{ \frac{418}{27} + \frac{56}{3}\zeta_3 - \frac{80}{9}\zeta_2 + \frac{418}{27}\omega + \frac{56}{3}\omega\zeta_3 - \frac{80}{9}\omega\zeta_2 \right\} + \frac{1}{\beta_0^2} C_F C_A^2 \left\{ -\frac{245}{3} - \frac{44}{3}\zeta_3 + \frac{536}{9}\zeta_2 - \frac{88}{5}\zeta_2^2 - \frac{245}{3}\omega - \frac{44}{3}\omega\zeta_3 + \frac{536}{9}\omega\zeta_2 - \frac{88}{5}\omega\zeta_2^2 \right\}, \quad \text{(C.36)}$$

Here, $L_\omega = \ln(1-\omega)$ and $\omega = 2\beta_0 a_s(\mu_R^2)\ln N$. And β_i's are the QCD β functions which are given by

$$\beta_0 = \frac{11}{3} C_A - \frac{2}{3} n_f\,,$$
$$\beta_1 = \frac{34}{3} C_A^2 - 2 n_f C_F - \frac{10}{3} n_f C_A,$$
$$\beta_2 = \frac{2857}{54} C_A^3 - \frac{1415}{54} C_A^2 n_f + \frac{79}{54} C_A n_f^2 + \frac{11}{9} C_F n_f^2 - \frac{205}{18} C_F C_A n_f + C_F^2 n_f. \quad \text{(C.37)}$$

C.5 The NSV resummed exponents $\overline{g}_i^q$

The resummation exponents $\overline{g}_i^q$ in (34), till three-loop, are given by

$$\overline{g}_1^q = \frac{1}{\beta_0} C_F \left\{ 4 L_\omega \right\}, \quad \text{(C.38)}$$

$$\overline{g}_2^q = \frac{1}{(1-\omega)} \Bigg[\frac{1}{\beta_0^2} C_F C_A n_f \left\{ -\frac{40}{3}\omega - \frac{40}{3} L_\omega \right\} + \frac{1}{\beta_0^2} C_F C_A^2 \left\{ \frac{136}{3}\omega + \frac{136}{3} L_\omega \right\} + \frac{1}{\beta_0^2} C_F^2 n_f \left\{ -8\omega - 8 L_\omega \right\} + \frac{1}{\beta_0} C_F n_f \left\{ \frac{40}{9}\omega \right\} + \frac{1}{\beta_0} C_F C_A \left\{ -\frac{268}{9}\omega + 8\omega\zeta_2 \right\} + C_F \left\{ -8 + 4L_{qr} - 4L_{fr} + 4L_{fr}\omega - 8\gamma_E \right\} \Bigg], \quad \text{(C.39)}$$

$$\overline{g}_3^q = \frac{1}{(1-\omega)^2} \Bigg[\frac{1}{\beta_0^3} C_F C_A^2 n_f^2 \left\{ \frac{200}{9}\omega^2 - \frac{200}{9} L_\omega^2 \right\} + \frac{1}{\beta_0^3} C_F C_A^3 n_f \left\{ -\frac{1360}{9}\omega^2 + \frac{1360}{9} L_\omega^2 \right\} + \frac{1}{\beta_0^3} C_F C_A^4 \left\{ \frac{2312}{9}\omega^2 - \frac{2312}{9} L_\omega^2 \right\} + \frac{1}{\beta_0^3} C_F^2 C_A n_f^2 \left\{ \frac{80}{3}\omega^2 - \frac{80}{3} L_\omega^2 \right\} + \frac{1}{\beta_0^3} C_F^2 C_A^2 n_f \left\{ -\frac{272}{3}\omega^2 + \frac{272}{3} L_\omega^2 \right\} + \frac{1}{\beta_0^3} C_F^3 n_f^2 \times \left\{ 8\omega^2 - 8 L_\omega^2 \right\} + \frac{1}{\beta_0^2} C_F C_A n_f^2 \left\{ \frac{400}{27}\omega - \frac{31}{3}\omega^2 + \frac{400}{27} L_\omega \right\}$$

$$
\begin{aligned}
&+\frac{1}{\beta_0^2}C_F C_A^2 n_f\Big\{-\frac{4040}{27}\omega+\frac{80}{3}\omega\zeta_2+\frac{1145}{9}\omega^2\\
&-\frac{40}{3}\omega^2\zeta_2-\frac{4040}{27}L_\omega+\frac{80}{3}L_\omega\zeta_2\Big\}+\frac{1}{\beta_0^2}C_F C_A^3\\
&\times\Big\{\frac{9112}{27}\omega-\frac{272}{3}\omega\zeta_2-\frac{2471}{9}\omega^2+\frac{136}{3}\omega^2\zeta_2+\frac{9112}{27}L_\omega\\
&-\frac{272}{3}L_\omega\zeta_2\Big\}+\frac{1}{\beta_0^2}C_F^2 n_f^2\Big\{\frac{80}{9}\omega-\frac{62}{9}\omega^2+\frac{80}{9}L_\omega\Big\}\\
&+\frac{1}{\beta_0^2}C_F^2 C_A n_f\Big\{-\frac{536}{9}\omega+16\omega\zeta_2+\frac{473}{9}\omega^2-8\omega^2\zeta_2\\
&-\frac{536}{9}L_\omega+16L_\omega\zeta_2\Big\}\\
&+\frac{1}{\beta_0^2}C_F^3 n_f\Big\{-2\omega^2\Big\}\\
&+\frac{1}{\beta_0}C_F n_f^2\Big\{\frac{16}{27}\omega-\frac{8}{27}\omega^2\Big\}+\frac{1}{\beta_0}C_F C_A n_f\Big\{\frac{836}{27}\omega\\
&+\frac{112}{3}\omega\zeta_3-\frac{160}{9}\omega\zeta_2-\frac{418}{27}\omega^2-\frac{56}{3}\omega^2\zeta_3+\frac{80}{9}\omega^2\zeta_2\\
&-\frac{80}{3}L_\omega+\frac{40}{3}L_\omega L_{qr}-\frac{80}{3}L_\omega\gamma_E\Big\}+\frac{1}{\beta_0}C_F C_A^2\Big\{\\
&-\frac{490}{3}\omega-\frac{88}{3}\omega\zeta_3+\frac{1072}{9}\omega\zeta_2-\frac{176}{5}\omega\zeta_2^2+\frac{245}{3}\omega^2\\
&+\frac{44}{3}\omega^2\zeta_3-\frac{536}{9}\omega^2\zeta_2+\frac{88}{5}\omega^2\zeta_2^2+\frac{272}{3}L_\omega\\
&-\frac{136}{3}L_\omega L_{qr}+\frac{272}{3}L_\omega\gamma_E\Big\}+\frac{1}{\beta_0}C_F^2 n_f\Big\{\frac{110}{3}\omega\\
&-32\omega\zeta_3-\frac{55}{3}\omega^2+16\omega^2\zeta_3-16L_\omega+8L_\omega L_{qr}\\
&-16L_\omega\gamma_E\Big\}+C_F n_f\Big\{\frac{352}{27}-\frac{88}{9}L_{qr}+\frac{4}{3}L_{qr}^2+\frac{40}{9}L_{fr}\\
&-\frac{80}{9}L_{fr}\omega+\frac{40}{9}L_{fr}\omega^2-\frac{4}{3}L_{fr}^2+\frac{8}{3}L_{fr}^2\omega-\frac{4}{3}L_{fr}^2\omega^2\\
&+\frac{176}{9}\gamma_E-\frac{16}{3}\gamma_E L_{qr}+\frac{16}{3}\gamma_E^2\Big\}+C_F C_A\Big\{-\frac{2416}{27}\\
&+28\zeta_3+16\zeta_2+\frac{532}{9}L_{qr}\\
&-8L_{qr}\zeta_2-\frac{22}{3}L_{qr}^2-\frac{268}{9}L_{fr}+8L_{fr}\zeta_2+\frac{536}{9}L_{fr}\omega\\
&-16L_{fr}\omega\zeta_2-\frac{268}{9}L_{fr}\omega^2+8L_{fr}\omega^2\zeta_2+\frac{22}{3}L_{fr}^2\\
&-\frac{44}{3}L_{fr}^2\omega+\frac{22}{3}L_{fr}^2\omega^2\\
&-\frac{1064}{9}\gamma_E+16\gamma_E\zeta_2+\frac{88}{3}\gamma_E L_{qr}-\frac{88}{3}\gamma_E^2\Big\}\Big],
\end{aligned}
\tag{C.40}
$$

C.6 The NSV resummed exponents h_{ij}^q

The resummation constants h_{ij}^q in Eq. (34), till three-loop, are given by

$$h_{00}^q=\frac{1}{\beta_0}C_F\Big\{-8L_\omega\Big\},\tag{C.41}$$

$$h_{01}^q=0,\tag{C.42}$$

$$
\begin{aligned}
h_{10}^q=&\frac{1}{(1-\omega)}\Big[\frac{1}{\beta_0^2}\beta_1 C_F\Big\{-8\omega-8L_\omega\Big\}+\frac{1}{\beta_0}C_F n_f\Big\{\\
&-\frac{80}{9}\omega\Big\}+\frac{1}{\beta_0}C_F C_A\Big\{\frac{536}{9}\omega-16\omega\zeta_2\Big\}+\frac{1}{\beta_0}C_F^2\Big\{\\
&-24\omega+32\gamma_E\omega\Big\}\\
&+C_F\Big\{8+8\omega-8L_{qr}+8L_{fr}\\
&-8L_{fr}\omega+16\gamma_E\Big\}\Big],
\end{aligned}
\tag{C.43}
$$

$$h_{11}^q=+\frac{1}{\beta_0}C_F^2\Big\{32\omega\Big\}+\frac{1}{(1-\omega)^2}\Big[\frac{1}{\beta_0}C_F^2\Big\{-4\omega\Big\}\Big],\tag{C.44}$$

$$
\begin{aligned}
h_{20}^q=&\frac{1}{(1-\omega)^2}\Big[\frac{1}{\beta_0^3}\beta_1^2 C_F\Big\{-4\omega^2+4L_\omega^2\Big\}+\frac{1}{\beta_0^2}\beta_2 C_F\\
&\times\Big\{4\omega^2\Big\}+\frac{1}{\beta_0^2}\beta_1 C_F n_f\Big\{\frac{80}{9}\omega-\frac{40}{9}\omega^2+\frac{80}{9}L_\omega\Big\}\\
&+\frac{1}{\beta_0^2}\beta_1 C_F C_A\Big\{-\frac{536}{9}\omega+16\omega\zeta_2+\frac{268}{9}\omega^2-8\omega^2\zeta_2\\
&-\frac{536}{9}L_\omega+16L_\omega\zeta_2\Big\}+\frac{1}{\beta_0^2}\beta_1 C_F^2\Big\{24\omega-12\omega^2\\
&-32\gamma_E\omega+16\gamma_E\omega^2+24L_\omega-32L_\omega\gamma_E\Big\}\\
&+\frac{1}{\beta_0}C_F n_f^2\Big\{-\frac{32}{27}\omega+\frac{16}{27}\omega^2\Big\}+\frac{1}{\beta_0}C_F C_A n_f\Big\{\\
&-\frac{1672}{27}\omega-\frac{224}{3}\omega\zeta_3+\frac{320}{9}\omega\zeta_2+\frac{836}{27}\omega^2\\
&+\frac{112}{3}\omega^2\zeta_3-\frac{160}{9}\omega^2\zeta_2\Big\}+\frac{1}{\beta_0}C_F C_A^2\Big\{\frac{980}{3}\omega\\
&+\frac{176}{3}\omega\zeta_3-\frac{2144}{9}\omega\zeta_2+\frac{352}{5}\omega\zeta_2^2-\frac{490}{3}\omega^2\\
&-\frac{88}{3}\omega^2\zeta_3+\frac{1072}{9}\omega^2\zeta_2-\frac{176}{5}\omega^2\zeta_2^2\Big\}+\frac{1}{\beta_0}C_F^2 n_f\Big\{\\
&-44\omega+64\omega\zeta_3+\frac{64}{3}\omega\zeta_2+22\omega^2-32\omega^2\zeta_3\\
&-\frac{32}{3}\omega^2\zeta_2-\frac{640}{9}\gamma_E\omega+\frac{320}{9}\gamma_E\omega^2\Big\}+\frac{1}{\beta_0}C_F^2 C_A\Big\{\\
&-\frac{604}{3}\omega+96\omega\zeta_3-\frac{208}{3}\omega\zeta_2+\frac{302}{3}\omega^2-48\omega^2\zeta_3\\
&+\frac{104}{3}\omega^2\zeta_2+\frac{4288}{9}\gamma_E\omega-128\gamma_E\omega\zeta_2-\frac{2144}{9}\gamma_E\omega^2\\
&+64\gamma_E\omega^2\zeta_2\Big\}+\frac{1}{\beta_0}C_F^3\Big\{-12\omega-192\omega\zeta_3+96\omega\zeta_2\\
&+6\omega^2+96\omega^2\zeta_3-48\omega^2\zeta_2\Big\}+\frac{1}{\beta_0}\beta_1 C_F\Big\{-16L_\omega\\
&+8L_\omega L_{qr}-16L_\omega\gamma_E\Big\}+C_F n_f\Big\{-\frac{656}{27}+\frac{32}{3}\zeta_2\\
&-\frac{80}{9}\omega+\frac{40}{9}\omega^2+\frac{80}{9}L_{qr}-\frac{80}{9}L_{fr}+\frac{160}{9}L_{fr}\omega\\
&-\frac{80}{9}L_{fr}\omega^2-\frac{160}{9}\gamma_E\Big\}+C_F C_A\Big\{\frac{2804}{27}-56\zeta_3\\
&-\frac{224}{3}\zeta_2+\frac{536}{9}\omega-16\omega\zeta_2-\frac{268}{9}\omega^2+8\omega^2\zeta_2\\
&-\frac{536}{9}L_{qr}+16L_{qr}\zeta_2+\frac{536}{9}L_{fr}-16L_{fr}\zeta_2
\end{aligned}
$$

$$
\begin{aligned}
&- \frac{1072}{9} L_{fr}\omega + 32 L_{fr}\omega\zeta_2 + \frac{536}{9} L_{fr}\omega^2 - 16 L_{fr}\omega^2\zeta_2 \\
&+ \frac{892}{9}\gamma_E - 32\gamma_E\zeta_2 \Big\} + C_F^2 \Big\{ - 8\zeta_2 + 24 L_{qr} - 24 L_{fr} \\
&+ 48 L_{fr}\omega - 24 L_{fr}\omega^2 - 28\gamma_E - 32\gamma_E L_{qr} + 32\gamma_E L_{fr} \\
&- 64\gamma_E L_{fr}\omega + 32\gamma_E L_{fr}\omega^2 + 56\gamma_E^2 \Big\} + \beta_0 C_F \Big\{ 16\zeta_2 \\
&- 16 L_{qr} + 4 L_{qr}^2 + 8 L_{fr} - 16 L_{fr}\omega + 8 L_{fr}\omega^2 - 4 L_{fr}^2 \\
&+ 8 L_{fr}^2\omega - 4 L_{fr}^2\omega^2 + 32\gamma_E - 16\gamma_E L_{qr} + 16\gamma_E^2 \Big\} \Big],
\end{aligned} \tag{C.45}
$$

$$
\begin{aligned}
h_{21}^q = \frac{1}{(1-\omega)^2} \Bigg[& \frac{1}{\beta_0^2}\beta_1 C_F^2 \Big\{ - 32\omega + 16\omega^2 - 32 L_\omega \Big\} \\
&+ \frac{1}{\beta_0} C_F^2 n_f \Big\{ - \frac{640}{9}\omega + \frac{320}{9}\omega^2 \Big\} + \frac{1}{\beta_0} C_F^2 C_A \\
&\times \Big\{ \frac{4288}{9}\omega - 128\omega\zeta_2 - \frac{2144}{9}\omega^2 + 64\omega^2\zeta_2 \Big\} + C_F C_A \\
&\times \Big\{ - 20 \Big\} + C_F^2 \Big\{ 20 - 32 L_{qr} \\
&+ 32 L_{fr} - 64 L_{fr}\omega + 32 L_{fr}\omega^2 + 48\gamma_E \Big\} \Bigg],
\end{aligned} \tag{C.46}
$$

$$
\begin{aligned}
h_{22}^q = \frac{1}{(1-\omega)^3} \Bigg[& \frac{1}{\beta_0} C_F^2 n_f \Big\{ - \frac{32}{27}\omega \Big\} \\
&+ \frac{1}{\beta_0} C_F^2 C_A \Big\{ \frac{176}{27}\omega \Big\} \Bigg].
\end{aligned} \tag{C.47}
$$

Appendix D: Resummation coefficients for the $\overline{N}$ exponentiation

For the case of $\overline{N}$ exponentiation, all the N-dependent resummed exponents namely $g_i^q(\overline{\omega})$, $\overline{g}_i^q(\overline{\omega})$, and $h_i^q(\overline{\omega})$ given in Eqs. (40) and (42), respectively can be obtained from the corresponding exponents in standard N-approach through setting all the γ_E terms to zero and replacing all the $\ln N$ terms by $\ln \overline{N}$ as well as all the $\mathcal{O}(1)$ ω terms by $\overline{\omega}$ as mentioned in Sect. 3. The N-independent constants $\bar{\tilde{g}}_0^q$ given in Eq. (39) can be obtained from their counterparts in standard N-approach by simply putting the γ_E terms equal to zero.

Appendix E: Resummation coefficients for the soft exponentiation

For the case of *soft exponentiation*, all the terms coming from the soft-collinear function Φ_q are exponentiated and hence this means all the contribution to the finite (N-independent) piece from the soft-collinear function is also being exponentiated. The resummation coefficients for the *soft exponentiation* denoted by $\tilde{g}_{0i}^{q,\mathrm{Soft}}$ and $g_i^{q,\mathrm{Soft}}$ in Eqs. (45) and (44), respectively can be obtained from their counterparts in standard N scheme as described below.

The N-independent constants $\tilde{g}_{0i}^{q,\mathrm{Soft}}$ in Eq. (45) can be put in the following form:

$$\tilde{g}_{01}^{q,\mathrm{Soft}} = \tilde{g}_{01}^q + \Delta_{\tilde{g}_{01}}^{q,\mathrm{Soft}}, \tag{E.48}$$

$$\tilde{g}_{02}^{q,\mathrm{Soft}} = \tilde{g}_{02}^q + \Delta_{\tilde{g}_{02}}^{q,\mathrm{Soft}}, \tag{E.49}$$

$$\tilde{g}_{03}^{q,\mathrm{Soft}} = \tilde{g}_{03}^q + \Delta_{\tilde{g}_{03}}^{q,\mathrm{Soft}}, \tag{E.50}$$

where the coefficients $\Delta_{\tilde{g}_{0i}}^{q,\mathrm{Soft}}$ are given by,

$$\Delta_{\tilde{g}_{01}}^{q,\mathrm{Soft}} = C_F \Big\{ - 16 + 14\zeta_2 + 6 L_{qr} - 2 L_{qr}^2 - 6 L_{fr} \Big\}, \tag{E.51}$$

$$
\begin{aligned}
\Delta_{\tilde{g}_{02}}^{q,\mathrm{Soft}} = C_F n_f \Big\{ & \frac{4085}{162} + \frac{4}{9}\zeta_3 - \frac{182}{9}\zeta_2 - \frac{418}{27} L_{qr} \\
&+ \frac{16}{3} L_{qr}\zeta_2 + \frac{38}{9} L_{qr}^2 - \frac{4}{9} L_{qr}^3 + \frac{2}{3} L_{fr} + \frac{16}{3} L_{fr}\zeta_2 \\
&- 2 L_{fr}^2 \Big\} + C_F C_A \Big\{ - \frac{51157}{324} + \frac{626}{9}\zeta_3 + \frac{1061}{9}\zeta_2 \\
&- \frac{32}{5}\zeta_2^2 + \frac{2545}{27} L_{qr} - 52 L_{qr}\zeta_3 - \frac{88}{3} L_{qr}\zeta_2 \\
&- \frac{233}{9} L_{qr}^2 + 4 L_{qr}^2\zeta_2 + \frac{22}{9} L_{qr}^3 - \frac{17}{3} L_{fr} + 24 L_{fr}\zeta_3 \\
&- \frac{88}{3} L_{fr}\zeta_2 + 11 L_{fr}^2 \Big\} + C_F^2 \Big\{ \frac{511}{4} - 60\zeta_3 - 166\zeta_2 \\
&+ \frac{402}{5}\zeta_2^2 - 93 L_{qr} + 48 L_{qr}\zeta_3 + 60 L_{qr}\zeta_2 + 50 L_{qr}^2 \\
&- 28 L_{qr}^2\zeta_2 - 12 L_{qr}^3 + 2 L_{qr}^4 + 93 L_{fr} - 48 L_{fr}\zeta_3 \\
&- 60 L_{fr}\zeta_2 - 36 L_{fr} L_{qr} + 12 L_{fr} L_{qr}^2 + 18 L_{fr}^2 \Big\},
\end{aligned} \tag{E.52}
$$

$$
\begin{aligned}
\Delta_{\tilde{g}_{03}}^{q,\mathrm{Soft}} = & C_F N_4 n_{fv} \Big\{ 8 - \frac{160}{3}\zeta_5 + \frac{28}{3}\zeta_3 + 20\zeta_2 - \frac{4}{5}\zeta_2^2 \Big\} \\
&+ C_F n_f^2 \Big\{ - \frac{190931}{6561} - \frac{832}{243}\zeta_3 + \frac{3224}{81}\zeta_2 + \frac{344}{135}\zeta_2^2 \\
&+ \frac{19676}{729} L_{qr} + \frac{32}{27} L_{qr}\zeta_3 - \frac{608}{27} L_{qr}\zeta_2 - \frac{812}{81} L_{qr}^2 \\
&+ \frac{32}{9} L_{qr}^2\zeta_2 + \frac{152}{81} L_{qr}^3 - \frac{4}{27} L_{qr}^4 + \frac{34}{9} L_{fr} \\
&+ \frac{32}{9} L_{fr}\zeta_3 - \frac{160}{27} L_{fr}\zeta_2 + \frac{4}{9} L_{fr}^2 + \frac{32}{9} L_{fr}^2\zeta_2 \\
&- \frac{8}{9} L_{fr}^3 \Big\} + C_F C_A n_f \Big\{ \frac{3400342}{6561} - \frac{8}{3}\zeta_5 - \frac{8576}{27}\zeta_3 \\
&- \frac{403498}{729}\zeta_2 + \frac{296}{3}\zeta_2\zeta_3 - \frac{140}{27}\zeta_2^2 - \frac{309838}{729} L_{qr} \\
&+ \frac{1448}{9} L_{qr}\zeta_3 + \frac{23336}{81} L_{qr}\zeta_2 - \frac{392}{15} L_{qr}\zeta_2^2 \\
&+ \frac{11752}{81} L_{qr}^2 - 16 L_{qr}^2\zeta_3 - 48 L_{qr}^2\zeta_2 - \frac{1948}{81} L_{qr}^3 \\
&+ \frac{16}{9} L_{qr}^3\zeta_2 + \frac{44}{27} L_{qr}^4 - 40 L_{fr} - \frac{400}{9} L_{fr}\zeta_3 \\
&+ \frac{2672}{27} L_{fr}\zeta_2 - \frac{8}{5} L_{fr}\zeta_2^2 - \frac{146}{9} L_{fr}^2 + 16 L_{fr}^2\zeta_3 \\
&- \frac{352}{9} L_{fr}^2\zeta_2 + \frac{88}{9} L_{fr}^3 \Big\} + C_F C_A^2
\end{aligned}
$$

$$\times\Bigg\{-\frac{51082685}{26244}-\frac{868}{9}\zeta_5$$

$$+\frac{505087}{243}\zeta_3-\frac{2272}{9}\zeta_3^2+\frac{1193026}{729}\zeta_2$$
$$-\frac{2336}{3}\zeta_2\zeta_3-\frac{4303}{135}\zeta_2^2+\frac{38272}{945}\zeta_2^3$$
$$+\frac{1045955}{729}L_{qr}+272L_{qr}\zeta_5-\frac{34928}{27}L_{qr}\zeta_3$$
$$-\frac{68552}{81}L_{qr}\zeta_2+\frac{176}{3}L_{qr}\zeta_2\zeta_3+\frac{340}{3}L_{qr}\zeta_2^2$$
$$-\frac{37364}{81}L_{qr}^2+176L_{qr}^2\zeta_3+\frac{1504}{9}L_{qr}^2\zeta_2-\frac{88}{5}L_{qr}^2\zeta_2^2$$
$$+\frac{5738}{81}L_{qr}^3-\frac{88}{9}L_{qr}^3\zeta_2-\frac{121}{27}L_{qr}^4+\frac{1657}{18}L_{fr}$$
$$-80L_{fr}\zeta_5+\frac{3104}{9}L_{fr}\zeta_3-\frac{8992}{27}L_{fr}\zeta_2+4L_{fr}\zeta_2^2$$
$$+\frac{493}{9}L_{fr}^2-88L_{fr}^2\zeta_3+\frac{968}{9}L_{fr}^2\zeta_2-\frac{242}{9}L_{fr}^3\Bigg\}$$

$$+C_F^2n_f\Bigg\{-\frac{56963}{486}-\frac{832}{9}\zeta_5+\frac{26080}{81}\zeta_3$$
$$+\frac{27410}{81}\zeta_2-\frac{296}{3}\zeta_2\zeta_3-\frac{5852}{27}\zeta_2^2+\frac{6947}{27}L_{qr}$$
$$-\frac{1208}{9}L_{qr}\zeta_3-\frac{8120}{27}L_{qr}\zeta_2+\frac{1328}{15}L_{qr}\zeta_2^2$$
$$-\frac{14948}{81}L_{qr}^2+\frac{136}{9}L_{qr}^2\zeta_3+\frac{1040}{9}L_{qr}^2\zeta_2$$
$$+\frac{1676}{27}L_{qr}^3-\frac{152}{9}L_{qr}^3\zeta_2-\frac{100}{9}L_{qr}^4+\frac{8}{9}L_{qr}^5$$
$$-\frac{3131}{27}L_{fr}+88L_{fr}\zeta_3+32L_{fr}\zeta_2+\frac{656}{15}L_{fr}\zeta_2^2$$
$$+\frac{872}{9}L_{fr}L_{qr}-\frac{80}{3}L_{fr}L_{qr}^2-\frac{32}{3}L_{fr}L_{qr}^2\zeta_2$$
$$+\frac{8}{3}L_{fr}L_{qr}^3+20L_{fr}^2-32L_{fr}^2\zeta_3-44L_{fr}^2\zeta_2$$
$$-12L_{fr}^2L_{qr}+4L_{fr}^2L_{qr}^2+12L_{fr}^3\Bigg\}+C_F^2C_A$$
$$\times\Bigg\{\frac{824281}{324}-\frac{5512}{9}\zeta_5-\frac{52564}{27}\zeta_3+\frac{592}{3}\zeta_3^2$$
$$-\frac{406507}{162}\zeta_2+\frac{3380}{3}\zeta_2\zeta_3+\frac{184474}{135}\zeta_2^2$$
$$-\frac{11824}{63}\zeta_2^3-\frac{14269}{6}L_{qr}+240L_{qr}\zeta_5+2252L_{qr}\zeta_3$$
$$+\frac{48536}{27}L_{qr}\zeta_2-696L_{qr}\zeta_2\zeta_3-\frac{6776}{15}L_{qr}\zeta_2^2$$
$$+\frac{208099}{162}L_{qr}^2-\frac{5644}{9}L_{qr}^2\zeta_3-\frac{6752}{9}L_{qr}^2\zeta_2$$
$$+\frac{344}{5}L_{qr}^2\zeta_2^2-\frac{10340}{27}L_{qr}^3+104L_{qr}^3\zeta_3$$
$$+\frac{1052}{9}L_{qr}^3\zeta_2+\frac{598}{9}L_{qr}^4-8L_{qr}^4\zeta_2-\frac{44}{9}L_{qr}^5$$
$$+\frac{25988}{27}L_{fr}-240L_{fr}\zeta_5-1364L_{fr}\zeta_3-44L_{fr}\zeta_2$$
$$+304L_{fr}\zeta_2\zeta_3-\frac{3608}{15}L_{fr}\zeta_2^2-\frac{5396}{9}L_{fr}L_{qr}$$
$$+456L_{fr}L_{qr}\zeta_3+\frac{500}{3}L_{fr}L_{qr}^2-48L_{fr}L_{qr}^2\zeta_3$$
$$+\frac{104}{3}L_{fr}L_{qr}^2\zeta_2-\frac{44}{3}L_{fr}L_{qr}^3-131L_{fr}^2+32L_{fr}^2\zeta_3$$
$$+242L_{fr}^2\zeta_2+66L_{fr}^2L_{qr}-22L_{fr}^2L_{qr}^2-66L_{fr}^3\Bigg\}$$
$$+C_F^3\Bigg\{-\frac{5599}{6}+1328\zeta_5-460\zeta_3+32\zeta_3^2$$
$$+\frac{4339}{6}\zeta_2-280\zeta_2\zeta_3-\frac{4152}{5}\zeta_2^2+\frac{109612}{315}\zeta_2^3$$
$$+\frac{1495}{2}L_{qr}-480L_{qr}\zeta_5-992L_{qr}\zeta_3-534L_{qr}\zeta_2$$
$$+608L_{qr}\zeta_2\zeta_3+\frac{1308}{5}L_{qr}\zeta_2^2-\frac{1051}{2}L_{qr}^2$$
$$+408L_{qr}^2\zeta_3+440L_{qr}^2\zeta_2-\frac{804}{5}L_{qr}^2\zeta_2^2+222L_{qr}^3$$
$$-96L_{qr}^3\zeta_3-120L_{qr}^3\zeta_2-68L_{qr}^4+28L_{qr}^4\zeta_2+12L_{qr}^5$$
$$-\frac{4}{3}L_{qr}^6-\frac{1495}{2}L_{fr}+480L_{fr}\zeta_5+992L_{fr}\zeta_3$$
$$+534L_{fr}\zeta_2-608L_{fr}\zeta_2\zeta_3-\frac{1308}{5}L_{fr}\zeta_2^2$$
$$+540L_{fr}L_{qr}-576L_{fr}L_{qr}\zeta_3-216L_{fr}L_{qr}\zeta_2$$
$$-294L_{fr}L_{qr}^2+96L_{fr}L_{qr}^2\zeta_3+120L_{fr}L_{qr}^2\zeta_2$$
$$+72L_{fr}L_{qr}^3-12L_{fr}L_{qr}^4-270L_{fr}^2+288L_{fr}^2\zeta_3$$
$$+108L_{fr}^2\zeta_2+108L_{fr}^2L_{qr}-36L_{fr}^2L_{qr}^2-36L_{fr}^3\Bigg\}. \tag{E.53}$$

The N-dependent coefficients $g_i^{q,\mathrm{Soft}}$ in Eq. (44) can be obtained as follows:

$$g_1^{q,\mathrm{Soft}}=g_1^q, \tag{E.54}$$
$$g_2^{q,\mathrm{Soft}}=g_2^q+a_s\,\Delta_{g_2}^{q,\mathrm{Soft}}, \tag{E.55}$$
$$g_3^{q,\mathrm{Soft}}=g_3^q+a_s\,\Delta_{g_3}^{q,\mathrm{Soft}}, \tag{E.56}$$

where the coefficients $\Delta_{g_i}^{q,\mathrm{Soft}}$ are given as,

$$\Delta_{g_2}^{\mathrm{Soft}}=C_F\Bigg\{2\zeta_2+2L_{qr}^2-8\gamma_EL_{qr}+8\gamma_EL_{fr}+8\gamma_E^2\Bigg\}, \tag{E.57}$$

$$\Delta_{g_3}^{\mathrm{Soft}}=C_Fn_f\Bigg\{-\frac{328}{81}+\frac{4}{9}\zeta_3-\frac{10}{9}\zeta_2+\frac{112}{27}L_{qr}-\frac{20}{9}L_{qr}^2$$
$$+\frac{4}{9}L_{qr}^3-\frac{224}{27}\gamma_E+\frac{80}{9}\gamma_EL_{qr}-\frac{8}{3}\gamma_EL_{qr}^2-\frac{80}{9}\gamma_EL_{fr}$$
$$+\frac{8}{3}\gamma_EL_{fr}^2-\frac{80}{9}\gamma_E^2+\frac{16}{3}\gamma_E^2L_{qr}-\frac{32}{9}\gamma_E^3\Bigg\}+C_FC_A$$
$$\times\Bigg\{\frac{2428}{81}-\frac{22}{9}\zeta_3+\frac{67}{9}\zeta_2-12\zeta_2^2-\frac{808}{27}L_{qr}+28L_{qr}\zeta_3$$
$$+\frac{134}{9}L_{qr}^2-4L_{qr}^2\zeta_2-\frac{22}{9}L_{qr}^3+\frac{1616}{27}\gamma_E-56\gamma_E\zeta_3$$
$$-\frac{536}{9}\gamma_EL_{qr}+16\gamma_EL_{qr}\zeta_2+\frac{44}{3}\gamma_EL_{qr}^2+\frac{536}{9}\gamma_EL_{fr}$$
$$-16\gamma_EL_{fr}\zeta_2-\frac{44}{3}\gamma_EL_{fr}^2+\frac{536}{9}\gamma_E^2-16\gamma_E^2\zeta_2$$
$$-\frac{88}{3}\gamma_E^2L_{qr}+\frac{176}{9}\gamma_E^3\Bigg\}. \tag{E.58}$$

Appendix F: Resummation coefficients for the all exponentiation

For the case of *All exponentiation*, the complete $\tilde{g}_0^q$ is being exponentiated along with the large-N pieces. This brings into modification only for the resummed exponent compared to the 'Standard N exponentiation'. We write the modified resummed exponents denoted by $g_i^{q,\mathrm{All}}$ in Eq. (47) in terms of exponents in standard N as,

$$g_1^{q,\mathrm{All}} = g_1^q, \tag{F.59}$$

$$g_2^{q,\mathrm{All}} = g_2^q + a_s\, \Delta_{g_2}^{q,\mathrm{All}}, \tag{F.60}$$

$$g_3^{q,\mathrm{All}} = g_3^q + a_s\, \Delta_{g_3}^{q,\mathrm{All}}, \tag{F.61}$$

where $\Delta_{g_i}^{q,\mathrm{All}}$ terms are found from exponentiating the complete $\tilde{g}_0^q$ prefactor and they are given as,

$$\Delta_{g_2}^{q,\mathrm{All}} = \tilde{g}_{01}^q, \tag{F.62}$$

$$\Delta_{g_3}^{q,\mathrm{All}} = \left(-\frac{(\tilde{g}_{01}^q)^2}{2} + \tilde{g}_{02}^q \right), \tag{F.63}$$

where the coefficients $\tilde{g}_{0i}^q$ are given in Appendix C.3.

References

1. R. Hamberg, W.L. van Neerven, T. Matsuura, A complete calculation of the order $\alpha - s^2$ correction to the Drell–Yan K factor. Nucl. Phys. B **359**, 343–405 (1991). https://doi.org/10.1016/S0550-3213(02)00814-3, https://doi.org/10.1016/0550-3213(91)90064-5
2. T. Matsuura, R. Hamberg, W.L. van Neerven, The contribution of the gluon–gluon subprocess to the Drell–Yan K factor. Nucl. Phys. B **345**, 331–368 (1990). https://doi.org/10.1016/0550-3213(90)90391-P
3. R.V. Harlander, W.B. Kilgore, Next-to-next-to-leading order Higgs production at hadron colliders. Phys. Rev. Lett. **88**, 201801 (2002). https://doi.org/10.1103/PhysRevLett.88.201801 arXiv:hep-ph/0201206
4. G. Altarelli, R. Ellis, G. Martinelli, Leptoproduction and Drell–Yan processes beyond the leading approximation in chromodynamics. Nucl. Phys. B **143**, 521 (1978). https://doi.org/10.1016/0550-3213(78)90067-6
5. G. Altarelli, R. Ellis, G. Martinelli, Large perturbative corrections to the Drell–Yan process in QCD. Nucl. Phys. B **157**, 461–497 (1979). https://doi.org/10.1016/0550-3213(79)90116-0
6. T. Matsuura, W. van Neerven, Second order logarithmic corrections to the Drell–Yan cross-section. Z. Phys. C **38**, 623 (1988). https://doi.org/10.1007/BF01624369
7. T. Matsuura, S. van der Marck, W. van Neerven, The order $\alpha^- s^2$ contribution to the K factor of the Drell–Yan process. Phys. Lett. B **211**, 171–178 (1988). https://doi.org/10.1016/0370-2693(88)90828-3
8. T. Matsuura, S. van der Marck, W. van Neerven, The calculation of the second order soft and virtual contributions to the Drell–Yan cross-section. Nucl. Phys. B **319**, 570–622 (1989). https://doi.org/10.1016/0550-3213(89)90620-2
9. W. van Neerven, E. Zijlstra, The $O(\alpha_s^2)$ corrected Drell–Yan K factor in the DIS and MS scheme. Nucl. Phys. B **382**, 11–62 (1992). https://doi.org/10.1016/0550-3213(92)90078-P
10. S. Moch, A. Vogt, Higher-order soft corrections to lepton pair and Higgs boson production. Phys. Lett. B **631**, 48–57 (2005). https://doi.org/10.1016/j.physletb.2005.09.061 arXiv:hep-ph/0508265
11. V. Ravindran, Higher-order threshold effects to inclusive processes in QCD. Nucl. Phys. B **752**, 173–196 (2006). https://doi.org/10.1016/j.nuclphysb.2006.06.025 arXiv:hep-ph/0603041
12. D. de Florian, J. Mazzitelli, A next-to-next-to-leading order calculation of soft-virtual cross sections. JHEP **12**, 088 (2012). https://doi.org/10.1007/JHEP12(2012)08, https://doi.org/10.1007/JHEP12(2012)088. arXiv:1209.0673
13. T. Ahmed, M. Mahakhud, N. Rana, V. Ravindran, Drell–Yan production at threshold to third order in QCD. Phys. Rev. Lett. **113**, 112002 (2014). https://doi.org/10.1103/PhysRevLett.113.112002 arXiv:1404.0366
14. T. Ahmed, M.C. Kumar, P. Mathews, N. Rana, V. Ravindran, Pseudo-scalar Higgs boson production at threshold N^3 LO and N^3 LL QCD. Eur. Phys. J. C **76**, 355 (2016). https://doi.org/10.1140/epjc/s10052-016-4199-1 arXiv:1510.02235
15. S. Catani, L. Cieri, D. de Florian, G. Ferrera, M. Grazzini, Threshold resummation at N^3LL accuracy and soft-virtual cross sections at N^3LO. Nucl. Phys. B **888**, 75–91 (2014). https://doi.org/10.1016/j.nuclphysb.2014.09.012 arXiv:1405.4827
16. Y. Li, A. von Manteuffel, R.M. Schabinger, H.X. Zhu, Soft-virtual corrections to Higgs production at N^3LO. Phys. Rev. D **91**, 036008 (2015). https://doi.org/10.1103/PhysRevD.91.036008 arXiv:1412.2771
17. C. Duhr, F. Dulat, B. Mistlberger, The Drell–Yan cross section to third order in the strong coupling constant. Phys. Rev. Lett. **125**, 172001 (2020). https://doi.org/10.1103/PhysRevLett.125.172001 arXiv:2001.07717
18. T. Ahmed, P. Banerjee, P.K. Dhani, M.C. Kumar, P. Mathews, N. Rana, V. Ravindran, NNLO QCD corrections to the Drell–Yan cross section in models of TeV-scale gravity. Eur. Phys. J. C **77**, 22 (2017). https://doi.org/10.1140/epjc/s10052-016-4587-6 arXiv:1606.08454
19. P. Banerjee, G. Das, P.K. Dhani, V. Ravindran, Threshold resummation of the rapidity distribution for Drell–Yan production at NNLO+NNLL. Phys. Rev. D **98**, 054018 (2018). https://doi.org/10.1103/PhysRevD.98.054018 arXiv:1805.01186
20. S. Majhi, P. Mathews, V. Ravindran, NNLO QCD corrections to the resonant sneutrino/slepton production at Hadron Colliders. Nucl. Phys. B **850**, 287–320 (2011). https://doi.org/10.1016/j.nuclphysb.2011.05.002 arXiv:1011.6027
21. V. Ravindran, On Sudakov and soft resummations in QCD. Nucl. Phys. B **746**, 58–76 (2006). https://doi.org/10.1016/j.nuclphysb.2006.04.008 arXiv:hep-ph/0512249
22. T. Ahmed, N. Rana, V. Ravindran, Higgs boson production through $b\bar{b}$ annihilation at threshold in N^3LO QCD. JHEP **10**, 139 (2014). https://doi.org/10.1007/JHEP10(2014)139 arXiv:1408.0787
23. M.C. Kumar, M.K. Mandal, V. Ravindran, Associated production of Higgs boson with vector boson at threshold N^3LO in QCD. JHEP **03**, 037 (2015). https://doi.org/10.1007/JHEP03(2015)037 arXiv:1412.3357
24. Y. Li, A. von Manteuffel, R.M. Schabinger, H.X. Zhu, N^3LO Higgs boson and Drell–Yan production at threshold: the one-loop two-emission contribution. Phys. Rev. D **90**, 053006 (2014). https://doi.org/10.1103/PhysRevD.90.053006 arXiv:1404.5839
25. G.F. Sterman, Summation of large corrections to short distance hadronic cross-sections. Nucl. Phys. B **281**, 310–364 (1987). https://doi.org/10.1016/0550-3213(87)90258-6

26. S. Catani, L. Trentadue, Resummation of the QCD perturbative series for hard processes. Nucl. Phys. B **327**, 323–352 (1989). https://doi.org/10.1016/0550-3213(89)90273-3
27. S. Moch, J.A.M. Vermaseren, A. Vogt, Higher-order corrections in threshold resummation. Nucl. Phys. B **726**, 317–335 (2005). https://doi.org/10.1016/j.nuclphysb.2005.08.005 arXiv:hep-ph/0506288
28. M. Bonvini, Threshold resummation for Drell–Yan production: theory and phenomenology. PoS DIS **2010**, 100 (2010). https://doi.org/10.22323/1.106.0100. arXiv:1006.5918
29. M. Bonvini, Resummation of soft and hard gluon radiation in perturbative QCD. Ph.D. thesis, Genoa U. (2012). arXiv:1212.0480
30. A.H. Ajjath, G. Das, M.C. Kumar, P. Mukherjee, V. Ravindran, K. Samanta, Resummed Drell–Yan cross-section at N^3LL. JHEP **10**, 153 (2020). https://doi.org/10.1007/JHEP10(2020)153 arXiv:2001.11377
31. C. Anastasiou, C. Duhr, F. Dulat, E. Furlan, T. Gehrmann, F. Herzog, B. Mistlberger, Higgs boson gluon-fusion production beyond threshold in N^3LO QCD. JHEP **03**, 091 (2015). https://doi.org/10.1007/JHEP03(2015)091 arXiv:1411.3584
32. M. Bonvini, S. Marzani, Resummed Higgs cross section at N^3LL. JHEP **09**, 007 (2014). https://doi.org/10.1007/JHEP09(2014)007 arXiv:1405.3654
33. G. Das, S. Moch, A. Vogt, Approximate four-loop QCD corrections to the Higgs-boson production cross section. Phys. Lett. B **807**, 135546 (2020). https://doi.org/10.1016/j.physletb.2020.135546 arXiv:2004.00563
34. N. Kidonakis, Soft and collinear enhancements to top quark and Higgs cross sections. Acta Phys. Pol. B **39**, 1593–1604 (2008). arXiv:0802.3381
35. E. Laenen, L. Magnea, G. Stavenga, On next-to-eikonal corrections to threshold resummation for the Drell–Yan and DIS cross sections. Phys. Lett. B **669**, 173–179 (2008). https://doi.org/10.1016/j.physletb.2008.09.037 arXiv:0807.4412
36. G. Grunberg, V. Ravindran, On threshold resummation beyond leading $1-x$ order. JHEP **10**, 055 (2009). https://doi.org/10.1088/1126-6708/2009/10/055 arXiv:0902.2702
37. S. Moch, A. Vogt, On non-singlet physical evolution kernels and large-x coefficient functions in perturbative QCD. JHEP **11**, 099 (2009). https://doi.org/10.1088/1126-6708/2009/11/099 arXiv:0909.2124
38. E. Laenen, L. Magnea, G. Stavenga, C.D. White, On next-to-eikonal exponentiation. Nucl. Phys. B Proc. Suppl. **205–206**, 260–265 (2010). https://doi.org/10.1016/j.nuclphysbps.2010.09.003 arXiv:1007.0624
39. E. Laenen, L. Magnea, G. Stavenga, C.D. White, Next-to-eikonal corrections to soft gluon radiation: a diagrammatic approach. JHEP **01**, 141 (2011). https://doi.org/10.1007/JHEP01(2011)141 arXiv:1010.1860
40. D. Bonocore, E. Laenen, L. Magnea, L. Vernazza, C.D. White, The method of regions and next-to-soft corrections in Drell–Yan production. Phys. Lett. B **742**, 375–382 (2015). https://doi.org/10.1016/j.physletb.2015.02.008 arXiv:1410.6406
41. D. Bonocore, E. Laenen, L. Magnea, S. Melville, L. Vernazza, C. White, A factorization approach to next-to-leading-power threshold logarithms. JHEP **06**, 008 (2015). https://doi.org/10.1007/JHEP06(2015)008 arXiv:1503.05156
42. M. Beneke, A. Broggio, S. Jaskiewicz, L. Vernazza, Threshold factorization of the Drell–Yan process at next-to-leading power. JHEP **07**, 78 (2019). https://doi.org/10.1007/JHEP07(2020)078 arXiv:1912.01585
43. M. Beneke, M. Garny, S. Jaskiewicz, R. Szafron, L. Vernazza, J. Wang, Leading-logarithmic threshold resummation of Higgs production in gluon fusion at next-to-leading power. JHEP **01**, 094 (2020). https://doi.org/10.1007/JHEP01(2020)094 arXiv:1910.12685
44. D. Bonocore, E. Laenen, L. Magnea, L. Vernazza, C. White, Non-abelian factorisation for next-to-leading-power threshold logarithms. JHEP **12**, 121 (2016). https://doi.org/10.1007/JHEP12(2016)121 arXiv:1610.06842
45. V. Del Duca, E. Laenen, L. Magnea, L. Vernazza, C. White, Universality of next-to-leading power threshold effects for colourless final states in hadronic collisions. JHEP **11**, 057 (2017). https://doi.org/10.1007/JHEP11(2017)057 arXiv:1706.04018
46. D. de Florian, J. Mazzitelli, S. Moch, A. Vogt, Approximate N^3LO Higgs-boson production cross section using physical-kernel constraints. JHEP **10**, 176 (2014). https://doi.org/10.1007/JHEP10(2014)176 arXiv:1408.6277
47. M. van Beekveld, E. Laenen, J. Sinninghe Damsté, L. Vernazza, Next-to-leading power threshold corrections for finite order and resummed colour-singlet cross sections. JHEP **05**, 114 (2021). https://doi.org/10.1007/JHEP05(2021)114 arXiv:2101.07270
48. T. Ahmed, M. Bonvini, M.C. Kumar, P. Mathews, N. Rana, V. Ravindran, L. Rottoli, Pseudo-scalar Higgs boson production at $N^3\,LO_A + N^3\,LL'$. Eur. Phys. J. C **76**, 663 (2016). https://doi.org/10.1140/epjc/s10052-016-4510-1 arXiv:1606.00837
49. A. Ajjath, P. Mukherjee, V. Ravindran, On next to soft corrections to Drell–Yan and Higgs boson productions. arXiv:2006.06726
50. T. Becher, M. Neubert, Infrared singularities of scattering amplitudes in perturbative QCD. Phys. Rev. Lett. **102**, 162001 (2009). https://doi.org/10.1103/PhysRevLett.102.162001, https://doi.org/10.1103/PhysRevLett.111.199905. arXiv:0901.0722
51. T. Becher, M. Neubert, On the structure of infrared singularities of gauge-theory amplitudes. JHEP **06**, 081 (2009). https://doi.org/10.1088/1126-6708/2009/06/081 arXiv:0903.1126
52. E. Gardi, L. Magnea, Factorization constraints for soft anomalous dimensions in QCD scattering amplitudes. JHEP **03**, 079 (2009). https://doi.org/10.1088/1126-6708/2009/03/079 arXiv:0901.1091
53. S. Catani, The singular behavior of QCD amplitudes at two loop order. Phys. Lett. B **427**, 161–171 (1998). https://doi.org/10.1016/S0370-2693(98)00332-3 arXiv:hep-ph/9802439
54. A.H. Ajjath, P. Mukherjee, V. Ravindran, Infrared structure of $SU(N) \times U(1)$ gauge theory to three loops. JHEP **08**, 156 (2020). https://doi.org/10.1007/JHEP08(2020)156 arXiv:1912.13386
55. A. Ajjath, P. Banerjee, A. Chakraborty, P.K. Dhani, P. Mukherjee, N. Rana, V. Ravindran, NNLO QCD⊕QED corrections to Higgs production in bottom quark annihilation. Phys. Rev. D **100**, 114016 (2019). https://doi.org/10.1103/PhysRevD.100.114016 arXiv:1906.09028
56. C. Anastasiou, C. Duhr, F. Dulat, F. Herzog, B. Mistlberger, Higgs boson gluon-fusion production in QCD at three loops. Phys. Rev. Lett. **114**, 212001 (2015). https://doi.org/10.1103/PhysRevLett.114.212001 arXiv:1503.06056
57. B. Mistlberger, Higgs boson production at hadron colliders at N^3LO in QCD. JHEP **05**, 028 (2018). https://doi.org/10.1007/JHEP05(2018)028 arXiv:1802.00833
58. C. Duhr, F. Dulat, B. Mistlberger, Higgs production in bottom-quark fusion to third order in the strong coupling. Phys. Rev. Lett. **125**, 051804 (2020). https://doi.org/10.1103/PhysRevLett.125.051804 arXiv:1904.09990
59. H. Georgi, S. Glashow, M. Machacek, D.V. Nanopoulos, Higgs bosons from two gluon annihilation in proton–proton collisions. Phys. Rev. Lett. **40**, 692 (1978). https://doi.org/10.1103/PhysRevLett.40.692
60. D. Graudenz, M. Spira, P. Zerwas, QCD corrections to Higgs boson production at proton–proton colliders. Phys. Rev. Lett. **70**, 1372–1375 (1993). https://doi.org/10.1103/PhysRevLett.70.1372
61. A. Djouadi, M. Spira, P. Zerwas, Production of Higgs bosons in proton colliders: QCD corrections. Phys. Lett. B **264**, 440–446 (1991). https://doi.org/10.1016/0370-2693(91)90375-Z

62. M. Spira, A. Djouadi, D. Graudenz, P. Zerwas, Higgs boson production at the LHC. Nucl. Phys. B **453**, 17–82 (1995). https://doi.org/10.1016/0550-3213(95)00379-7 arXiv:hep-ph/9504378
63. S. Catani, D. de Florian, M. Grazzini, Higgs production in hadron collisions: soft and virtual QCD corrections at NNLO. JHEP **05**, 025 (2001). https://doi.org/10.1088/1126-6708/2001/05/025 arXiv:hep-ph/0102227
64. R.V. Harlander, W.B. Kilgore, Soft and virtual corrections to proton proton → H + x at NNLO. Phys. Rev. D **64**, 013015 (2001). https://doi.org/10.1103/PhysRevD.64.013015 arXiv:hep-ph/0102241
65. C. Anastasiou, K. Melnikov, Higgs boson production at hadron colliders in NNLO QCD. Nucl. Phys. B **646**, 220–256 (2002). https://doi.org/10.1016/S0550-3213(02)00837-4 arXiv:hep-ph/0207004
66. S. Catani, D. de Florian, M. Grazzini, P. Nason, Soft gluon resummation for Higgs boson production at hadron colliders. JHEP **07**, 028 (2003). https://doi.org/10.1088/1126-6708/2003/07/028 arXiv:hep-ph/0306211
67. V. Ravindran, J. Smith, W.L. van Neerven, NNLO corrections to the total cross-section for Higgs boson production in hadron–hadron collisions. Nucl. Phys. B **665**, 325–366 (2003). https://doi.org/10.1016/S0550-3213(03)00457-7 arXiv:hep-ph/0302135
68. M. Bonvini, R.D. Ball, S. Forte, S. Marzani, G. Ridolfi, Updated Higgs cross section at approximate N^3LO. J. Phys. G **41**, 095002 (2014). https://doi.org/10.1088/0954-3899/41/9/095002 arXiv:1404.3204
69. C. Anastasiou, C. Duhr, F. Dulat, E. Furlan, T. Gehrmann, F. Herzog, B. Mistlberger, Higgs boson gluon-fusion production at threshold in N^3LO QCD. Phys. Lett. B **737**, 325–328 (2014). https://doi.org/10.1016/j.physletb.2014.08.067 arXiv:1403.4616
70. A. Idilbi, X.-D. Ji, J.-P. Ma, F. Yuan, Threshold resummation for Higgs production in effective field theory. Phys. Rev. D **73**, 077501 (2006). https://doi.org/10.1103/PhysRevD.73.077501 arXiv:hep-ph/0509294
71. C. Anastasiou, C. Duhr, F. Dulat, E. Furlan, F. Herzog, B. Mistlberger, Soft expansion of double-real-virtual corrections to Higgs production at N^3LO. JHEP **08**, 051 (2015). https://doi.org/10.1007/JHEP08(2015)051 arXiv:1505.04110
72. C.W. Bauer, S. Fleming, D. Pirjol, I.W. Stewart, An effective field theory for collinear and soft gluons: heavy to light decays. Phys. Rev. D **63**, 114020 (2001). https://doi.org/10.1103/PhysRevD.63.114020 arXiv:hep-ph/0011336
73. C.W. Bauer, D. Pirjol, I.W. Stewart, Soft collinear factorization in effective field theory. Phys. Rev. D **65**, 054022 (2002). https://doi.org/10.1103/PhysRevD.65.054022 arXiv:hep-ph/0109045
74. C.W. Bauer, S. Fleming, D. Pirjol, I.Z. Rothstein, I.W. Stewart, Hard scattering factorization from effective field theory. Phys. Rev. D **66**, 014017 (2002). https://doi.org/10.1103/PhysRevD.66.014017 arXiv:hep-ph/0202088
75. S. Catani, M.L. Mangano, P. Nason, L. Trentadue, The resummation of soft gluons in hadronic collisions. Nucl. Phys. B **478**, 273–310 (1996). https://doi.org/10.1016/0550-3213(96)00399-9 arXiv:hep-ph/9604351
76. M. Bonvini, S. Forte, G. Ridolfi, The threshold region for Higgs production in gluon fusion. Phys. Rev. Lett. **109**, 102002 (2012). https://doi.org/10.1103/PhysRevLett.109.102002 arXiv:1204.5473
77. M. Bonvini, L. Rottoli, Three loop soft function for N^3LL' gluon fusion Higgs production in soft-collinear effective theory. Phys. Rev. D **91**, 051301 (2015). https://doi.org/10.1103/PhysRevD.91.051301 arXiv:1412.3791
78. M. Bonvini, S. Marzani, C. Muselli, L. Rottoli, On the Higgs cross section at N^3LO+N^3LL and its uncertainty. JHEP **08**, 105 (2016). https://doi.org/10.1007/JHEP08(2016)105 arXiv:1603.08000
79. M. Bonvini, A.S. Papanastasiou, F.J. Tackmann, Matched predictions for the $b\bar{b}H$ cross section at the 13 TeV LHC. JHEP **10**, 053 (2016). https://doi.org/10.1007/JHEP10(2016)053 arXiv:1605.01733
80. A.H. Ajjath, A. Chakraborty, G. Das, P. Mukherjee, V. Ravindran, Resummed prediction for Higgs boson production through $b\bar{b}$ annihilation at N^3LL. JHEP **11**, 006 (2019). https://doi.org/10.1007/JHEP11(2019)006 arXiv:1905.03771
81. M. Cacciari, S. Catani, Soft gluon resummation for the fragmentation of light and heavy quarks at large x. Nucl. Phys. B **617**, 253–290 (2001). https://doi.org/10.1016/S0550-3213(01)00469-2 arXiv:hep-ph/0107138
82. D. Westmark, J.F. Owens, Enhanced threshold resummation formalism for lepton pair production and its effects in the determination of parton distribution functions. Phys. Rev. D **95**, 056024 (2017). https://doi.org/10.1103/PhysRevD.95.056024 arXiv:1701.06716
83. P. Banerjee, G. Das, P.K. Dhani, V. Ravindran, Threshold resummation of the rapidity distribution for Higgs production at NNLO+NNLL. Phys. Rev. D **97**, 054024 (2018). https://doi.org/10.1103/PhysRevD.97.054024 arXiv:1708.05706
84. G. Lustermans, J.K.L. Michel, F.J. Tackmann, Generalized threshold factorization with full collinear dynamics. arXiv:1908.00985
85. A.H. Ajjath, P. Mukherjee, V. Ravindran, A. Sankar, S. Tiwari, On next to soft threshold corrections to DIS and SIA processes. JHEP **04**, 131 (2021). https://doi.org/10.1007/JHEP04(2021)131 arXiv:2007.12214
86. A.H. Ajjath, P. Mukherjee, V. Ravindran, A. Sankar, S. Tiwari, On next to soft corrections for Drell–Yan and Higgs boson rapidity distributions beyond N^3LO. Phys. Rev. D **103**, L111502 (2021). https://doi.org/10.1103/PhysRevD.103.L111502 arXiv:2010.00079
87. S. Moch, J.A.M. Vermaseren, A. Vogt, The three loop splitting functions in QCD: the nonsinglet case. Nucl. Phys. B **688**, 101–134 (2004). https://doi.org/10.1016/j.nuclphysb.2004.03.030 arXiv:hep-ph/0403192
88. A. Vogt, S. Moch, J.A.M. Vermaseren, The three-loop splitting functions in QCD: the singlet case. Nucl. Phys. B **691**, 129–181 (2004). https://doi.org/10.1016/j.nuclphysb.2004.04.024 arXiv:hep-ph/0404111
89. A. Gonzalez-Arroyo, C. Lopez, F. Yndurain, Second order contributions to the structure functions in deep inelastic scattering. 1. Theoretical calculations. Nucl. Phys. B **153**, 161–186 (1979). https://doi.org/10.1016/0550-3213(79)90596-0
90. G. Curci, W. Furmanski, R. Petronzio, Evolution of parton densities beyond leading order: the nonsinglet case. Nucl. Phys. B **175**, 27–92 (1980). https://doi.org/10.1016/0550-3213(80)90003-6
91. W. Furmanski, R. Petronzio, Singlet parton densities beyond leading order. Phys. Lett. B **97**, 437–442 (1980). https://doi.org/10.1016/0370-2693(80)90636-X
92. R. Hamberg, W. van Neerven, The correct renormalization of the gluon operator in a covariant gauge. Nucl. Phys. B **379**, 143–171 (1992). https://doi.org/10.1016/0550-3213(92)90593-Z
93. R. Ellis, W. Vogelsang, The evolution of parton distributions beyond leading order: the singlet case. arXiv:hep-ph/9602356
94. G. Soar, S. Moch, J. Vermaseren, A. Vogt, On Higgs-exchange DIS, physical evolution kernels and fourth-order splitting functions at large x. Nucl. Phys. B **832**, 152–227 (2010). https://doi.org/10.1016/j.nuclphysb.2010.02.003 arXiv:0912.0369
95. J. Ablinger, A. Behring, J. Blümlein, A. De Freitas, A. von Manteuffel, C. Schneider, The three-loop splitting functions $P_{qg}^{(2)}$ and $P_{gg}^{(2,N_F)}$. Nucl. Phys. B **922**, 1–40 (2017). https://doi.org/10.1016/j.nuclphysb.2017.06.004 arXiv:1705.01508
96. S. Moch, B. Ruijl, T. Ueda, J.A.M. Vermaseren, A. Vogt, Four-loop non-singlet splitting functions in the planar limit and beyond.

JHEP **10**, 041 (2017). https://doi.org/10.1007/JHEP10(2017)041 arXiv:1707.08315
97. G. Das, S.-O. Moch, A. Vogt, Soft corrections to inclusive deep-inelastic scattering at four loops and beyond. JHEP **03**, 116 (2020). https://doi.org/10.1007/JHEP03(2020)116 arXiv:1912.12920
98. V.V. Sudakov, Vertex parts at very high-energies in quantum electrodynamics. Sov. Phys. JETP **3**, 65–71 (1956)
99. A.H. Mueller, On the asymptotic behavior of the Sudakov form-factor. Phys. Rev. D **20**, 2037 (1979). https://doi.org/10.1103/PhysRevD.20.2037
100. J.C. Collins, Algorithm to compute corrections to the Sudakov form-factor. Phys. Rev. D **22**, 1478 (1980). https://doi.org/10.1103/PhysRevD.22.1478
101. A. Sen, Asymptotic behavior of the Sudakov form-factor in QCD. Phys. Rev. D **24**, 3281 (1981). https://doi.org/10.1103/PhysRevD.24.3281
102. T.O. Eynck, E. Laenen, L. Magnea, Exponentiation of the Drell–Yan cross-section near partonic threshold in the DIS and MS-bar schemes. JHEP **06**, 057 (2003). https://doi.org/10.1088/1126-6708/2003/06/057 arXiv:hep-ph/0305179
103. A. Vogt, Efficient evolution of unpolarized and polarized parton distributions with QCD-PEGASUS. Comput. Phys. Commun. **170**, 65–92 (2005). https://doi.org/10.1016/j.cpc.2005.03.103 arXiv:hep-ph/0408244
104. M. Beneke, A. Broggio, M. Garny, S. Jaskiewicz, R. Szafron, L. Vernazza, J. Wang, Leading-logarithmic threshold resummation of the Drell–Yan process at next-to-leading power. JHEP **03**, 043 (2019). https://doi.org/10.1007/JHEP03(2019)043 arXiv:1809.10631
105. A. Buckley, J. Ferrando, S. Lloyd, K. Nordström, B. Page, M. Rüfenacht, M. Schönherr, G. Watt, LHAPDF6: parton density access in the LHC precision era. Eur. Phys. J. C **75**, 132 (2015). https://doi.org/10.1140/epjc/s10052-015-3318-8 arXiv:1412.7420
106. L.A. Harland-Lang, A.D. Martin, P. Motylinski, R.S. Thorne, Parton distributions in the LHC era: MMHT 2014 PDFs. Eur. Phys. J. C **75**, 204 (2015). https://doi.org/10.1140/epjc/s10052-015-3397-6 arXiv:1412.3989
107. T. Gehrmann, E.W.N. Glover, T. Huber, N. Ikizlerli, C. Studerus, Calculation of the quark and gluon form factors to three loops in QCD. JHEP **06**, 094 (2010). https://doi.org/10.1007/JHEP06(2010)094 arXiv:1004.3653